MICROBES ACROSS SPACE AND TIME:

MICROBIAL COMPOSITION THROUGHOUT DELAWARE WATERS, INVERTEBRATES AND SEDIMENTS

by

Malique R. Bowen

A dissertation submitted to the Faculty of the University of Delaware in partial fulfillment of the requirements for the degree of Doctor of Philosophy in Marine Bioscience

Summer 2025

MICROBES ACROSS SPACE AND TIME:

MICROBIAL COMPOSITION THROUGHOUT DELAWARE WATERS, INVERTEBRATES AND SEDIMENTS

by

Malique R. Bowen

Approved: _____
Katharina Billups, Ph.D.
Director of the School of Marine Science & Policy

Approved: _____
Fabrice Veron, Ph.D.
Dean of the College of College of Earth, Ocean & Environment

Approved: _____
Louis F. Rossi, Ph.D.
Vice Provost for Graduate and Professional Education and
Dean of the Graduate College

I certify that I have read this dissertation and that in my opinion it meets the academic and professional standard required by the University as a dissertation for the degree of Doctor of Philosophy.

Signed: _____

Jennifer F. Biddle, Ph.D.
Professor in charge of dissertation

I certify that I have read this dissertation and that in my opinion it meets the academic and professional standard required by the University as a dissertation for the degree of Doctor of Philosophy.

Signed: _____

Thomas Hanson, Ph.D.
Member of dissertation committee

I certify that I have read this dissertation and that in my opinion it meets the academic and professional standard required by the University as a dissertation for the degree of Doctor of Philosophy.

Signed: _____

Christopher Main, Ph.D.
Member of dissertation committee

I certify that I have read this dissertation and that in my opinion it meets the academic and professional standard required by the University as a dissertation for the degree of Doctor of Philosophy.

Signed: _____

Andrew Wozniak, Ph.D.
Member of dissertation committee

ACKNOWLEDGMENTS

I would like to express my deepest gratitude for everyone I have met along this journey. While this dissertation is a product of direct help and support, there are plenty of people who supplied moral support through various ways and for that I am grateful.

I would like to thank my previous advisors Dr. Melanie Langford and Dr. Christy Wolovich for nurturing a young scientific mind which led me to working with my current advisor, Dr. Jennifer Biddle. Jen, I will always be forever appreciative for your continued support and gentle parenting. Dr. Biddle, you have been a great force and positive influence not only on my scientific journey but my life as well.

Further thanks for every intern I worked with in the lab and every Biddle Lab member past and present. Thank you to other early and senior career scientists for collaboration throughout every completed and forgotten experiment.

Thank you to Delaware SeaGrant and National Science Foundation for funding a various portion of this work. Thank you to the University of Delaware and the Nancy Fosters Fellowship for funding my graduate degree.

TABLE OF CONTENTS

LIST OF TABLES

LIST OF FIGURES

ABSTRACT

Microbes are ubiquitous across all environments on the planet, accounting for approximately 15% of the planet's total biomass. Technological advancements in microbiology have revolutionized our ability to understand microbial diversity and function. Where traditional culture-based techniques once limited our view to a small fraction of microbial life, modern tools such as metagenomics, high-throughput sequencing, and environmental DNA (eDNA) analysis now provide a comprehensive view of entire microbial communities. The work presented in this thesis integrates microbiological approaches to explore water quality, sediment biogeochemistry, and invertebrate biodiversity in Delaware's estuarine ecosystems. By applying advanced molecular techniques to microbial communities in water, sediment, and biological samples, this research provides a multidimensional view of ecosystem health and function. The findings contribute to the broader field of environmental microbiology and offer practical insights for managing water resources, protecting biodiversity, and understanding the microbial influence of ecological change.

INTRODUCTION

Microbes are ubiquitous across all environments on the planet, accounting for approximately 15% of the planet's total biomass (Bar-On, Phillips & Milo, 2018). These microscopic organisms are foundational to the structure and function of ecosystems, serving as primary producers, decomposers, and symbionts (Allison & Martiny, 2008; Azam et al., 1983; Delgado-Baquerizo et al., 2016). They play key roles in the degradation of organic matter, nutrient regeneration, and the stabilization of ecological communities (Allison & Martiny, 2008; Azam et al., 1983; Delgado-Baquerizo et al., 2016). Their roles span geological timescales, linking past environmental conditions with today's functioning ecosystems.

Technological advancements in microbiology have revolutionized our ability to understand microbial diversity and function (Koonin et al., 2021). Where traditional culture-based techniques once limited our view to a small fraction of microbial life, modern tools such as metagenomics and high-throughput sequencing analysis now provide a comprehensive view of entire microbial communities including the uncultivated majority of microbes (Riesenfeld et al., 2004; Shakya et al., 2019; Tringe et al., 2005). These advanced molecular and genomic tools have shifted our view on the role of microbes from passive indicators to active participants in ecosystem processes. For example, microbes mediate critical transformations such as carbon cycling, pollutant degradation, and nutrient sequestration (Schimel & Schaeffer, 2012; Dubey et al., 2019;

Rafeeq et al., 2022). These processes can directly affect water quality, greenhouse gas emissions, and long-term ecological stability (Galloway et al., 2008; Sala et al., 2000; Zhang et al., 2024). As such, microbial data are increasingly used to inform ecosystem models, environmental policies, and restoration strategies.

One of the most direct and impactful roles of microbes is in supporting the health of multicellular organisms and ecosystems (Yatsunenko et al., 2012). The gut microbiome, for instance, is critical to digestion, immune function, and disease resistance across a wide range of animals, including humans (Belkaid & Hand, 2014; Perler, Friedman & Wu, 2023; Yatsunenko et al., 2012). These gut microbiomes intersect with broader ecosystems and can be observed entering and potentially contaminating environments. Microbial source tracking (MST) methods utilize specific genetic markers or whole-community signatures to trace fecal contamination back to humans, livestock, or wildlife (Shanks & Korajkic, 2020). These techniques are especially important for managing water quality in areas, where identifying and mitigating pollution sources can reduce health risks and inform land-use planning (Scott et al., 2002). Thus, shifts in microbial populations can signal environmental disturbances or contamination, making them valuable bioindicators of ecosystem health (Astudillo-García et al., 2019; Astudillo-García et al., 2019; Astudillo-García et al., 2019).

In aquatic environments, especially estuarine and coastal systems, microbes function as both indicators and drivers of ecosystem resilience (Garrison, 2021). The microbial composition of surface waters, sediments, and host organisms reflects ongoing environmental change, land-use practices, and contamination sources (Wagg, Widmer, & Van Der Heijden, 2018). In sediment ecosystems, microbial activity governs organic matter decomposition and long-term carbon burial, processes strongly influenced by redox conditions, temperature, and nutrient availability (Reimers et al., 2013; Cook et al., 2007). Furthermore, sedimentary microbes provide insight into carbon storage dynamics and the environmental conditions that govern organic matter burial (Jorgensen, 2011). Microbial metabolic pathways such as sulfate reduction, methanogenesis, and anaerobic respiration can directly influence how carbon is stabilized or released from sediments (Berton, 2014; Dang et al., 2020; Widdel & Bak, 1992). Redox potential, temperature, and nutrient gradients interact with microbial activity to regulate long-term carbon sequestration, which is especially important in coastal environments that serve as critical carbon sinks (Kallmeyer et al., 2012; Middelburg, 2019).

Marine sediments have been widely studied via metagenomics and other cultivation-independent techniques, which have revolutionized our understanding of microbial diversity and functional potential in these complex ecosystems (Gilbert & Dupont, 2011; Mason et al., 2014). These high-throughput approaches have provided high resolution snapshots of taxonomic microbial communities and their metabolic potential (Biddle et al., 2008; Mason et al., 2014). However, ample amount of data produced through these -omic approaches also raises critical questions about the ecological relevance of

observations made at a single time point, often collected with a single sample. Temporal variability, redox gradients, and physicochemical fluxes may influence microbial community structure and activity in ways that are difficult to capture through static, sequence-based methods alone (Findlay & Watling, 1998; Frindte et al., 2016, Vignesh et al., 2014). As such, there is a growing need to reintroduce culture-dependent techniques into modern studies. These methods enable direct observation of microbial physiology, interactions, and responses to environmental change, offering a powerful evidence-based framework to test and refine hypotheses generated through cultivation-independent studies. Collectively, the work presented in this thesis integrates microbiological approaches to explore water quality, sediment biogeochemistry, and invertebrate gut microbiomes in Delaware's coastal ecosystems. By applying advanced molecular techniques to microbial communities in water, sediment, and biological samples, and also incorporating cultivation-based microcosm enrichments, this research provides a multidimensional view of coastal microbial systems. The findings contribute to the broader field of environmental microbiology and offer practical insights for managing water resources, understanding biodiversity, and interpreting environmental data on microbial physiology.

REFERENCES

1. Bar-On, Y. M., Phillips, R., & Milo, R. (2018). The biomass distribution on Earth. *Proceedings of the National Academy of Sciences*, *115*(25), 6506-6511.
2. Allison, S. D., & Martiny, J. B. H. (2008). *Resistance, resilience, and redundancy in microbial communities*. Proceedings of the National Academy of Sciences, 105(Supplement 1), 11512–11519. [https://doi.org/10.1073/pnas.0801925105]
3. Azam, F., Fenchel, T., Field, J. G., Gray, J. S., Meyer-Reil, L. A., & Thingstad, F. (1983). *The ecological role of water-column microbes in the sea*. Marine Ecology Progress Series, 10, 257–263. https://doi.org/10.3354/meps010257
4. Delgado-Baquerizo, M., Maestre, F. T., Reich, P. B., Jeffries, T. C., Gaitan, J. J., Encinar, D., ... & Singh, B. K. (2016). *Microbial diversity drives multifunctionality in terrestrial ecosystems*. Nature Communications, 7, 10541. [https://doi.org/10.1038/ncomms10541]
5. Falkowski, P. G., Fenchel, T., & Delong, E. F. (2008). *The microbial engines that drive Earth's biogeochemical cycles*. Science, 320(5879), 1034–1039. https://doi.org/10.1126/science.1153213

6. Schimel, J. P., & Schaeffer, S. M. (2012). Microbial control over carbon cycling in soil. *Frontiers in microbiology*, *3*, 348.
7. Galloway, J. N., Dentener, F. J., Capone, D. G., Boyer, E. W., Howarth, R. W., Seitzinger, S. P., & Colbert, D. M. (2008). *Transformation of the nitrogen cycle: Recent trends, questions, and potential solutions*. Science, 320(5878), 889-892. https://doi.org/10.1126/science.1136675
8. Dubey, A., Malla, M. A., Khan, F., Chowdhary, K., Yadav, S., Kumar, A., ... & Khan, M. L. (2019). Soil microbiome: a key player for conservation of soil health under changing climate. *Biodiversity and Conservation*, *28*, 2405-2429.
9. Koonin, E. V., Makarova, K. S., & Wolf, Y. I. (2021). Evolution of microbial genomics: conceptual shifts over a quarter century. *Trends in microbiology*, *29*(7), 582-592.
10. Rafeeq, H., Qamar, S. A., Nguyen, T. A., Bilal, M., & Iqbal, H. M. (2022). Microbial degradation of environmental pollutants. In *Biodegradation and biodeterioration at the nanoscale* (pp. 509-528). Elsevier.
11. Riesenfeld, C. S., Schloss, P. D., & Handelsman, J. (2004). Metagenomics: genomic analysis of microbial communities. *Annu. Rev. Genet.*, *38*(1), 525-552.
12. Sala, O. E., Stuart Chapin, F. I. I. I., Armesto, J. J., Berlow, E., Bloomfield, J., Dirzo, R., ... & Wall, D. H. (2000). Global biodiversity scenarios for the year 2100. *science*, *287*(5459), 1770-1774.

13. Shakya, M., Ahmed, S. A., Davenport, K. W., Flynn, M. C., Lo, C. C., & Chain, P. S. (2020). Standardized phylogenetic and molecular evolutionary analysis applied to species across the microbial tree of life. *Scientific reports*, *10*(1), 1723.
14. Tringe, S. G., Von Mering, C., Kobayashi, A., Salamov, A. A., Chen, K., Chang, H. W., ... & Rubin, E. M. (2005). Comparative metagenomics of microbial communities. *Science*, *308*(5721), 554-557.
15. Zhang, Z., Zhang, Q., Chen, B., Yu, Y., Wang, T., Xu, N., ... & Qian, H. (2024). Global biogeography of microbes driving ocean ecological status under climate change. *Nature Communications*, *15*(1), 4657.
16. Belkaid, Y., & Hand, T. W. (2014). *Role of the microbiota in immunity and inflammation*. Cell, 157(1), 121-141. https://doi.org/10.1016/j.cell.2014.03.011
17. Garrison, C. E. (2021). *Microbial Community Response to Environmental Change During the Anthropocene*. East Carolina University.
18. Yi, J., Lo, L. S. H., & Cheng, J. (2020). Dynamics of microbial community structure and ecological functions in estuarine intertidal sediments. *Frontiers in Marine Science*, *7*, 585970.
19. Astudillo-García, C., Hermans, S. M., Stevenson, B., Buckley, H. L., & Lear, G. (2019). Microbial assemblages and bioindicators as proxies for ecosystem health status: potential and limitations. *Applied microbiology and biotechnology*, *103*, 6407-6421.

20. Scott, T. M., Rose, J. B., Jenkins, T. M., Farrah, S. R., & Lukasik, J. (2002). Microbial source tracking: current methodology and future directions. *Applied and environmental microbiology*, *68*(12), 5796-5803.
21. Dang, H. (2020). Grand challenges in microbe-driven marine carbon cycling research. *Frontiers in Microbiology*, *11*, 1039.
22. Perler, B. K., Friedman, E. S., & Wu, G. D. (2023). The role of the gut microbiota in the relationship between diet and human health. *Annual review of physiology*, *85*(1), 449-468.
23. Shanks, O. C., & Korajkic, A. (2020). Microbial source tracking: characterization of human fecal pollution in environmental waters with HF183 quantitative real-time PCR. In *Microbial forensics* (pp. 71-87). Academic Press.
24. Wagg, C., Dudenhöffer, J. H., Widmer, F., & Van Der Heijden, M. G. (2018). Linking diversity, synchrony and stability in soil microbial communities. *Functional ecology*, *32*(5), 1280-1292.
25. Yatsunenko, T., Rey, F. E., Manary, M. J., Trehan, I., Dominguez-Bello, M. G., Contreras, M., ... & Gordon, J. I. (2012). Human gut microbiome viewed across age and geography. *nature*, *486*(7402), 222-227.
26. Berton, R. (2014). Microbial pathways of carbon degradation and stabilization in marine sediments. Geobiology, 12(6), 545-560. https://doi.org/10.1111/gbi.12101
27. Jørgensen, B. B. (2011). Sulfate reduction and other anaerobic microbial processes in marine sediments. In Ecology of Marine Sediments (pp. 116-131). Wiley-Blackwell. https://doi.org/10.1002/9781444316568.ch7

28. Kallmeyer, J., et al. (2012). Global distribution of microbial abundance and biomass in subseafloor sediments. Proceedings of the National Academy of Sciences, 109(40), 16213-16216. https://doi.org/10.1073/pnas.1203849109

29. Middelburg, J. J. (2019). The role of microbes in the burial and cycling of carbon in estuaries and coastal sediments. Geophysical Research Letters, 46(16), 9394–9403. https://doi.org/10.1029/2019GL083700

30. Widdel, F., & Bak, F. (1992). Anaerobic degradation of fatty acids by sulphate-reducing bacteria. FEMS Microbiology Reviews, 103(1–2), 199-221. https://doi.org/10.1111/j.1574-6976.1992.tb05560.x

31. Gilbert, J. A., & Dupont, C. L. (2011). Microbial metagenomics: beyond the genome. *Annual review of marine science*, *3*(1), 347-371.

32. Mason, O. U., Scott, N. M., Gonzalez, A., Robbins-Pianka, A., Bælum, J., Kimbrel, J., ... & Jansson, J. K. (2014). Metagenomics reveals sediment microbial community response to Deepwater Horizon oil spill. *The ISME journal*, *8*(7), 1464-1475.

33. Findlay, R. H., & Watling, L. (1998). Seasonal variation in the structure of a marine benthic microbial community. *Microbial ecology*, *36*, 23-30.

34. Frindte, K., Allgaier, M., Grossart, H. P., & Eckert, W. (2016). Redox stability regulates community structure of active microbes at the sediment–water interface. *Environmental Microbiology Reports*, *8*(5), 798-804.

35. Vignesh, S., Dahms, H. U., Emmanuel, K. V., Gokul, M. S., Muthukumar, K., Kim, B. R., & James, R. A. (2014). Physicochemical parameters aid microbial

community? A case study from marine recreational beaches, Southern India. *Environmental monitoring and assessment*, *186*, 1875-1887.

36. Reimers, C. E., Alleau, Y., Bauer, J. E., Delaney, J., Girguis, P. R., Schrader, P. S., & Stecher III, H. A. (2013). Redox effects on the microbial degradation of refractory organic matter in marine sediments. *Geochimica et Cosmochimica Acta*, *121*, 582-598.
37. Cook, P. L., Veuger, B., Böer, S., & Middelburg, J. J. (2007). Effect of nutrient availability on carbon and nitrogen incorporation and flows through benthic algae and bacteria in near-shore sandy sediment. *Aquatic Microbial Ecology*, *49*(2), 165-180.
38. Biddle, J. F., Fitz-Gibbon, S., Schuster, S. C., Brenchley, J. E., & House, C. H. (2008). Metagenomic signatures of the Peru Margin subseafloor biosphere show a genetically distinct environment. *Proceedings of the National Academy of Sciences*, *105*(30), 10583-10588.

IDENTIFYING POTENTIAL INTRODUCED SOURCES OF POLLUTION IN DELAWARE WATERSHEDS

Introduction

Recent reports state that 50% of the United States (US) tested waterways are still classified as impaired, nearly 50 years after the Environmental Protection Agency's (EPA) Clean Water Act (CWA) was implemented (Environmental Integrity Report, 2022). Impaired water bodies present higher risks that surpass EPA standards supporting wildlife, recreation, or human consumption (Davis et al, 2022). Among the US waterways, Delaware leads with 97% of its rivers and streams and 100% of its estuaries classified as impaired according to the 2022 Environmental Integrity Report (Environmental Integrity Report, 2022). Delaware's Department of Natural Resources and Environmental Control (DNREC) has monitored these waterways according to water quality standards outlined in the CWA. The most common method used for determining biological pollution is the total maximum daily load (TMDL) which quantifies waterborne pathogens (U.S. EPA, 2019; Faraji & Afshar, 2021). The TMDL for biological pollution is based on culturable fecal coliforms from the fecal indicator bacteria (FIB) genus *Enterococcus*. During monitoring, Delaware establishes freshwater and marine water criteria for Primary Contact Recreation (swimming; fresh - 185; marine - 925 colonies of FIB per 100 mL water) and Secondary Contact Recreation (boating; fresh - 104; marine - 520 colonies of FIB per 100 mL water) warnings, which limits the

use of recreational waters (DNREC, 2014). In the past 20 years, there have been over 138 recreational advisories or beach closures in Delaware due to high bacterial loads (DNREC, 2014).

Quantifying biological pollutants (i.e. FIB) without identification of the source only allows watershed stakeholders limited control for mitigating potential biological pollution (Hyer & Mayer, 2004). Pollutant sources can either be of point or nonpoint origin where point sources are easily identifiable and nonpoint sources are diffused and not easily identifiable (Xepapadeas, 2011). Tests, such as microbial source tracking (MST), were developed to better distinguish nonpoint sources for mitigation practices (Stoeckel & Harwood, 2007). Traditional MST utilizes local genomic reference libraries, high-throughput sequences, and Bayesian statistical models to pair most likely host-specific genetic markers of potential fecal origins in an environmental sample (Stoeckel & Harwood, 2007; Harwood et al., 2013). MST has made significant advancement over the last two decades in accurately identifying point sources of human microbial pollution; however, there has been little advancement in accurately identifying nonpoint-source microbial pollution from wildlife and agricultural livestock (Harwood et al., 2013). Traditional uses of MST are dependent on small and limited reference libraries, usually containing <10 different fecal hosts, consisting of specific human, agricultural and domesticated animal microbial markers, which may limit their accuracy (Hyer & Mayer, 2004, Shrestha et al. 2020).

Recent MST studies attempt more explicit testing of individual microbial markers from host-associated (i.e., human, dog, cattle and shorebird) FIB to trace fecal pollution; however, the use of such specific genes excludes other domestic or wild sources. MST results based on constrained host identifiers can also be affected by environmental factors such as precipitation, temperature, and sedimentation (Shrestha et al., 2020; Reitz et al., 2021). On Chicago lakeshores, MST via specific-gene quantitative PCR determined genetic biomarkers for dog and agricultural livestock increased after heavy precipitation events, using five source markers from three different hosts (Shrestha et al., 2020). Increasing host identifiers by using whole microbial community signatures, and not just specific genes, in the initial MST analysis, or community-based MST, may improve accurate identification of host fecal pollution beyond environmental effects in watersheds. For example, in a Lake Superior estuary, wastewater treatment plants, and not geese or other wildlife were determined to be the main sources of contamination during community-based MST, using 11 fecal hosts (Brown et al., 2017). Geese and gulls were found to be a minor source component in this study, and restricted geographically, showing that native wildlife and human development have the potential to alter the microbial structure in waterways by water-use and proximity to the watershed, showing the power of total community analysis in source tracking (Brown et al., 2017). Improved methods that use machine learning to do unsupervised source selection and enable sparse identification of source environments means that now large reference source libraries are better able to be used during community-based MST (An et al., 2022).

Delaware is home to major watersheds that drain water from areas of mixed land-use and many are influenced through tidal interactions with the Delaware Bay. A source tracking study, using 9 fecal hosts, (Main et al. 2021) done in Love Creek, Delaware used whole microbial community signatures in the SourceTracker2 software (Knights et al., 2011) to determine that many of the areas tested in the watershed were impaired from unknown sources; however, this study did observe an increase in domestic (cat and dog) sources throughout the summer months which coincides with the higher human population of the tourist season. This initial Love Creek study concluded that site-specific variability of FIB may be attributed to environmental factors (e.g., salinity, seasonality, temperature, tides) and/or host presence near the sampled locations in the Delaware watershed (Main et al., 2021).

We expanded on this previous study with the goal of analyzing waterways over an extended timeframe with a more complete reference library, including domestic and wild animals, using a recently improved microbial source tracking software Source Tracking with Environment SeLection (STENSL) (An et al., 2022). We aimed to expand the reference library for source tracking to include a robust sampling of potential sources, including 20 potential fecal hosts, and performed microbial source tracking with waters of the Broadkill, Murderkill, and Love Creek watersheds of Delaware. Of the three watersheds, Love Creek is a less populated watershed, therefore; we expect to see less human related pollution and more influence from animals. Broadkill is surrounded by nature reserves, rural lands with agricultural activity, and has a higher human population than Love Creek. We expect Broadkill to display a larger influence by human-related

sources and a range of animals and an even higher influence of humans in the Murderkill, which has the highest human population of the 3 watersheds. The reference library created for this work expands the potential human, domestic, and wild fecal sources, allowing for a more accurate identification of potential fecal origins to water samples. Our observations reveal that wild and domestic animals are not major contributors to microbial pollution in Delaware. The most significant source determined across the samples was from human origin. The results of this study, along with the generated large reference libraries, can be broadly relevant to identifying fecal pollution origin within mid-Atlantic waterways as well as elsewhere.

Methods

Sample Collection & Processing

Surface water samples were collected bi-monthly throughout the Broadkill (n = 118) and Murderkill (n = 87) watersheds from January 2020 to November 2021 by DNREC and monthly from the Love Creek (n = 39) watershed in summer 2021 using 2-Liter bottles (Figure 1; Table S1, S2). Locations were chosen based on standard observation sites for state water sampling. Fecal material was collected from seventeen genera of domestic and native animals, influent and effluent wastewater treatment and influent community septic system throughout southern Delaware and stored at -80°C (Table 1; Table S2). Fecal samples consisted of fresh and aged samples collected throughout 2020 and 2021, species origin was determined by visual inspection prior to

collection. Domestic fecal samples (cat, cattle, chicken, dog, goat, horse, pig, rabbit, and sheep) were collected fresh while the age of wild-collected samples is unknown, all samples were visually identified when the animal was not present. Sediment samples were collected from all 3 watersheds in summer 2021 (n = 14; sediment) using modified 5mL syringes to collect the top 5 cm of sediment. Influent wastewater samples (n= 20; wastewater) were collected by Delaware Department of Health and Human services, Division of Public Health, as part of their influent wastewater monitoring program for COVID from 12 wastewater treatment plants across the state. Samples were collected from four plants in New Castle County, one in Kent County, and seven in Sussex County. These samples were pasteurized in liquid prior to the hand-off for research and filtering for DNA extraction. DNREC provided effluent wastewater samples (n= 2; wastewater) from the Kent County Wastewater Treatment Plant and influent septic system samples (n= 6; septic) from a community septic system at Seaford Mobile Garden Homes.

Sediment and fecal samples were homogenized with 20 mL of 1X Phosphate buffered saline (PBS) (Fisher Scientific, Waltham MA) to create a slurry to ensure microbial homogeneity across individual samples. All liquid samples were vigorously shaken prior to being filtered on mixed cellulose esters membrane 0.22 um filters and stored at -80°C. DNA was extracted from all filter, fecal and control samples using the Qiagen DNeasy PowerSoil Pro kit (Germantown, MD). Controls for extraction were run as PBS for fecal samples and filtered ultrapure water for the water samples. Control samples were sent for sequencing, regardless of if DNA was measured. Extracted DNA was sent to the UCONN MARS facility for amplicon sequencing of the 16S rRNA gene

targeting the V4 region (primers 515F and 806R) using the Illumina MiSeq paired-end sequencing platform via the v2 2x250 base pair kit (Illumina) following their standard protocol (Parada et al., 2016).

Raw forward and reverse sequences were paired, and quality checked (QC) but quality reads were low quality for reverse sequences; therefore, the forward sequences that passed QC were further processed using the 16S rRNA gene analysis pipeline implemented in MOTHUR version 1.46.1 (Schloss et al., 2009). Forward sequences were quality filtered using MOTHUR, yielding amplicons ranging in sizes of 130-200 bp in lengths, where ambiguous nucleotides and homopolymer stretches were removed. We opted against the use of amplicon sequence variants (ASV) considering the amount of available computation and created operational taxonomic units (OTU). OTUs were created with a 3% dissimilarity and were aligned and classified against the Silva SSU database, version 138 in MOTHUR version 1.46.1 (Gurevich et al., 2013). Prior to further downstream analysis, nontarget OTUs, i.e. chloroplast and mitochondria, and taxa <1% were removed from representative sequences. Information of sequenced controls can be found in Table 2.9 where controls averaged <452 amplicon sequences, whereas fecal and water samples returned over 35,000 sequences on average.

Diversity analysis of all sources was carried out using the PRIMER 7 statistical package for community ecology (Clarke & Gorley, 2006). Order level classified OTUs were assigned a representative for beta diversity analysis among samples. Bray-Curtis dissimilarity matrices were used for non-metric dimensional scaling (NMDS) to visualize

beta diversity of source and sink OTUs. An OTU table was created with representative sequences for use in STENSL by default parameters established in STENSLE.R code (An et al., 2022).

Additional data considered

We combine our analyses with those performed by the Delaware Department of Natural Resources and Environmental Control (DNREC) and retrieved via the Delaware Open Data portal (data.delaware.gov). These include Enterococcus counts using Enterolert (ASTM Method D6503-99; IDEXX systems, Westbrook, ME), taken at the same time and locations as the water samples in our study, and numbers of septic tank permits per watershed.

Data accessibility statement

All sequences have been deposited in the National Center for Biotechnology Information (NCBI) database under BioProject PRJNA996235. A limited source database has been previously described in a companion paper (Bowen et al., 2024).

Table 2.1. Fecal sources used to build reference library

Source	Environment	Diet	Samples
Cat	Domestic	Carnivore	6
Cattle	Domestic	Herbivore	9
Chicken	Domestic	Omnivore	10
Deer	Domestic	Herbivore	11
Dog	Domestic	Omnivore	7
Duck	Wild	Omnivore	5
Fox	Wild	Omnivore	6
Goat	Wild	Herbivore	9
Goose	Wild	Herbivore	10
Horse	Domestic	Herbivore	3
Otter	Wild	Omnivore	4
Pig	Domestic	Omnivore	10
Rabbit	Domestic	Herbivore	5
Raccoon	Wild	Omnivore	10
Septic	Human	n/a	6
Sediment	n/a	n/a	14
Sheep	Domestic	Herbivore	10
Squirrel	Wild	Omnivore	3
Turkey	Wild	Omnivore	2
Wastewater Treatment	Human	n/a	22

Figure 2.1 Map of sampling sites across Murderkill (A), Broadkill (B) and Love Creek (C) watersheds. Exact geographical locations of sampling site as contained in Table 2.2.

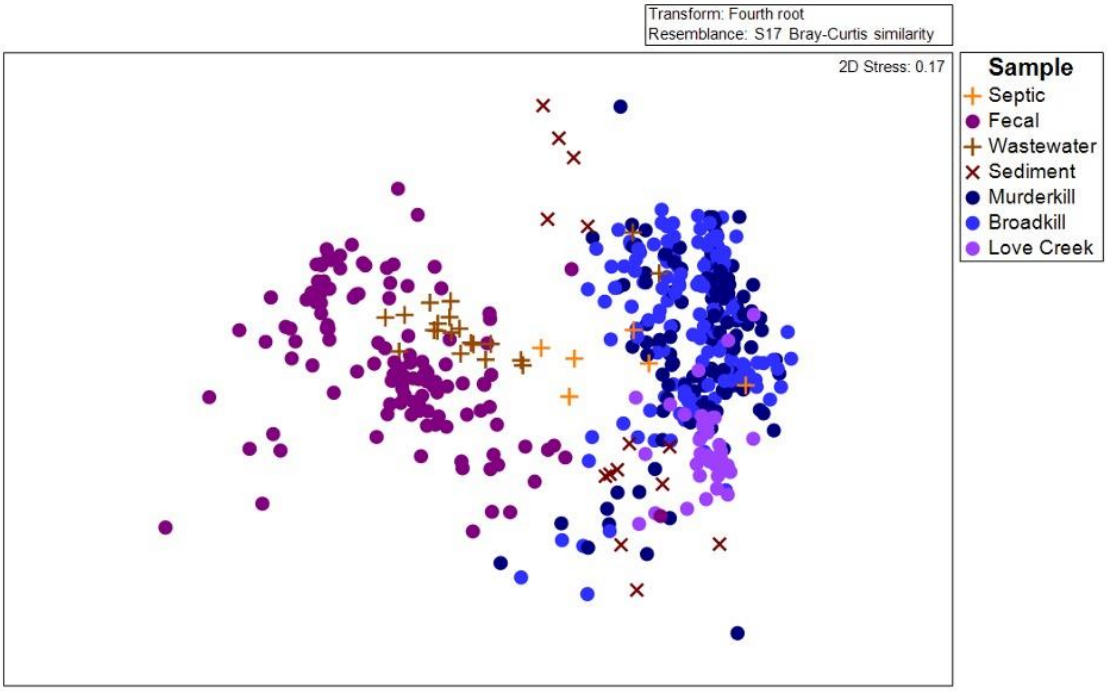

Figure 2.2 Non-metric dimensional scaling (NMDS) of source (fecal, septic, sediment, wastewater) and sink (Murderkill, Broadkill and Love Creek waters) samples using Bray-Curtis similarity matrix transformed to the fourth root.

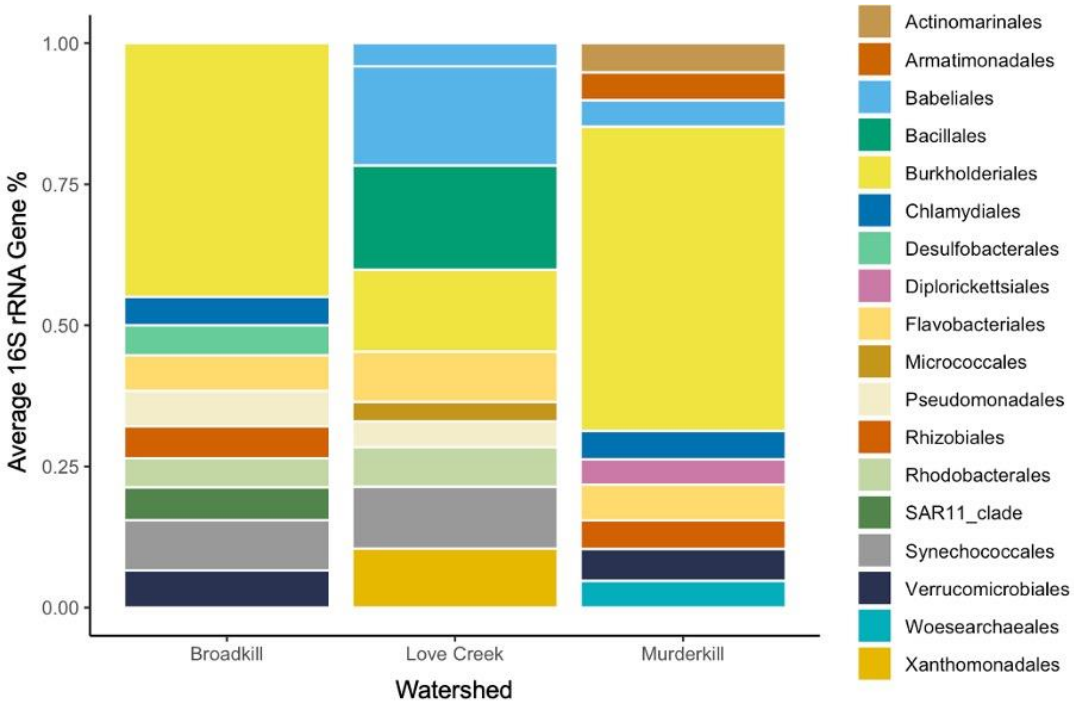

Figure 2.3 Relative abundance of representative microbiomes of watersheds as determined by 16S rRNA gene amplicon sequencing. The top 10 microbial Orders across watersheds are shown.

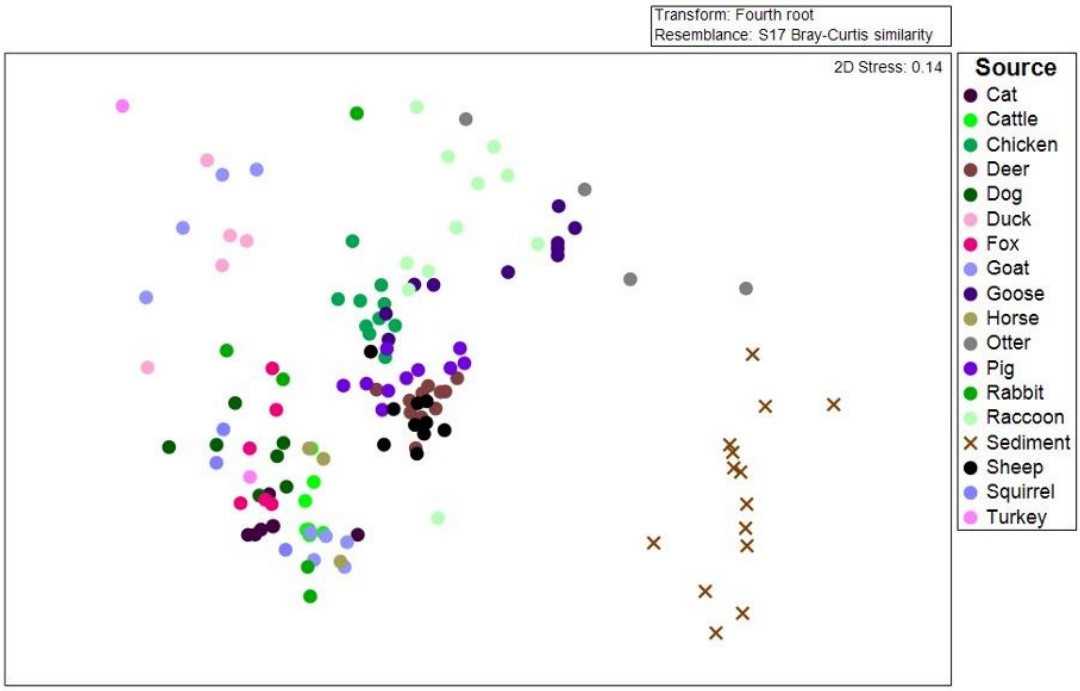

Figure 2.4 Non-metric dimensional scaling (NMDS) of fecal and sediment sources using Bray-Curtis similarity matrix transformed to the fourth root. Human sources (Figure 2) are not shown so that fecal sources can be more easily seen.

Results

We created a robust library of potential sources for fecal material and bacterial pollution from a geographically relevant area in Delaware. A total of 121 fecal samples, 14 sediment samples and 30 human-related samples (septic and wastewater) were collected and processed as source samples (Table 2.2). We also collected and processed 258 water samples across 3 watershed systems across 2 years to serve as sink samples (Table 2.4). The microbial signature of the sinks are distinct when compared to fecal and wastewater source microbial signatures, displaying little overlap. Non-metric dimensional scaling of all samples revealed that septic microbial signatures are nestled between

fecal/wastewater samples and watershed samples, with 3 septic samples are nestled with watershed microbial signatures (Figure 2.2). Microbial signatures of sediment samples group more closely with watershed samples than fecal sources. Taxonomic analysis of sink samples revealed OTU representatives belonging to the Order Burkholderiales were present and abundant across all three watersheds (Murderkill 29%, Broadkill 23% and Love Creek 15%) potentially causing a convergence of microbial signatures across watersheds with some sediment and septic samples (Figure 2.3; Table 2.5). Although Order Burkholderiales are abundant in all three watersheds, they all retain unique community structures through Orders such as Flavobacteriales (3%) and Verrucomicrobiales (3%) in the Murderkill watershed, Orders Synechococcales (5%) and Verrucomicrobiales (3%) in the Broadkill watershed, and Orders Bacillales (14%) and Babeliales (11%) in the Love Creek watershed (Figure 2.3; Table 2.5).

All fecal, sediment, and wastewater sources contained one or more fecal representative such as Lachnospirales, Bacteroidales, and Lactobacillaes (Table 2.5). Order Lactobacillales was the most prominent in Chicken (57%), Duck (38%), Goose (18%), Pig (25%), Racoon (9%), and Turkey (59%) sources. Order Lachnospirales was most prominent in Deer (32%), Dog (18%), Fox (18%), Horse (28%), and Squirrel (44%) sources (Table 2.4). Order Oscillospirales was most prominent in Bull (23%), Goat (26%), Rabbit (16%), and Sheep (17%) sources (Table 2.5). Order Burkholderials was prominent in wastewater treatment samples (38%) and human samples (43%); whereas sediment samples exhibit diversity in common gut and environmental representatives

across watersheds (i.e. Orders Clostridiales, Anaerolineales, Desulfobacterales, and Campylobacterales) (Table 2.5). The Order Coriobacteriales was only prominent in Cat (30%) sources whereas Order Clostridiales was only prominent in Otter (22%) sources (Table 2.5). Though some prominent microbial taxa are shared among sources, the microbial signatures of fecal sources are noticeably different than sediment sources as shown by non-metric dimensional scaling (Figure 2.4). Although wild fecal sources have unknown freshness of collection, deer, fox, and squirrel microbial signatures group closely to their host origin whereas duck, goose, otter, raccoon, and turkey microbial signatures are not grouped closely (Figure 2.4). In contrast, all samples used for domestic sources group closely by host origin with the exception of goat (Figure 2.4).

STENSL analyses using source microbiomes as the reference library displayed varied source inputs among the three watersheds tested (Figure 2.5). Human-related sources including septic sources and treated facility sewage runoff were consistently identified across all three watersheds in the Broadkill and Murderkill watersheds (Figure 2.5B,C). All watersheds presented unknown assigned sources with Love Creek having, on average, >60% of samples assigned to unknown sources followed by Broadkill with >50% on average, and Murderkill with >50% on average (Figure 2.5). Murderkill samples presented 20% human-related assigned sources on average; whereas Broadkill presented 20% wastewater treatment facility assigned sources on average, as well as varied source input from wildlife assigned sources (Figure 2.5A,B).

STENSL Assigned Sources for Murderkill Watershed

Murderkill River displayed consistent source contributions from human and treatment facility assigned sources. On average, approximately ~20% of STENSL assigned sources belonged to human and/or treatment facility sources. Individual animal sources here were inconsistent where they often contributed to <1% of the assigned sources identified in a sample. STENSL identified wildlife sources including chicken, deer, fox, goose, otter, rabbit, and raccoon <3% across all Murderkill samples. Sediment assigned sources were consistently found at location Murderkill 6 and account for approximately 20% of the assigned sources at this sampling location (Figure 2.1; Figure 2.5A). One location-specific sampling event, in May 2020, showed sediment as the most prominent identifiable contaminating source. In general, after January 2021, there is a decrease in identifiable sources through November 2021. During this time period, the most often assigned sources are human-based signals of septic and wastewater (Figure 2.5A).

STENSL Assigned Sources for Broadkill Watershed

Broadkill displayed consistent source contributions from human and wastewater assigned sources with the addition of otter assigned sources (Figure 2.5B). On average, approximately ~20% of STENSL assigned sources belonged to human and/or treatment facility sources. STENSL identified wildlife sources including bull, goose, otter, rabbit, raccoon, squirrel, and turkey totaling, on average, <8% across all Broadkill samples. Animal assigned sources only occurred in specific times such as goose in July/September

2020 and November 2021 and rabbit in July/September 2020 (Figure 2.5B). Identifiable sources are extremely high in July and September 2020 and are very low in July and September 2021 (Figure 2.5B).

STENSL Assigned Sources for Love Creek Watershed

Love Creek was sampled monthly through from May to November 2020, which included major weather events in July and October (Figure 2.5C). After weather events in July and October, sediment assigned sources were even across samplings sites in Love Creek (Figure 2.5C). Smaller contributions to Love Creek assigned sources included otter and raccoon assigned sources. The human-associated contributions at Love Creek were seen only in the upriver samples at station 1, and not in any repeated or consistent manner, being very high in May 2021 and to a lesser extent in June, August and November 2021 (Figure 2.5B). Only in August 2021 does the human source extend to station 2, further downriver.

Microbial Source Tracking Overlapped with Traditional Enterococcus Counts

We compared the source prediction with the measured Enterococcus counts for the Broadkill and Murderkill watersheds (Figure 2.6). We see that the peaks of Enterococcus counts occur in summer months, repeatedly, but that the sources predicted during these peaks are not necessarily consistent. In both watersheds, the Enterococcus counts are high in September 2020, while the major source predicted is human-related.

However, in 2021, when Enterococcus peaks in July, the major source predicted is unknown. The Murderkill watershed exceeded primary contact recreation levels in 44 of the 87 samples, 12 of these samples exceeded even secondary contact recreation levels (Figure 2.5; Table 2.6). The Broadkill watershed exceeded primary contact recreation levels in 48 of the 118, 15 exceeded secondary levels (Figure 2.5; Table 2.6).

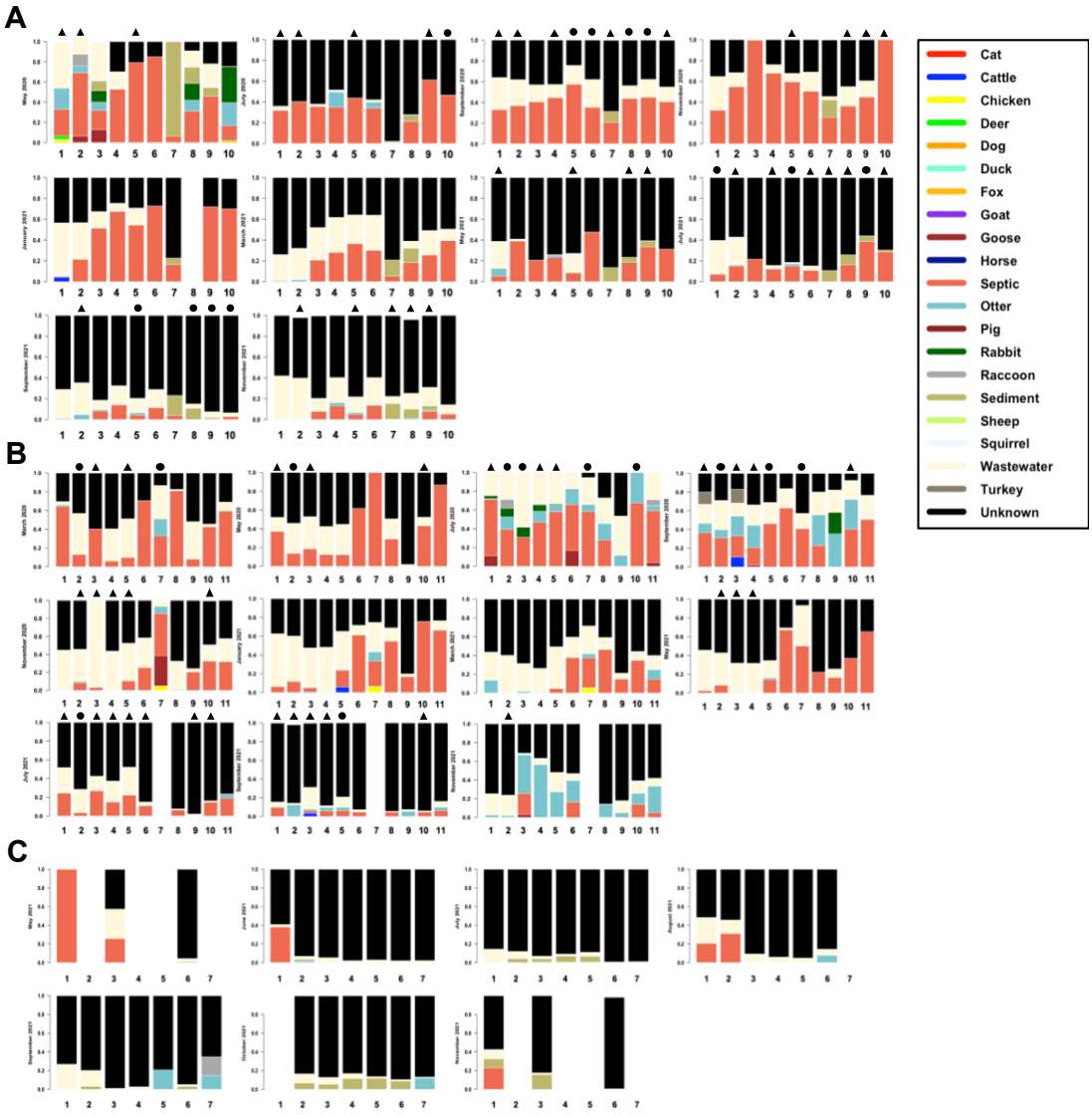

Figure 2.5 Stacked-bar plot of host-assigned sources estimated by STENSL in the Murderkill River n=87 (A), Broadkill River n= 118 (B) and Love Creek n=39 (C) watersheds. Station numbering reflects map locations shown in Figure 1, with the most inland sample as the lowest number and sample number increasing towards the coast. Samples from Murderkill and Broadkill watersheds that exceeded Primary Contact Recreation Levels are indicated by triangles and samples that exceeded Secondary Contact Recreation levels are indicated by circles. The following are in the legend but not displayed in the graph due to no signal: cat, dog, goat, horse, sheep and squirrel.

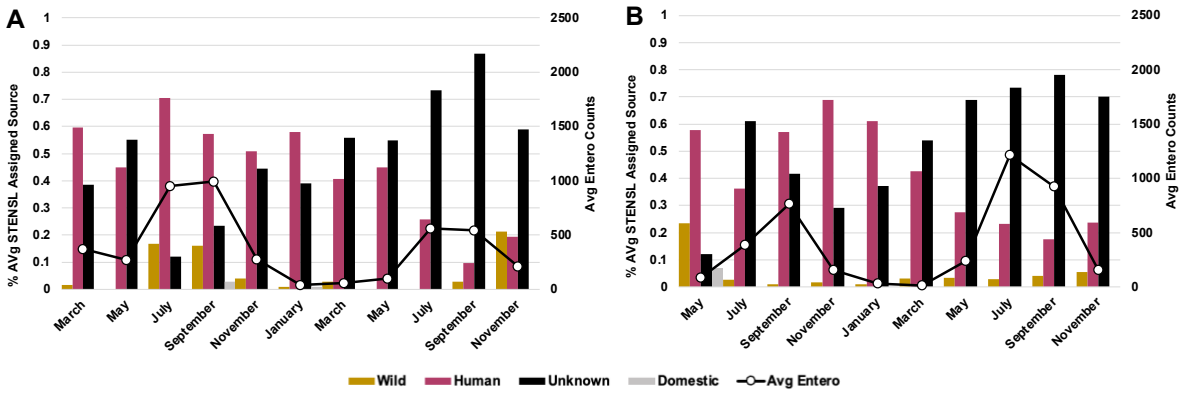

Figure 2.6 Average of STENSL assignments grouped by Wild, Domestic, Human, or Unknown origin, overlayed with average *Enterococcus* counts by month for Broadkill (A) and Murderkill (B) watersheds. Full data available in Table S6.

Discussion & Conclusion

We built a reference library of 158 samples for 17 native fauna, 3 types of human-related waste, and native sediment that served as potential sources and that allowed us to

use a holistic approach to examine microbial impairment in Delaware watersheds. We identified bacterial Orders commonly found in gut microbiomes known to serve as FIB, such as Lachnospirales, Bacteroidales, Clostridales, and Lactobacillaes, in our source sequences. Previous studies have suggested that feces compositional shifts over time could impact source tracking efforts (Devane et al. 2023), we consider that our community data is robust enough and better reflects a typical output to overland sources. Our reference library showed effectiveness in source-tracking and disagreed with previous studies performed in the Love Creek area, which used much smaller reference libraries. Our study shows that wild and domestic animals have a minor impact on waters, overshadowed by the contributions of humans or natural systems (sediment) alone and unknown sources.

We noted significant differences per watershed tested and hypothesize that these impacts are based on land use in and around the watersheds. The Murderkill watershed has 7811 permitted septic systems followed by Broadkill with 7182 and Love Creek with 2328 (DNREC, 2024). Therefore, it is not surprising that the Murderkill and Broadkill watersheds have approximately 20% assigned sources to human-related sources. The Broadkill and Murderkill watersheds are located in more densely populated regions of the state, which likely explains the stark difference in assigned sources compared to Love Creek. As a smaller, tidally driven waterbody, Love Creek consists of majority human-assigned sources that decreased as sampling locations approach the open bay whereas we observed the opposite from unknown-assigned sources. Our observation of fecal sources

in Love Creek aligned with prior studies stating that tidal cycles may have influence over identifiable fecal sources (Devane, et al., 2023). Although we were able to assign potential prominent fecal sources to samples from the Broadkill and Murderkill watersheds, the Love Creek watershed contained mostly unknown sources. In contrast to the previous study, we did not see an increase in domestic or wildlife sources (Main et al. 2019); however, we did observe a decrease in human-assigned sources as sampling went further downstream toward the mouth of the bay where freshwater and marine water mix potentially diluting human-assigned sources.

Similar microbial taxa were seen across sources and sinks which agrees with other studies indicating that watersheds receive a variety of microbial input from varied sources (Brown et al., 2017). Specific taxa may drive these similarities. For example, Murderkill and Love Creek showed sediment-assigned sources and the microbial taxa that may drive this similarity are Bacteroidales, Burkholderiales, Rhizobiales, and Desulfobactales, as they were found in both the sediment and water samples. The order Bacteroidales is the only taxon listed that is usually linked to the human gut; whereas the order Desulfobacterales is a sulfate-reducer that is used in wastewater treatment facilities and found in sewage runoff (Ormerod et al., 2016; Biswas & Turner, 2012). Turkey was identified as a source in the Broadkill, potentially since the orders Bacteroidales, Corynebacteriales and Lachnospirales were identified in both turkey and water samples. There are many potential hosts contributing to the shared taxa between the water and animals, but the most common and abundant shared taxa is the order Burkholderiales.

Burkholderiales is a common environmental taxon found in the natural environment; however, in this study it is abundant across both human-related sources (influent septic waste and wastewater treatment outflow) and water samples. Burkholderiales consists of many genera that carry out important roles in nutrient cycling such as ammonia oxidation which have been adopted by companies that manage and treat sewage (Ruprecht et al., 2021; Fan et al., 2017). Many genera in this order are also found in human guts as pathogens and as members of the gut microbiome in many animals. This relationship of shared taxa among gut and environmental communities across sources and sinks help reinforce the expansion of the reference library size needed to use the whole microbial community to identify potential host origin. These 3 orders of bacteria are common members of many gut microbiomes, so we interpret our wildlife sources with caution. While it is possible that a few abundant taxa influenced our results from the STENSL software, the use of the whole microbial community in analyses should lessen such biases.

Enterococcus counts observed for the Broadkill watershed in 2020 were elevated in the summer where majority of STENSL assigned sources were of human origin, but as unknown sources increased in 2021 the observed Enterococcus counts decreased (Figure 2.6A). *Enterococcus* counts observed for the Murderkill watershed in 2020 were also elevated when the majority of STENSL assigned sources were of human origin, but as *Enterococcus* counts increased, we observed a decrease in human-assigned sources (Figure 2.6B). This suggests that the seasonal increase in *Enterococcus* has multiple

influencing features, of which the major feature is seasonal high temperatures. We also note that during the 2020 sampling event, the COVID pandemic created a lockdown where there was likely greater pressure on the household infrastructure within Delaware. This may be why the human influence on *Enterococcus* was better detected in 2020 and not 2021 (Figure 2.6). It is important to note that the influence of wild and domestic animal sources is not well correlated with any *Enterococcus* counts. Though we observed consistent human-related sources to be the main contributors to microbial structure in Delaware watersheds, there is still work to be done to fully explain the origin of this signal. Future work would include the use of coliform specific genetic markers incorporated with the use of 16S rRNA microbial community-based source tracking using the STENSL software to better track harmful contamination instead of potential contamination as suggested from our study.

In this study, we showed that we could use an expanded reference library consisting of whole microbial communities in STENSL software to identify potential fecal origins in Delaware watersheds. We present the most likely sources of microbial impairment in three Delaware watersheds as determined via community-based MST using amplicon sequencing of the 16S rRNA gene for whole microbial communities in brackish and freshwater samples. While the TMDL is the standard practice that utilizes culture-based measurements that track FIB explicitly, the incorporation of the whole microbial community in the reference library allowed us to better understand the actual impact sources can have on the microbial community and furthermore, water quality. We

also provided a 16S rRNA amplicon gene reference library that can be used in other microbial source tracking studies across the mid north-Atlantic United States. Our results suggest these methods can identify likely sources which can be used to better assess bacterial contamination using source tracking in future studies and management.

REFERENCES

An, U., Shenhav, L., Olson, C. A., Hsiao, E. Y., Halperin, E., & Sankararaman, S. (2022). STENSL: Microbial Source Tracking with ENvironment SeLection. *Msystems*, *7*(5), e00995-21.

Biswas, K., & Turner, S. J. (2012). Microbial community composition and dynamics of moving bed biofilm reactor systems treating municipal sewage. *Applied and environmental microbiology*, *78*(3), 855-864.

Bowen, M., Farag, I. F., Main, C. R., & Biddle, J. F. (2024). Reference library for microbial source tracking in the mid-Atlantic United States. *Microbiology Resource Announcements*, *13*(1), e00674-23.

Brown, C., Staley, C., Wang, P., Dalzell, B., Chun, C.L., Sadowsky, M.J. (2017). A high-throughput DNA-sequencing approach for determining sources of fecal bacteria in a Lake Superior estuary. *Environmental Science and Technology* 51(15), 8263-8271.

Clarke, K., & Gorley, R. (2006). Plymouth routines in multivariate ecological research. *Plymouth Marine Laboratory, Londres, Inglaterra*, *2*, 24-30.

Davis, L. J., Milligan, R., Stauber, C. E., Jelks, N. O., Casanova, L., & Ledford, S. H. (2022). Environmental injustice and *Escherichia coli* in urban streams: Potential for community-led response. *Wiley Interdisciplinary Reviews: Water*, 9(3), e1583. https://doi.org/10.1002/wat2.1583

Department of Natural Resources and Environmental Control (DNREC), D. of W. (2024). *Permitted septic systems: Delaware Open Data Portal*. data.delaware.gov. https://data.delaware.gov/Energy-and-Environment/Permitted-Septic-Systems/mv7j-tx3u/about_data

Department of Natural Resources and Environmental Control (DNREC), (2014). Surface Water

Quality Standards (2014). Retrieved from http://regulations.delaware.gov/AdminCode/title7/7000/7400/7401.pdf

Devane, M. L., Taylor, W., Dupont, P. Y., Armstrong, B., Weaver, L., & Gilpin, B. J. (2023).

Exploring the Bacterial Community in Aged Fecal Sources from Dairy Cows: Impacts on Fecal Source Tracking. Microorganisms, 11(5), 1161.

Environmental Integrity Report: The Clean Water Act at 50 (2022). The Environmental Integrity Project. Link: https://environmentalintegrity.org/wp-content/uploads/2022/03/CWA-report-UPDATED-8.9.23.pdf

Fan, X. Y., Gao, J. F., Pan, K. L., Li, D. C., & Dai, H. H. (2017). Temporal dynamics of bacterial communities and predicted nitrogen metabolism genes in a full-scale wastewater treatment plant. *RSC advances*, *7*(89), 56317-56327.

Faraji, E., & Afshar, A. (2021). Regret-Based Decision Making for Total Maximum Daily Load Allocation under Climate Change Scenarios; Application of Charged System Search Algorithm. 58-48 ,(6)*31*

Gurevich, A., Saveliev, V., Vyahhi, N., & Tesler, G. (2013). QUAST: quality assessment tool for genome assemblies. *Bioinformatics*, *29*(8), 1072-1075.

Harwood, V. J., Staley, C., Badgley, B. D., Borges, K., & Korajkic, A. (2014). Microbial source tracking markers for detection of fecal contamination in environmental waters: relationships between pathogens and human health outcomes. *FEMS microbiology reviews*, *38*(1), 1-40.

Hyer, K. E., & Mayer, D. L. (2004). Enhancing fecal coliform total maximum daily load models through bacterial source tracking 1. *JAWRA Journal of the American Water Resources Association*, *40*(6), 1511-1526.

Knights, D., Kuczynski, J., Charlson, E. S., Zaneveld, J., Mozer, M. C., Collman, R. G., ... & Kelley, S. T. (2011). Bayesian community-wide culture-independent microbial source tracking. *Nature methods*, *8*(9), 761-763.

Main, C. R., Tyler, R., & Huerta, S. (2021). Microbial Source Tracking in the Love Creek Watershed, Delaware (USA). *Delaware Journal of Public Health*, *7*(1), 22.

Ormerod, K. L., Wood, D. LA, Lachner, N., Shaan, G. L., Daly, J. N, Parsons, J. D., Dal'Molin, C. GO, et al. (2016). "Genomic characterization of the uncultured Bacteroidales family S24-7 inhabiting the guts of homeothermic animals." *Microbiome* 4: 1-17.

Parada, A. E., Needham, D. M., & Fuhrman, J. A. (2016). Every base matters: assessing small subunit rRNA primers for marine microbiomes with mock communities, time series and global field samples. *Environmental microbiology*, *18*(5), 1403-1414.

Schloss, P. D., Westcott, S. L., Ryabin, T., Hall, J. R., Hartmann, M., Hollister, E. B., ... & Weber, C. F. (2009). Introducing mothur: open-source, platform-independent, community-supported software for describing and comparing microbial communities. *Applied and environmental microbiology*, *75*(23), 7537-7541.

Shrestha, A., Kelty, C. A., Sivaganesan, M., Shanks, O. C., & Dorevitch, S. (2020). Fecal pollution source characterization at non-point source impacted beaches under dry and wet weather conditions. Water Research, 182, 116014.

Stoeckel, D. M., & Harwood, V. J. (2007). Performance, design, and analysis in microbial source tracking studies. *Applied and environmental microbiology*, *73*(8), 2405-2415.

Reitz, A., Hemric, E., & Hall, K. K. (2021). Evaluation of a multivariate analysis modeling approach identifying sources and patterns of nonpoint fecal pollution in a mixed-use watershed. *Journal of Environmental Management*, *277*, 111413.

Ruprecht, J. E., Birrer, S. C., Dafforn, K. A., Mitrovic, S. M., Crane, S. L., Johnston, E. L., ... &

Glamore, W. C. (2021). Wastewater effluents cause microbial community shifts and change trophic status. *Water research*, *200*, 117206.

USEPA. "Method 1696: Characterization of Human Fecal Pollution in Water by HF183/BacR287 TaqMan quantitative polymerase chain reaction (qPCR) assay." (2019).

Xepapadeas, A. (2011). The economics of non-point-source pollution. *Annu. Rev. Resour. Econ.*, *3*(1), 355-373.

ASSESSING SKELETON SHRIMP (*CAPRELLA SP*) DIVERSITY AND THEIR ASSOCIATED MICROBIOME IN THE MID-ATLANTIC UNITED STATES

Introduction

Amphipods are considered key marine species, serving in marine ecosystems as herbivores, detritivores and scavengers. The biodiversity in marine ecosystems has drastically declined in recent years due to over-fishing, climate change, and other anthropogenic impacts (Halpern et al., 2015; McCauley et al., 2015). The IUCN World Conservation Congress has called for full protection of at least 30% of global oceans to effectively conserve marine biodiversity (IUCN, 2016). However, progress has been slow, since priority has been given to known threatened areas of high species richness and biodiversity (Jefferson et al., 2021). To identify these threatened areas, mapping global species distribution in marine ecosystems is crucial for uncovering vulnerable areas of species richness and biodiversity (Momtazi & Saeedi, 2024). Within marine invertebrates, Amphipoda, an often-overlooked order, currently has over ten thousand recognized species and 79% of these inhabit marine ecosystems (WoRMS, 2023). These organisms often serve as indicators of aquatic pollution and play an essential role in marine food webs worldwide (Dauvin, 2018; Dauby, Nyssen & Broyer, 2003). Expanding our understanding of marine amphipod distribution and biodiversity is key to identifying priority areas to help meet the IUCN's Ocean protection goals.

Marine amphipod research primarily focuses on their function in food webs and ecotoxicology, leaving just ~6% of total amphipod research to focus on geographical distribution (Bhoi, Dubey & Patro, 2023; Glazier, 2014). Though there are natural means of amphipod dispersal, many species have historically been introduced by way of ballast waters (Gollasch et al., 2002). Caprellid species, commonly known as skeleton shrimp, are native amphipods across North American coastal ecosystems. Native caprellid species, such as *Caprella penantis* and *Caprella* laevis, are found in a variety of marine habitats along both the Atlantic and Pacific coasts, typically in intertidal zones, rocky shorelines, and eelgrass beds (Feldmann et al., 2015). These species play a significant role in benthic food webs, serving as prey for larger invertebrates and fish while also participating in organic matter decomposition (Thiel & Wellborn, 1999). However, non-native caprellid species, such as *Caprella mutica*, have been introduced to North America, likely through ballast water from ships, and have begun to spread across different regions, including parts of the Atlantic and Pacific coastlines (Gollasch et al., 2002; Boudouresque et al., 2012). The introduction of non-native Caprellids can potentially disrupt local ecosystems, outcompeting native species for food and space, and altering community dynamics (Häfner et al., 2009). As such, the presence of both native and nonnative Caprellids in North America highlights the need for continued monitoring and research on their distribution, ecological roles, and potential role in coastal biodiversity.

Along with geographic distribution, studies of gut microbiomes provide valuable information since marine invertebrate gut microbiomes can reflect their lifestyle and habitat (Carrier & Reitzel, 2018). These microbiomes are highly adapted to the diet and environmental conditions, influencing digestion, nutrient absorption, and immune function (Carrier & Reitzel, 2018; Chan et al., 2021; Cui et al., 2025). Marine amphipods living in environments with high organic matter, such as coastal areas, often harbor diverse microbial communities that help break down complex compounds (Chan et al., 2021; Zhang et al., 2019). In contrast, marine amphipods living in oligotrophic waters may have simpler, more specialized microbiomes that reflect the lower diversity in resources (Cui et al., 2025). For example, the gut microbiome of two hadal amphipods occupying the Mariana and Japan trench were found to exhibit similar microbial communities but significantly different abundances correlated with higher carbohydrate metabolism in the carbon limited Mariana trench inhabitants (Zhang et al., 2019). This intricate relationship between amphipods and their gut microbiota underscores the important role of microbes in enabling the survival and ecological function of these organisms across diverse marine ecosystems.

Distinct microbial signatures can be used to differentiate not only between various diets, lifestyles, but are also distinct between marine invertebrates (Bates et al., 2011; McFall-Ngai et al., 2013; Zaneveld et al., 2017, León-Zayas et al., 2020). When microbiome data are coupled with morphological observations, we can infer broader ecological roles that invertebrates play in their environments. For example, sea

cucumbers exhibit a higher abundance of sulfate-reducing bacteria in their gastrointestinal tracts, which may aid in metabolizing sulfate-rich nutrients from their diet (Zhang et al., 2019). Furthermore, studies have shown the gut microbiome of hadal living amphipods have a high abundance of carbohydrate and lipid metabolism genes and chemotaxis and motility genes that promote survival in nutrient poor conditions (Chan et al., 2021). However, the microbiome of many marine invertebrates, particularly amphipods, remain understudied

Here we describe the species diversity of Caprellids in the coastal Delaware Bay. In addition, we examined the gut microbiome of the two most prominent species identified during the study. The data presented here establishes the presence of six Caprellid species in the Delaware Bay, three of which have not previously been documented on the North American Atlantic coast and four which have not been previously reported as being observed in the Delaware Bay, to our knowledge. Furthermore, we present the first description of the gut microbiome among two Caprellid species, which harbors both sulfate reducers and sulfur oxidizers, and compare their gut microbiomes to other marine invertebrate gut microbiomes. This study further adds to known marine invertebrate biodiversity of Delaware Bay and gut associated microbiomes.

Methods

The study area is located within the Delaware Bay (Delaware, USA), specifically boating docks (38.788402 N, -75162095 W), that consists of various floating substrates where macroalgae congregate creating densely populated invertebrate communities. This area is tidally influenced and experiences substantial boating and human activity.

We aimed to better describe the Caprella spp. composition of Delaware Bay, so we intentionally sampled mature specimen by hand in summer 2023 and 2024 from floating substrates (buoys, ropes, & docks) within our study area. Specimen were brought back to the lab in small seawater tanks with air stones for morphological identification. Live specimens were observed using a compound dissecting scope and identified using relevant reference literature (Paz-Rios, Guerra-Garcia, & Ardisson, 2014; McCain, 1968; Guerra-García et al., 2016). Species identifications were made visually, based on coloration, body structure, and appendage size and length. Males and females were separated based on expected sexually dimorphic sizing between sexes and the presence of eggs or live young exclusively found on females.

Selected caprellids were removed with sterile forceps and stored in sterile 1X PBS at 4°C until gut contents were aseptically removed from *Caprella equilibria* (n=14), *Caprella penantis* (n=8), and *Caprella mutica* (n=1) for DNA extraction. Genetic material was extracted from the guts using the Qiagen DNeasy PowerSoil Pro kit (Germantown, Maryland) by placing the entire gut into the extraction. Extracted DNA

was sent to the UCONN MARS facility for amplicon sequencing of the 16S rRNA gene targeting the V4 region (primers 515F and 806R) using the Illumina MiSeq paired-end sequencing platform via the v2 2x250 base pair kit (Illumina) following their standard protocol (Parada et al., 2016). Raw forward and reverse sequences were paired, and quality checked; sequences that passed QC were further processed using the 16S rRNA gene analysis pipeline implemented in MOTHUR version 1.46.1 (Schloss et al., 2009). Forward and reverse sequences were aligned and quality filtered using MOTHUR, yielding amplicons ranging in sizes of 130-200 bp in lengths, where ambiguous nucleotides and homopolymer stretches were removed. Operational taxonomic units (OTU) were created with a 3% dissimilarity and were aligned and classified against the Silva SSU database, version 138 (Gurevich et al., 2013). Prior to further downstream analysis, nontarget OTUs, i.e. chloroplast and mitochondria, and taxa <1% were removed from representative sequences. Relative 16S rRNA gene abundance was averaged across triplicate sampling of caprellid samples.

Diversity analyses of the gut microbiomes were performed in R using the following packages: VEGAN and tidyverse (Dixon, 2003; Wickham et al., 2019). Order level classified OTUs were assigned a representative for beta diversity analysis among samples. Bray-Curtis dissimilarity matrices were used for non-metric dimensional scaling (NMDS) to visualize beta diversity between caprellid species and sex. Molecular data has been deposited in the NCBI repository under XXXXXXX and caprellid images have been uploaded to the FigShare repository under XXXX.

Results

We examined literature and database information to compile all known caprellids in North America at the time of our study (Table 3.1). Prior to our study, *C. mutica, C. linearis* and *C. equilibria* had previously been seen on the US Atlantic Coast. We then collected a total of 150 caprellids and identified 6 different species based on pronounced morphological features in the Delaware Bay over two summer seasons (Figure 3.1; Table 3.3). *C. equilibria* were distinguished by elongated body plan that included extended pereonite 1 and extended pair of antennae 1 (Guerra-García et al., 2016). *C. laeviuscula* were distinguished by their distinct blotting coloration across their pereion, thin oval-shaped pereopods, and elongated antennae 1 (Caine, 1991). *C. linearis* were distinguished by dense setae covered antenna 1, brown/green coloration, and small oval shaped pereopods (McCain, 1968). *C. mutica* were distinguished by their rows of spines down their pereion, dense setae covering the gnathopods and thoracic segments, and blue coloration above the eyes (Arimoto, 1976). *C. penantis* were distinguished by their similar length of both pair of antennae and wide, circular shaped pereopods (Paz-Rios, Guerra-Garcia, & Ardisson). *C. scaura* were similarly distinguished by elongated body plan that included extended pereonite 1 and extended pair of antennae 1 with the addition of a pronounced rostrum on the cephalon (Guerra-García et al., 2016). Due to sexually dimorphic body plans, we further used brooding pound size, shape, and coloration to aid species identification. Of the total caprellids collected, 65% were male and 35% were female (Table 3.2). Among the surveyed amphipods, we identified *C. equilibria* (41%),

C. laeviuscula (3%), *C. linearis* (10%), *C. mutica* (13%), *C. penantis* (18%), and *C. scaura* (14%) (Table 3.2).

The gut microbiome was assessed for the two most prominent taxa, *C. equilibria* and *C. penantis* and 1 sample of a minor taxon, *C. mutica*, was also included. A total of 24 samples were processed, with 24 passing quality control parameters. The gut microbiomes were diverse, consisting of common gut taxa such as Bacteroidales, Camplyobacterales, Lachnospirales, and Lactobacillales (Figure 3.2). Though the gut microbiome is diverse among samples, Enterobacterales was the only abundant microbial order identified across samples (Figure 3.2; Table 3.4). Enterobacterales was the most abundant taxa seen in both species across males and females (Figure 3.2). There was no statistically significant difference seen between the three *Caprella* spp. samples.

Several sulfate-reducing taxa were observed between the *C. equilibria* and *C. penantis*, such as Desulfuromonadales, Desulfobulbales and Pseudomonadales (Figure 2). The microbial order Desulfobulbales represented ~50% of the gut community in three of the fourteen *C. equilibria* gut microbiomes (Figure 3.2). Sulfur-oxidizing taxa were also seen across species including Thiotrichales and Rhodobacterales (Figure 3.2). The gut microbial composition observed is diverse within the caprellid species, however, beta-analysis (NMDS) revealed that the female gut microbiome is more similar than the males across species (Figure 3.3).

We examined if the caprellid invertebrates had similar gut microbes to other marine invertebrates, especially for sulfur-cycling bacteria. When comparing gut microbial taxa of other marine invertebrates from other literature, an average of 38% of

the gut community is involved in sulfur related metabolisms between caprellids (*C. equilibria* & *C. penantis*), echinoderms (*O. kinbergi*, *O. mirabilis*, *O. sarsii vadicola*, *S. sladeni, and T. gratilla elatensis*) and a mollusk (*A. marisindica*) (Figure 3.4). The average most abundant sulfur-related microbial order in caprellids were Enterobacterales (44%), followed by Rhodobaterales (7%) and Thiotricales (7%) (Figure 3.5). The echinoderms share more similar sulfur related taxa as Rhodobacterales (5%), Flavobacterales (5%), and Spirochaetales (1%) were identified in all echinoderm species gut communities (Figure 3.5). The sulfur related microbial orders in the reported mollusk species were Fusobacteria (35%) and Clostridiales (20%) (Figure 3.5).

Table 3.1. Caprellid species observed on North American coastline as documented in the World Register of Marine Species (WoRMS) (Ahyong et al., Accessed 2025).

Species	Region Found	First Documented
Caprella andreae	U.S. Gulf Coast	1836
Caprella equilibra	U.S. East & West Coasts	1818
Caprella laeviuscula	U.S. West Coast	1977
Caprella linearis	U.S. East & West Coasts	1935
Caprella mendax	U.S. West Coast	1836
Caprella mutica	U.S. East Coast	1935
Caprella penantis	U.S. Gulf Coast	1836
Caprella scaura	U.S. Gulf Coast	1836
Caprella mendax	U.S. West Coast	1836

Table 3.2. Caprellids morphologically identified in 2023 and 2024 from Delaware Bay (n=150). Species previously identified on the East coast indicated by an asterisk.

Species	Total Collected
*Caprella equilibra**	42 ♂ 20 ♀
Caprella laeviuscula	4 ♂ 1 ♀
*Caprella linearis**	14 ♂ 2 ♀
*Caprella mutica**	10 ♂ 9 ♀
Caprella penantis	16 ♂ 11 ♀
Caprella scaura	12 ♂ 9 ♀

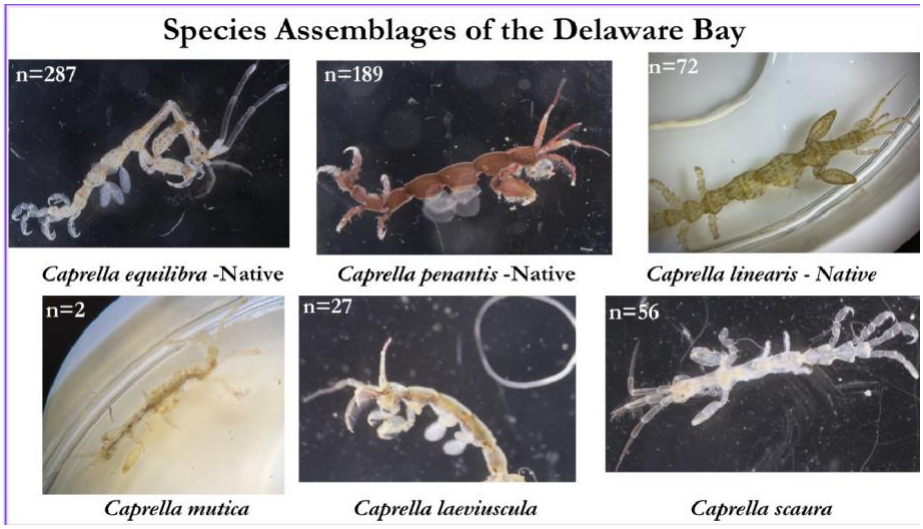

Figure 3.1. Photos depicting a representative caprellid species (*C. equilibria, C penantis, C. linearis, C. mutica, C. laeviuscula,* and *C. scaura*) identified in the study.

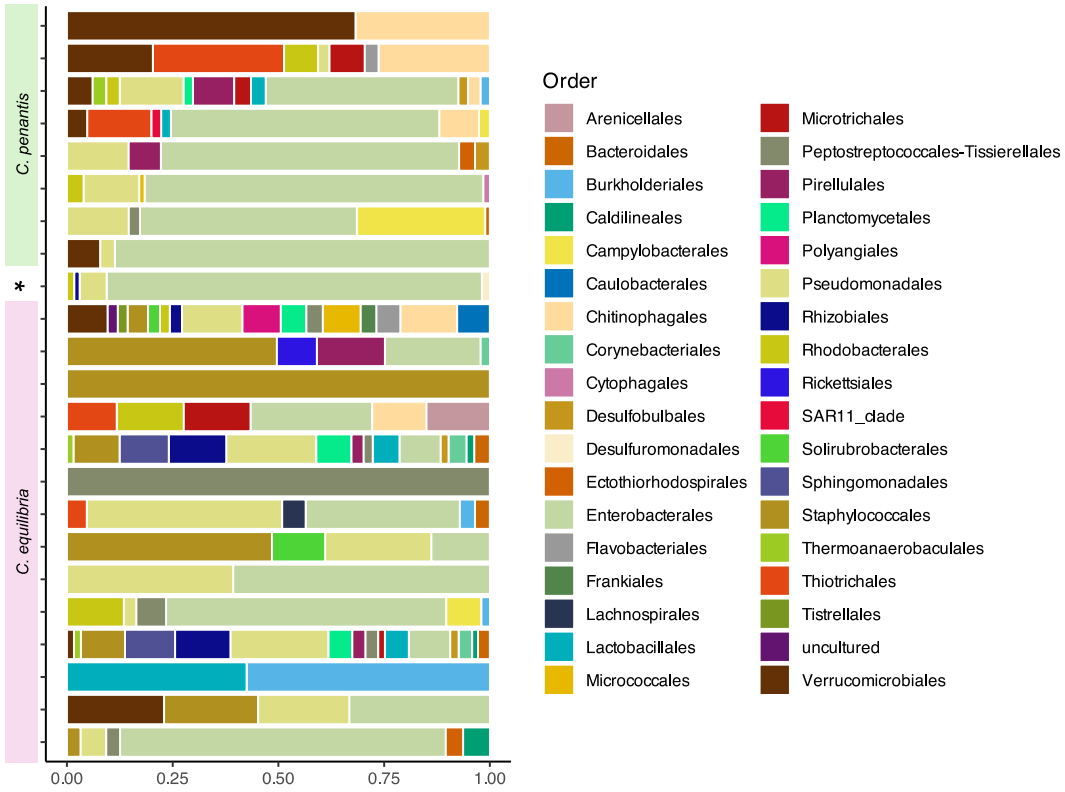

Figure 3.2. Microbial orders based on 16S rRNA gene percent abundance *from C. penantis, C. equilibria* and *C. mutica* gut microbiomes (indicated with an asterisk). Data shows a diverse gut microbiome across species and sexes with a dominant abundance of Enterobacterales among Caprellids. Microbial Orders present at <1% abundance have been removed to simplify visualization of abundant taxa.

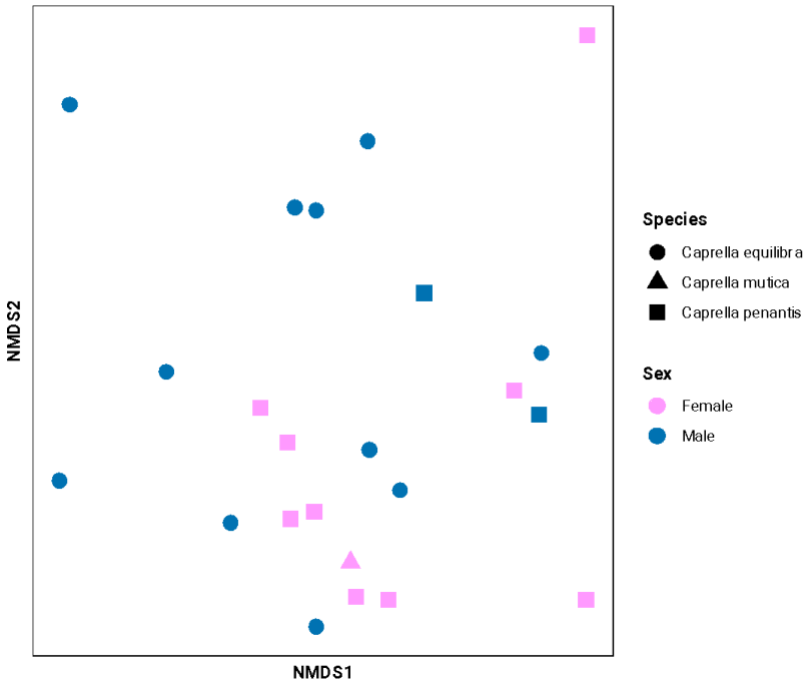

Figure 3.3. Non-metric Dimensional Scaling (NMDS) of a Bray-Curtis similarity matrix from the taxonomic identification of the 16S rRNA gene sequences organized by caprellid species and sample gender. Data was double square-root transformed (Stress = 0.15).

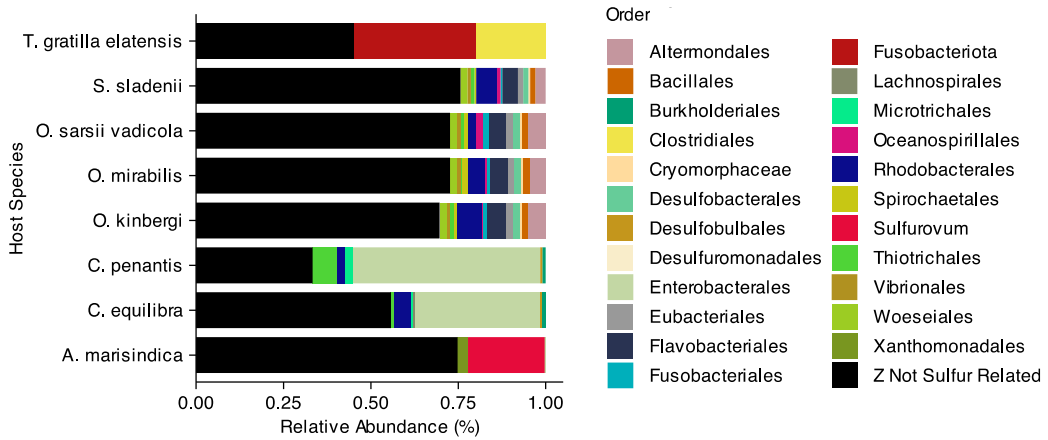

Figure 3.4. Stacked bar plot of Order level microbial taxa that are involved in sulfur cycling found in the guts of marine invertebrates in this study *C. equilibria*, *C. penantis*, *A. marisindica* (Yang et al., 2022), *O. mirabilis* (Dong et al., 2021), *O. kinbergi* (Dong et al., 2021), *S. sladeni* (Dong et al., 2021), *O. sarsii vadicola* (Dong et al., 2021), and *T. gratilla elatensis* (Masasa et al, 2023).

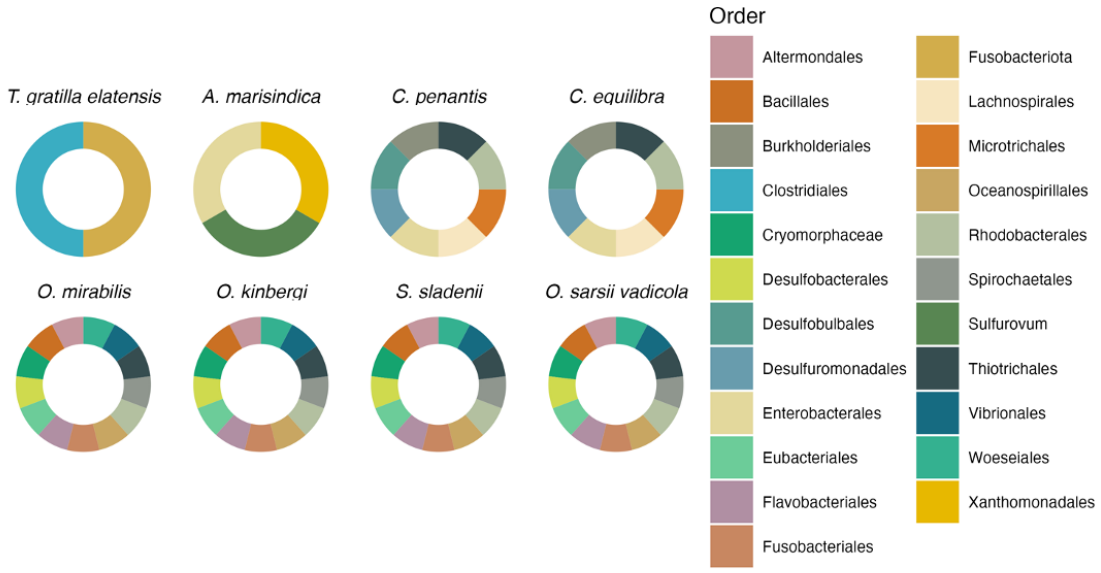

Figure 3.5. Comparative donut charts of marine invertebrate gut microbial taxa classified to the Order level that are capable of sulfur metabolism. The data consist of data collected from our study with *C. penantis* and *C. equilibria* as well as data collected from other studies on *A. marisindica* (Yang et al., 2022), *O. mirabilis* (Dong et al., 2021), *O. kinbergi* (Dong et al., 2021), *S. sladeni* (Dong et al., 2021), *O. sarsii vadicola* (Dong et al., 2021), and *T. gratilla elatensis* (Masasa et al, 2023).

Discussion & Conclusion

We morphologically identified six caprellid spp in a small ecoregion of the coastal Delaware Bay. Two of these species have not been previously observed in this region based on published reports (Ahyong et al., 2025). This study also provides a brief first look at the caprellid gut microbiome offering insight to the gut microbiome of these overlooked marine amphipods.

While the specific range of *Caprella* spp. is uncertain along much of the North Atlantic US coastline, three of the six species identified in this study are native to the North Atlantic, including *C. linearis, C. equilibria, and C. penantis* (Guerra-Garcia & Figueroa, 2009; Foster & LeCroy, 1991). *C. mutica* is the only established nonnative species found in this study that has been previously identified on the North Atlantic coast (Gollasch et al., 2002; Boudouresque et al., 2012). C *laeviuscula* and *C. scaura* have been seen on the North Pacific coastline of the US but neither have been said to inhabit the North Atlantic US coastline (Foster & LeCroy, 2000). All six species were found cohabiting red and brown algal substrates at the sampling sites, forming a diverse assemblage of native and non-native caprellid species not previously documented in the Delaware Bay. The apparent establishment of two additional non-native species in this localized ecoregion highlights the need for continued monitoring and more comprehensive assessments of amphipod biodiversity in the area.

The gut microbiome observed in the three caprellid species was highly diverse, but microbiomes were not distinct by species. Such microbial diversity of the gut microbiome could be beneficial to the host health, including enhanced immune responses and the production of essential dietary metabolites that support physiological functions and ecological adaptations (e.g., Sommer & Bäckhed, 2013; Thaiss et al., 2016). Recent studies on echinoderm gut microbiota have revealed complex microbial communities involved in nutrient breakdown and biogeochemical processes such as the sulfur cycling

(e.g., Hakim, 2015; Yao et al., 2019). Consistent with findings from other marine invertebrates, our analysis identified microbial taxa capable of both sulfate reduction (e.g., Desulfovibrio spp.) and sulfur oxidation (e.g., Sulfurimonas spp.) (Jørgensen, Findlay & Pellerin, 2019; Goffredi et al., 2008). Given the sulfate-rich nature of marine environments, many benthic invertebrates have evolved mechanisms to regulate internal sulfur levels and mitigate potential toxicity (Canfield et al., 2005). However, the synergistic role of sulfate-reducing and sulfur-oxidizing bacteria in invertebrate gut ecosystems remains poorly understood, potentially constituting a cryptic sulfur involvement in these hosts (Canfield et al., 2010). The high microbial diversity found in these caprellids may also reflect the heterogeneity of their diet, as their foraging styles can be scavengers, detritivores, and filter-feeders inhabiting substrate-rich, sulfate-dense marine environments (Caine, 1977).

We did find that gender of the caprellid organism showed more variance than species designation, with female samples appearing more similar to one another than to male samples. Gut studies of marine invertebrates do not usually separate by gender of sample, but since sampling occurred in breeding season, it may suggest that hormonal differences influence gut microbiomes. This would be an interesting phenomenon to pursue further in future studies.

Given this study captures only a fraction of the likely caprellid diversity present in the entire Delaware Bay and the Atlantic coast of North America, it underscores the need for more comprehensive investigations of the caprellid assemblages and their ecological roles. Future research should incorporate both morphological and molecular identification

methods to more accurately resolve species-level diversity within the region. Expanding gut microbiome analyses to include a larger sample size and broader species representation, separated by gender, would offer deeper insights into the dietary habits and ecological lifestyles of caprellid species, thereby enhancing our understanding of their functional roles in sulfur-rich marine ecosystems.

REFERENCES

1. Halpern, B. S., Frazier, M., Potapenko, J., Casey, K. S., Koenig, K., Longo, C., ... & Walbridge, S. (2015). Spatial and temporal changes in cumulative human impacts on the world's ocean. Nature communications, 6(1), 7615.
2. McCauley, D. J., Pinsky, M. L., Palumbi, S. R., Estes, J. A., Joyce, F. H., & Warner, R. R. (2015). Marine defaunation: animal loss in the global ocean. Science, 347(6219), 1255641.
3. IUCN. (2016). Increasing marine protected area coverage for effective marine biodiversity conservation. In WCC-2016-Res-050-EN, World Conservation Congress, Hawai 'i, United States of America, 1–10 September 2016.
4. Jefferson, T., Costello, M. J., Zhao, Q., & Lundquist, C. J. (2021). Conserving threatened marine species and biodiversity requires 40% ocean protection. Biological Conservation, 264, 109368.
5. Momtazi, F., & Saeedi, H. (2024). Exploring latitudinal gradients and environmental drivers of amphipod biodiversity patterns regarding depth and habitat variations. Scientific Reports, 14(1), 30547.
6. Board, W. E. (2014). World register of marine species. 2016.
7. Dauvin, J. C. (2018). Twenty years of application of Polychaete/Amphipod ratios to assess diverse human pressures in estuarine and coastal marine environments: A review. Ecological Indicators, 95, 427-435.

8. Dauby, P., Nyssen, F., & De Broyer, C. (2003). Amphipods as food sources for higher trophic levels in the Southern Ocean: a synthesis. Antarctic biology in a global context, 129-134.
9. Bhoi, G., Dubey, S. K., & Patro, S. (2023). Marine benthic amphipods (Amphipoda) of India: an assessment on their biodiversity, distribution and significance. Thalassas: An International Journal of Marine Sciences, 39(1), 215-233.
10. Kohler, S. A., Parker, M. O., & Ford, A. T. (2018). Species-specific behaviours in amphipods highlight the need for understanding baseline behaviours in ecotoxicology. *Aquatic Toxicology*, *202*, 173-180.
11. Gollasch, S., MacDonald, E., Belson, S., Botnen, H., Christensen, J. T., Hamer, J. P., ... & Wittling, T. (2002). Life in ballast tanks. Invasive aquatic species of Europe. Distribution, impacts and management, 217-231.
12. Carrier, T. J., & Reitzel, A. M. (2018). The hologenome across environments and the implications of a host-associated microbial repertoire. *Frontiers in Ecology and Evolution*, 6, 186.
13. Chan, J., Geng, D., Pan, B., Zhang, Q., & Xu, Q. (2021). Metagenomic insights into the structure and function of intestinal microbiota of the hadal amphipods. *Frontiers in Microbiology*, *12*, 668989.
14. Zhang, W., Watanabe, H. K., Ding, W., Lan, Y., Tian, R. M., Sun, J., ... & Qian, P. Y. (2019). Gut microbial divergence between two populations of the hadal

amphipod Hirondellea gigas. *Applied and Environmental Microbiology*, *85*(1), e02032-18.

15. Cui, Y., Xiao, Y., Wang, Z., Ji, P., Zhang, C., Li, Y., ... & Yu, X. (2025). Microbial community structure and functional traits involved in the adaptation of culturable bacteria within the gut of amphipods from the deepest ocean. *Microbiology Spectrum*, *13*(1), e00723-24.
16. Bates, S. T., Berg-Lyons, D., Caporaso, J. G., Walters, W. A., Knight, R., & Fierer, N. (2011). Examining the global distribution of dominant archaeal populations in soil. *The ISME Journal*, 5(5), 908–917.
17. McFall-Ngai, M. J., Hadfield, M. G., Bosch, T. C., Carey, H. V., Domazet-Lošo, T., Douglas, A. E., Eberl, G., Fukami, T., Gilbert, S. F., Hentschel, U., & et al. (2013). Animals in a bacterial world, a new imperative for the life sciences. *Proceedings of the National Academy of Sciences*, 110(9), 3229–3236.
18. Zaneveld, J. R., McMinds, R., & Thurber, R. V. (2017). Stress and stability: Applying the Anna Karenina principle to animal microbiomes. *Nature Microbiology*, 2(11), 17121.
19. Zhang, X., Liu, Y., Zhang, H., & Zhang, J. (2019). Characterization of the gut microbiota in sea cucumbers and its role in nutrient metabolism. *Frontiers in Microbiology*, 10, 1001.
20. Guerra-García, J. M., & Tierno de Figueroa, J. M. (2009). What do caprellids (Crustacea: Amphipoda) feed on? Marine Biology, 156(9), 1881–1890. https://doi.org/10.1007/s00227-009-1216-1

21. Foster, J. M., & LeCroy, S. E. (1991). Caprellid amphipods (Crustacea: Amphipoda: Caprellidea) from the northern Gulf of Mexico. *Gulf Research Reports*, 8(3), 271–283. https://aquila.usm.edu/gcr/vol8/iss3/6/

22. Cook, E. J., Jahnke, M., Kerckhof, F., Minchin, D., Faasse, M., Boos, K., & Ashton, G. (2007). European expansion of the introduced amphipod *Caprella mutica* Schurin, 1935. *Aquatic Invasions*, 2(4), 411–421. https://doi.org/10.3391/ai.2007.2.4.11

23. Foster, J. M., & LeCroy, S. E. (2000). An annotated checklist of the amphipod crustaceans of the Gulf of Mexico. Gulf Research Reports, 16(1), 1–23. https://aquila.usm.edu/gcr/vol16/iss1/9/

24. Sommer, F., & Bäckhed, F. (2013). The gut microbiota — masters of host development and physiology. *Nature Reviews Microbiology*, 11(4), 227–238.

25. Thaiss, C. A., et al. (2016). The microbiome and innate immunity. *Nature*, 535(7610), 65–74.

26. Hakim, J. A. (2015). *Comparison of gut microbiomes in laboratory cultured sea urchins revealing selective attributes of microbial composition based upon their feed and surroundings*. The University of Alabama at Birmingham.

27. Yao, Q., Yu, K., Liang, J., Wang, Y., Hu, B., Huang, X., ... & Qin, Z. (2019). The composition, diversity and predictive metabolic profiles of bacteria associated with the gut digesta of five sea urchins in Luhuitou fringing reef (northern South China Sea). *Frontiers in microbiology*, *10*, 1168.

28. Jørgensen, B. B., Findlay, A. J., & Pellerin, A. (2019). The biogeochemical sulfur cycle of marine sediments. *Frontiers in microbiology*, *10*, 849.

29. Goffredi, S. K., Jones, W. J., Erhlich, H., Springer, A., & Vrijenhoek, R. C. (2008). Epibiotic bacteria associated with the recently discovered Yeti crab, Kiwa hirsuta. *Environmental Microbiology*, *10*(10), 2623-2634.

30. Canfield, D. E., et al. (2005). The sulfur cycle. In *Biogeochemistry* (pp. 97–122). Elsevier.

31. Canfield, D. E., Stewart, F. J., Thamdrup, B., De Brabandere, L., Dalsgaard, T., Delong, E. F., ... & Ulloa, O. (2010). A cryptic sulfur cycle in oxygen-minimum–zone waters off the Chilean coast. *Science*, *330*(6009), 1375-1378..

32. Caine, E. A. (1977). Feeding mechanisms and possible resource partitioning of the Caprellidae (Crustacea: Amphipoda) from Puget Sound, USA. *Marine Biology*, *42*(4), 331-336.

33. Ahyong, S.; Boyko, C.B.; Bernot, J.; Brandão, S.N.; Daly, M.; De Grave, S.; de Voogd, N.J.; Gofas, S.; Hernandez, F.; Hughes, L.; Neubauer, T.A.; Paulay, G.; van der Meij, S.; Boydens, B.; Decock, W.; Dekeyzer, S.; Goharimanesh, M.; Vandepitte, L.; Vanhoorne, B.; Adlard, R.; Agatha, S.; Ahn, K.J.; Alonso, M.V.; Alvarez, B.; Alves, K.; Amler, M.R.W.; Amorim, V.; Anderberg, A.; Andrés-Sánchez, S.; Ang, Y.; Antić, D.; Antonietto, L.S..; Arango, C.; Artois, T.; Atkinson, S.; Auffenberg, K.; Bailly, N.; Baldwin, B.G.; Bank, R.; Barber, A.; Barrett, R.L.; Bartsch, I.; Bellan-Santini, D.; Bergh, N.; Bernard, C.; Berrios Ortega, F.J.; Berta, A.; Bezerra, T.N.; Bhandari, P.; Bieler, R.; Blanco, S.; Blasco-

Costa, I.; Blazewicz, M.; Bledzki, L.A.; Bock, P.; Bonifacino, M.; Böttger-Schnack, R.; Bouchet, P.; Boury-Esnault, N.; Bouzan, R.; Boxshall, G.; Bradshaw, C.; Bray, R.; Brito Seixas, A.L.; Browning, J.; Bruhl, J.J.; Bruneau, A.; Budaeva, N.; Bueno-Villegas, J.; Calvo Casas, J.; Campos-Filho, I.S.; Cárdenas, P.; Carstens, E.; Carvalho, A.B.G.D.; Cedhagen, T.; Chan, B.K.; Chan, T.Y.; Chernyshev, A.; Choong, H.; Christenhusz, M.; Churchill, M.; Cole, E.; Collins, A.G.; Collins, G.E.; Collins, K.; Consorti, L.; Copilaș-Ciocianu, D.; Corbari, L.; Cordeiro, R.; Costa, S.M.; Costa, V.M.d.M.; Costa Corgosinho, P.H.; Coste, M.; Crandall, K.A.; Cremonte, F.; Cribb, T.; Cutmore, S.; Dahdouh-Guebas, F.; Daneliya, M.; Dauvin, J.C.; Davie, P.; De Broyer, C.; de Lima Ferreira, P.; de Mazancourt, V.; de Moura Oliveira, L.; Decker, P.; Defaye, D.; Dekker, H.; DeSalle, R.; Di Capua, I.; Dippenaar, S.; Dohrmann, M.; Dolan, J.; Domning, D.; D'Onofrio, R.; Downey, R.; Dreyer, N.; Duke, N.C.; Eisendle, U.; Eitel, M.; Eleaume, M.; Elliott, T.; Enghoff, H.; Epler, J.; Esquete Garrote, P.; Evenhuis, N.L.; Ewers-Saucedo, C.; Faber, M.; Figueroa, D.; Fišer, C.; Ford, B.A.; Ford, K.A.; Fordyce, E.; Foster, W.; Fransen, C.; Freire, S.; Fujimoto, S.; Furuya, H.; Galbany-Casals, M.; Gale, A.; Galea, H.; Gao, T.; García-Moro, P.; Garic, R.; Garnett, S.; Gaviria-Melo, S.; Gebauer, S.; Gerken, S.; Gibson, D.; Gibson, R.; Gil, A.; Gil, J.; Gittenberger, A.; Glasby, C.; Glenner, H.; Glover, A.; Goetghebeur, P.; Gómez-Noguera, S.E.; Gonçalves, G.O.; Gondim, A.I.; Gonzalez, B.C.; González-Elizondo, M.d.S.; González-Gallego, L.; González-Solís, D.; Goodwin, C.; Gostel, M.; Grabowski, M.; Grossi, M.; Guerra-García,

J.M..; Guerrero, J.M.; Guidetti, R.; Guiry, M.D.; Gutierrez, D.; Hadfield, K.A.; Hajdu, E.; Halanych, K.; Hallermann, J.; Hayward, B.W.; Hegna, T.A.; Heiden, G.; Hendrycks, E.; Hennen, D.; Herbert, D.; Herrera Bachiller, A.; Hipp, A.L.; Hodda, M.; Høeg, J.; Hoeksema, B.; Holovachov, O.; Hooge, M.D.; Hooper, J.N.; Horton, T.; Houart, R.; Hroudová, Z.; Huys, R.; Hyžný, M.; Iniesta, L.F.M.; Iseto, T.; Iwataki, M.; Janssen, R.; Jaume, D.; Jazdzewski, K.; Jersabek, C.D.; Jiménez-Mejías, P.; Jin, X.F.; Jóźwiak, P.; Jung, M.; Kabat, A.; Kajihara, H.; Kakui, K.; Kantor, Y.; Karanovic, I.; Karapunar, B.; Karthick, B.; Kathirithamby, J.; Katinas, L.; Kilian, N.; Kim, S.; Kim, Y.H.; King, R.; Kirk, P.M.; Klautau, M.; Kociolek, J.P.; Köhler, F.; Konowalik, K.; Kotov, A.; Kovács, Z.; Kremenetskaia, A.; Kristensen, R.M.; Kroh, A.; Kulikovskiy, M.; Kullander, S.; Kupriyanova, E.; Lacroix-Carignan, É.; Lamaro, A.; Lambert, G.; Larridon, I.; Lazarus, D.; Le Coze, F.; Le Roux, M.; LeCroy, S.; Leduc, D.; Lefkowitz, E.J.; Lemaitre, R.; Léveillé-Bourret, É.; Licher, M.; Lichter-Marck, I.H.; Lim, S.C.; Lindsay, D.; Liu, Y.; Loeuille, B.; Lois, R.; Lörz, A.N.; Lu, Y.F.; Luceño Garcés, M.; Ludwig, m.; Lundholm, N.; Maciel Silva, J.; Macpherson, E.; Mah, C.; Mamos, T.; Manconi, R.; Mańko, M.; Mapstone, G.; Marco Rosado, N.; Marek, P.E.; Marhold, K.; Markello, K.; Márquez-Corro, J.I.; Marshall, B.; Marshall, D.J.; Martin, P.; Martín-Bravo, S.; Martinez Arbizu, P.; Maslakova, S.; McFadden, C.; McInnes, S.J.; McKenzie, R.; Means, J.; Mees, J.; Mejía-Madrid, H.H.; Meland, K.; Merrin, K.L.; Mesterházy, A.; Míguez, M.; Miller, J.; Mills, C.; Moestrup, Ø.; Mokievsky, V.; Molodtsova, T.; Mooi, R.; Morales-Alonso, A.; Morandini, A.C.;

Moreira da Rocha, R.; Morel, J.; Moreyra C., L.D.; Moritz, L.; Morrow, C.; Mortelmans, J.; Muasya, M.A.; Müller, A.; Muñoz Gallego, A.R.; Muñoz Schüler, P.; Musco, L.; Naczi, R.F.C.; Nascimento, J.B.; Nesom, G.; Neto Silva, M.d.S.; Neubert, E.; Neuhaus, B.; Ng, P.; Nguyen, A.D.; Nielsen, S.; Nishikawa, T.; Norenburg, J.; Nunes, C.; O'Hara, T.; Opresko, D.; Osawa, M.; Osigus, H.J.; Ota, Y.; Páll-Gergely, B.; Panero, J.L.; Parra-Gómez, A.; Patterson, D.; Pedram, M.; Pelser, P.; Peña Santiago, R.; Perbiche-Neves, G.; Pereira, J.d.S..; Pereira, P.H.M.; Pereira, S.G.G.; Pereira-Silva, L.; Perez-Losada, M.; Petrescu, I.; Pfingstl, T.; Piasecki, W.; Pica, D.; Picton, B.; Pignatti, J.; Pilger, J.F.; Pinheiro, U.; Pisera, A.B.; Poatskievick Pierezan, B.; Polhemus, D.; Poore, G.C.; Potapova, M.; Praxedes, R.A.; Půža, V.; Rasaminirina, F.; Read, G.; Reich, M.; Reimer, J.D.; Reip, H.; Resende Bueno, V.; Reuscher, M.; Reynolds, J.W.; Reznicek, A.A.; Richling, I.; Rimet, F.; Rink, G.; Ríos, P.; Rius, M.; Rodríguez, E.; Rogers, D.C.; Rosenberg, G.; Rützler, K.; Sá, H.A.B..; Saavedra, M.; Sabater, L.M.; Sabbe, K.; Sabroux, R.; Saiz-Salinas, J.; Sala, S.; Samimi-Namin, K.; Sánchez Santos, N.; Sánchez-Villegas, R.; Santagata, S.; Santos, S.; Santos, S.G.; Santos Filho, M.A.B.d.; Sanz Arnal, M.; Sar, E.; Saucède, T.; Schärer, L.; Schierwater, B.; Schilling, E.; Schmidt-Lebuhn, A.; Schneider, L.; Schneider, S.; Schönberg, C.; Schrével, J.; Schuchert, P.; Schweitzer, C.; Segers, H.; Semple, J.C.; Senna, A.R.; Sennikov, A.; Serejo, C.; Shaik, S.; Shamsi, S.; Sharma, J.; Shear, W.A.; Shenkar, N.; Short, M.; Sicinski, J.; Sierwald, P.; Silva, M.L.C.N.; Silva da Silva Filho, P.J.; Simmons, E.; Simpson, D.A.; Sinniger, F.; Sinou, C.; Sivell, D.; Smit,

H.; Smit, N.; Smol, N.; Sørensen, M.V.; Souza-Filho, J.F..; Spalink, D.; Spelda, J.; Starr, J.R.; Sterrer, W.; Steyn, H.M.; Stoev, P.; Stöhr, S.; Suárez-Morales, E.; Susanna, A.; Suttle, C.; Swalla, B.J.; Takahashi, K.T.; Tanaka, M.; Tandberg, A.H.; Tang, D.; Tasker, M.; Taylor, J.; Taylor, J.; Taylor, K.; Tchesunov, A.; Temereva, E.; ten Hove, H.; ter Poorten, J.J.; Thirouin, K.; Thomas, J.D.; Thomas, W.W.; Thuesen, E.V.; Thurston, M.; Thuy, B.; Timi, J.T.; Todaro, A.; Todd, J.; Tucker, G.C.; Turon, X.; Tyler, S.; Uetz, P.; Urbatsch, L.; Uribe-Palomino, J.; Urtubey, E.; Utevsky, S.; Uy, M.; Vacelet, J.; Vader, W.; Väinölä, R.; Valdés-Florido, A.; Valls Domedel, G.; Van de Vijver, B.; van Haaren, T.; van Soest, R.W.; Vanreusel, A.; Vázquez-García, B.; Venekey, V.; Verhoeff, T.; Verloove, F.; Villaverde, T.; Vinarski, M.; Vonk, R.; Vos, C.; Vouilloud, A.A.; Walker-Smith, G.; Walter, T.C.; Watling, L.; Wayland, M.; Wesener, T.; Wetzel, C.E.; Whipps, C.; White, K.; Wieneke, U.; Williams, D.M.; Williams, G.; Williams, N.; Wilson, K.L.; Wilson, R.; Witkowski, J.; Xanthos, M.; Xavier, J.; Xu, K.; Yano, O.; Zanol, J.; Zeidler, W.; Zhang, S.; Zhao, Z.; Zullini, A. (2025). World Register of Marine Species. Available from https://www.marinespecies.org at VLIZ. Accessed 2025-05-22. doi:10.14284/170

34. León-Zayas, R., McCargar, M., Drew, J. A., & Biddle, J. F. (2020). Microbiomes of fish, sediment and seagrass suggest connectivity of coral reef microbial populations. *PeerJ*, *8*, e10026.
35. Zhang, W., Watanabe, H. K., Ding, W., Lan, Y., Tian, R. M., Sun, J., ... & Qian, P. Y. (2019). Gut microbial divergence between two populations of the hadal

amphipod Hirondellea gigas. *Applied and Environmental Microbiology*, *85*(1), e02032-18.

36. Chan, J., Geng, D., Pan, B., Zhang, Q., & Xu, Q. (2021). Metagenomic insights into the structure and function of intestinal microbiota of the hadal amphipods. *Frontiers in Microbiology*, *12*, 668989.
37. Masasa, M., Kushmaro, A., Nguyen, D., Chernova, H., Shashar, N., & Guttman, L. (2023). Spatial succession underlies microbial contribution to food digestion in the gut of an algivorous sea urchin. *Microbiology spectrum*, *11*(3), e00514-23.
38. Yang, Y., Sun, J., Chen, C., Zhou, Y., Van Dover, C. L., Wang, C., ... & Qian, P. Y. (2022). Metagenomic and metatranscriptomic analyses reveal minor-yet-crucial roles of gut microbiome in deep-sea hydrothermal vent snail. *Animal Microbiome*, *4*, 1-17.
39. Dong, Y., Li, Y., He, P., Wang, Z., Fan, S., Zhang, Z., ... & Xu, Q. (2021). Gut microbial composition and diversity in four ophiuroid species: divergence between suspension feeder and scavenger and their symbiotic microbes. *Frontiers in Microbiology*, *12*, 645070.
40. McCain, J. C. (1968). The Capreillidae (Crustacea: Amphipoda) of the Western North Atlantic. Bulletin of the United States National Museum.
41. Paz-Ríos, C. E., Guerra-García, J. M., & Ardisson, P. L. (2014). Caprellids (Crustacea: Amphipoda) from the Gulf of Mexico, with observations on Deutella mayeri, redescription of Metaprotella hummelincki, a taxonomic key and zoogeographical comments. Journal of Natural History, 48(41-42), 2517-2578.

42. Guerra-García, J. M., Hachero-Cruzado, I., González-Romero, P., Jiménez-Prada, P., Cassell, C., & Ros, M. (2016). Towards integrated multi-trophic aquaculture: lessons from caprellids (Crustacea: Amphipoda). *PLoS One*, *11*(4), e0154776.
43. Arimoto, I. (1976). Taxonomic studies of caprellids (Crustacea, Amphipoda, Caprellidae) found in the Japanese and adjacent waters. *Special Publications from the Seto Marine Biological Laboratory*, *3*, iii-229.
44. Caine, E. A. (1991). Reproductive behavior and sexual dimorphism of a caprellid amphipod. *Journal of Crustacean Biology*, *11*(1), 56-63.

INFLUENCE OF SEASONAL SUCCESSION ON MICROBIOLOGICAL AND PHYSIOCHEMICAL COMPOSITION IN SHALLOW ESTUARINE SEDIMENTS

Introduction

Marine sediments harbor diverse and abundant microbial populations and are estimated to contain 15% of microbial biomass on the planet (Kallmeyer et al., 2012; Bar-On, Phillps & Milo, 2018). Our current understanding of microbial life in marine sediments is that life becomes slow growing or dormant with increased depth due to a lack of new organic matter and stable environmental conditions (Lloyd et al., 2020; Lennon & Jones, 2011). Many researchers have used shallow coastal sediments as a conduit to the deep biosphere of marine sediments (Rambo et al. 2019; Petro et al. 2019; Lloyd et al. 2020; Engelen & Cypionka, 2008). However, the general term of marine sediments also includes shallow coastal sediments, which have a large amount of buried organic matter and are described as very biologically active (Gattuso, Frankignoulle & Wollast, 1998; Yi, Shing Him Lo & Cheng, 2020). Therefore, these shallow coastal sediments may not work under the same constraints expected in deep ocean sediments. Hence the relevance of shallow coastal sediment systems to the deep biosphere remains to be determined.

Environmental variability across marine sedimentary ecosystems (i.e. estuaries, deep sea, mudflats) may provide different physiochemical parameters that could impact

our current understanding of subsurface life and marine sediment carbon burial. For example, estuarine waters and surface sediments may experience drastic changes in water-level, temperature, salinity, and seasonal nutrient deposition whereas deep-sea surface sediments do not experience much variation (Yi, Shing Him Lo & Cheng, 2020; Crump & Bowen, 2024; Rice et al., 1986). Much of our knowledge on buried organic matter degradation in marine sediments is based on work in deep sea marine sediments (Arndt et al., 2013). In marine sediments, a portion of dissolved organic matter (DOM) is chemically altered and becomes resistant to biological degradation, referred to as humic substances (Arndt et al., 2013). In marine sediments of the Chesapeake Bay, humic-like substances have been seen to increase with depth whereas the opposite occurrs for biological activity, which typically decreases with depth (Burdige, Kline & Chen, 2004). The physiochemical factors that affect DOM in deep sea sediments may differ from those of shallow subsurface sediments and present an important relationship with endemic sedimentary microbial life.

Perturbations in the physiochemical environment such as nutrient availability, temperature, CO_2, or pH could stimulate or suppress microbial growth (Ruan et al., 2023). Some typical sedimentary bacterial phyla such as Bacillota and Bacteroidota have been shown to respond rapidly to their environments while others exhibit a slower response time (Ruan et al., 2023). While the physiochemical environment can affect microbial life, microbes can also help create environmental fluctuations, such as the bioavailability of DOM (LaRowe et al., 2020). In Delaware Bay, the amount and type of DOM is controlled by salinity and seasonal biological succession, which impact what can be deposited to the seafloor surface (Powers et al., 2014). Seasonal control such as temperature are well known to impact surface communities (Cartaxana et al., 2015), but yearly temperature data is not widely recorded or available for estuarine sediments. Recent work showed that very shallow (1cm-5cm) coastal sediment types experience varied temperature dynamics that align with seasonal influence (Douglas et al., 2024). Temperature can be a major environmental contributor when discussing selective degradation in marine sediments, metabolic activity, and bioavailability of DOM (Weston & Joye, 2005; Malinverno & Martinez, 2015), but the depth and extent to which seasonal temperatures can impact coastal sediment communities is not well constrained.

In this study, we examined the subsurface changes that occur in the microbial communities of shallow coastal sediments. We present the biological and physiochemical results from three sediment depths in temperate, shallow estuarine sediments over the course of one year. The data collected from 50 cm sediment cores across four seasons

include total organic carbon (TOC), total nitrogen (TN), temperature, and DOM composition measured via fluorescence excitation-emission matrix spectroscopy (EEMs) coupled with the microbial community composition and abundance. The results allow us to examine the transformation of organic matter in marine sediments, and furthermore its impact on microbial life on seasonal timescales in seasonally impacted marine sediments. We show that seasonal blooms of microbes occur within the shallow sediment column, with differing archaeal and bacterial responses.

Methods

Samples were collected from the benthos of the Broadkill River at the end of Oyster Rocks Road in Delaware (38.80216 N, -75.20326 W). During 2024, 50cm sediment cores were collected monthly. The temperature was recorded for the atmosphere, water, and sediment depths at 1cm, 5cm, 10cm, 12-14cm, and 38-40cm on site, using the digital thermometer DeltaTrak (Model 11050). Sediment cores were additionally collected in January 2023, April 2023, July 2024, and October 2023 and were sectioned and stored at -80C until analysis. Analyses were performed on the sections from 12-14cm, 38-40cm and 48-50 cm. Previous work indicates that sediments beneath 6cm at this location are aged over 100 years (Rambo et al. 2019).

TOC/TN Analysis: Total organic carbon and nitrogen analysis was performed on sediment samples subsampled from each seasonal core and depth. Samples were acidified

using 1M HCl to remove inorganic carbon prior to analyzing samples using standard protocol on the Costech Instruments Elemental Combustion System (ECS). Triplicate samples of 2.5 mg of sediment were analyzed for carbon and nitrogen quantification.

DOC Analysis: Porewater was extracted from 2g of thawed sediment and diluted in milli-q water (1:9) in triplicate. Samples were acidified to pH 2 using 2 M HCl prior to measurements of made by high temperature catalytic oxidation (Emery et al., 1971; Sharp et al., 1993) using a Shimadzu TOC-Vcph analyzer. Dissolved organic carbon (DOC) was quantified using non-dispersive infrared detection. DOC concentrations were calculated along with a standard curve generated from measurements of potassium hydrogen phthalate solutions of known concentrations. Aliquots of surface seawater (SSR; Lot# 10-22) and mid-depth seawater reference (MSR; Lot# 10-22) samples from the Consensus Reference Material Project of Hansell Organic Biogeochemistry Laboratory (University of Miami, Florida, USA) were analyzed with in-house standards of ethylenediaminetetraacetic acid and phenylalanine during runs to monitor instrumental precision and accuracy. Standard concentrations within +- 10% of certified values were considered acceptable for QA/QC purposes.

DOM Analysis: Excitation-emission matrix spectra (EEMs) were obtained using a spectrofluorometer (Aqualog, Horiba) to characterize chromophoric and fluorophoric DOM. Milli-q water was used as a blank to adjust spectral intensities. Porewater was extracted from 2g of thawed sediment and diluted in milli-q water (1:9) in triplicate.

EEMs were measured with a 150-W Xenon lamp at 2 nm excitation wavelength intervals between 230 and 700 nm, with emission data collected at 4.65-nm intervals from 245 to 822 nm. EEMs were normalized to Raman Units, and corrected for inner filter effects, 1st and 2nd order Rayleigh scattering using processing tools in Aqualog software. We used R (version 1.46.1) packages "staRdom" and "eemR" to calculate and analyze CDOM and FDOM as well as biological, humification, and fluorescence indices (Pucher et al. 2019). Further details on analytical parameters are outlined by Ouyan et al., 2024 (Ouyang et al., 2024). Dissolved organic carbon (DOC) was measured by high temperature catalytic oxidation (Emery et al., 1971; Sharp et al., 1993) using a Shimadzu TOC-Vcph analyzer.

DNA Extraction and Analysis: 1g of sediment was collected from each seasonal core and depth, and DNA was extracted in triplicate using 0.25g of sediment in the Qiagen DNeasy PowerSoil Pro kit (Germantown, Maryland) following manufacturer instructions. Extracted DNA was used for total quantitative abundance of bacteria and archaea using ThermoScientific maxima SYBR Green qPCR Master Mix and run on a Mx5005P thermocycler. Bacterial 16S rRNA gene counts were determined using B1114F and B1275R primers (Yoshimura, Biddle & York, 2018) and archaeal 16S rRNA gene counts used A915F and A1059R primers (Yoshimura, Biddle & York, 2018). Standard curves were created using a 9-fold dilution series of PCR products made with these primers from environmental samples.

DNA was sent to the UCONN MARS facility for amplicon sequencing of the 16S rRNA gene targeting the V4 region (primers 515F and 806R) using the Illumina MiSeq

paired-end sequencing platform via the v2 2x250 base pair kit (Illumina) following their standard protocol (Parada et al., 2016). Raw forward and reverse sequences were paired, and quality checked; sequences that passed QC were further processed using the 16S rRNA gene analysis pipeline implemented in MOTHUR version 1.46.1 (Schloss et al., 2009). Forward and reverse sequences were aligned and quality filtered using MOTHUR, yielding amplicons ranging in sizes of 130-200 bp in lengths, where ambiguous nucleotides and homopolymer stretches were removed. We opted against the use of amplicon sequence variants (ASV) considering the amount of available computation and created operational taxonomic units (OTU). OTUs were created with a 3% dissimilarity and were aligned and classified against the Silva SSU database, version 138 (Gurevich et al., 2013). Prior to further downstream analysis, nontarget OTUs, i.e. chloroplast and mitochondria, and taxa <1% were removed from representative sequences. Relative 16S rRNA gene abundance was averaged across triplicate sampling of sediment samples.

Diversity analyses of sediments were performed in R using the following packages: VEGAN and tidyverse (Dixon, 2003; Wickham et al., 2019). OTUs were classified to the Class level and assigned a representative for beta diversity analysis among samples. Bray-Curtis dissimilarity matrices were used for non-metric dimensional scaling (NMDS) to visualize beta diversity of sediment depths at different seasons. Statistical significance of TOC and TN across seasons and depths were calculated using one-way ANOVA. Adjusted p-values were calculated using Tukey multiple comparisons

of means. Data has been deposited in the NCBI repository under BioProject number PRJNA1265397.

Results

Yearly Temperature

We analyzed subsurface estuarine sediments for temperature, geochemistry and microbial populations by taxonomy and abundance seasonally for a year. The average temperature of the water and sediment was warmest in summer months (water 27.1°C; 1cm 26.4°C, 38-40cm 23.5°C) and coldest in winter months (water 8.0°C; 1cm 8.06°C, 38-40cm 7.66°C) (Figure 4.1; Table 4.1). In the deepest sediment depth measured, the temperature impacts were similar to the overlying water throughout the year, in that water temperatures changed 19.2°C between January (6.3°C) and July (25.5°C), and the shallowest sediment depth temperatures changed 20.9°C between February (7°C) and July (27.9°C) (Table 4.1). However, the temperature differential between depths was narrower at individual sampling times than when comparing separate depths across month and season (Table 4.1). Temperatures throughout the sediment core exhibited a 1-3°C range difference from shallow to deep, except in May where there was a 4.2°C difference between the shallowest (23.1°C) and deepest (18.9°C) depths (Figure 4.1; Table 4.1). The deepest sediment depth measured warmer than the shallowest sediment depth in October by 2.7°C, November by 1°C and December by 1.2°C (Figure 4.1; Table 4.1).

Geochemistry

The average total nitrogen ranged from 0.313 to 1.38 mg of N/g and the average total organic carbon ranged from 9.81 to 16.57 mg of C/g (Figure 4.2; Table 4.2). The total nitrogen (TN) exhibited no statistical significance in variation across season or by depth (Figure 4.2A). Total organic carbon (TOC) decreased with depth in the spring core but increased with depth in fall and winter cores and was consistent with depth in the summer core (Figure 4.2B). TOC only exhibited significant statistical variation at 12-14cm depth (p-value = 0.015) between spring and fall cores (adjusted p-value = 0.009). Due to destructive sampling for biological measurements, these nitrogen and carbon values indicate that the background of sedimentary material was relatively consistent across cores collected for this project.

We utilized fluorescence excitation-emission matrix spectroscopy (EEMs) to examine the extractable organic material from the core material. EEMs utilizes specific wavelengths to differentiate between chromoflouric (CDOM) and fluorophoric (FDOM) forms of organic matter pools in the environment. The specific UV absorbance at 254 nm (SUVa254), a measure of DOM aromaticity, ranged from 14.42 to 20.83 L mg-C^{-1} m^{-1}(Figure 4.3; Table 4.3). The humification index (HIX), biological index (BIX) and fluorescence index (FI) from EEMs ranged from 1.56 to 1.81, 0.92 to 1.09 and 1.20 to 1.27, respectively (Figure 4.3; Table 4.3). Marine-like humic DOM (m) ranged from 0.01 to 0.04, while humic-like DOM (a) ranged from 0.06 to 0.08 Raman units (RU)

(Figure 4.3; Table 4.3). Tryptophan-like DOM (t) ranged from 0.05 to 0.08 RU and tyrosine-like DOM (b) ranged from 0.1 to 0.15 RU (Figure 4.3; Table 4.3). Dissolved organic carbon ranged between 34-47 micromolar across all samples (Table 4.3).

Specific ultraviolet absorbance (SUVa254) values varied across samples and were highest at 48-50cm depth in the summer core and lowest at the same depth in the winter core (Figure 4.3). In the summer core, SUVa254 increased with depth, whereas in the spring and winter cores, the highest concentrations were observed at the 38-40 cm depth (Figure 4.3). Humic-like DOM (m and a) was most abundant in the summer core (Figure 4.3). Marine-like humic DOM (m) increased with depth in the summer core but decreased with depth in the winter core, while concentrations remained consistent throughout the cores in spring and fall (Figure 4.3). Marine-like humic DOM was lowest at depth 48-50 cm in the winter core (Figure 4.3). Humic-like DOM (a) was lowest at 12-14 cm depth in fall (Figure 4.3). In the fall, summer, and spring cores humic-like DOM showed similar trends of increasing with depth while concentrations decreased with depth in the winter core (Figure 4.3).

Tryptophan and tyrosine-like DOM exhibited peak concentrations at the deepest depth in the summer core (Figure 4.3). Tryptophan-like DOM increased with depth in the summer and fall cores, decreased with depth in the winter core, and remained consistent in the spring core (Figure 4.3). Tryptophan-like (t) DOM peaked at 48-50 cm in the summer core, while it was lowest at 12-14 cm in the fall core (Figure 4.3). Tyrosine-like

(b) DOM was the highest at 48-50 cm in the summer core and lowest at 12-14 cm in the spring core (Figure 4.3). In both summer and spring cores, tyrosine-like DOM increased with depth in but decreased with depth in the winter cores (Figure 4.3).

The humification index (HIX) showed an increase in humification with depth in the spring, fall, and winter cores but a decrease by depth in the summer core (Figure 4.3). HIX was highest at 12-14 cm in the summer core and lowest at the same depth in the fall core (Figure 4.3). The fluorescence index (FI) increased by depth in spring, fall, and winter cores but decreased by depth in the summer core (Figure 4.3). FI values were highest at 38-40 cm in the spring core and lowest at 12-14 cm in the spring and winter cores (Figure 4.3). The biological index (BIX) suggested an increase in recent biological activity with increasing depth in the summer core, remained consistent with depth in the spring core, and decreased with depth in the fall and winter cores (Figure 4.3). The BIX index was the highest at 12-14 cm in the fall core and lowest at the same depth in the summer core (Figure 4.3).

Microbial Composition and Abundance

We observed similar microbial compositions across both seasons and depths. Dehalococcoidia, Anaerolineae, Bathyarchaeia, and Phycisphaerae were the most abundant class-level taxa observed across season and depth (Figure 4.4). We observed subtle shifts in taxa abundance and composition across seasons and depths (Figure 4.4). In the winter core, Alphaproteobacteria, Aminicenantia, and Methanomicrobia, and

unclassified taxa increased in the 12-14 cm depth taxa whereas Parcubacteria, Clostrida, and Lokiarcheia increased at 38-40 cm and Nanoarcheia and Phycisphaerae increased at 48-50 cm (Figure 4.4). In spring, Paracubacteria appeared as an abundant taxon at 38-40 cm and 48-50 cm depths (Figure 4.4). In the summer core, Plantomycetes and Alphaproteobacteria decreased with depth while the relative abundance of Bathyarchaeia increased with depth (Figure 4.4). In the fall core, Thermoplasmata decreased with depth and Clostridia increased with depth (Figure 4.4). The top 15 averaged microbial classes seemed similar, however beta-diversity analysis (NDMS) on these samples show that the microbial composition does vary across sample season, depth, and even biological replicates (Figure 4.5). The largest variation is seen in the deepest summer samples, with the least variation in spring samples.

Average quantitative PCR (qPCR) 16S rRNA gene copies ranged from $1.50x10^{10}$ to $4.22x10^{11}$ genes/g sediment using archaeal primers and $1.89x10^{11}$ to $2.50x10^{12}$ genes/g sediment using bacterial primers (Figure 4.6; Table 4.5). Archaeal 16S rRNA gene copies generally increased in fall, summer, and winter cores with depth, but peak in spring at depth 38-40cm ($4.22x10^{11}$ genes/g sediment), ~20-fold higher than other seasonal cores, and are lowest in the winter core at the same depth ($1.95x10^{10}$ genes/g sediment) (Figure 4.6A). Bacterial 16S rRNA gene copies generally increase with depth in the summer, fall, and winter cores but decrease with depth in the spring core (Figure 4.6B). Bacterial gene copies are ~15-fold higher overall in the summer core than other seasons and peak at depth 38-40 cm ($2.50x10^{12}$ genes/g sediment) but are lowest in the spring core ($1.43x10^{11}$ genes/g sediment) at depth 48-50 cm (Figure 4.6B).

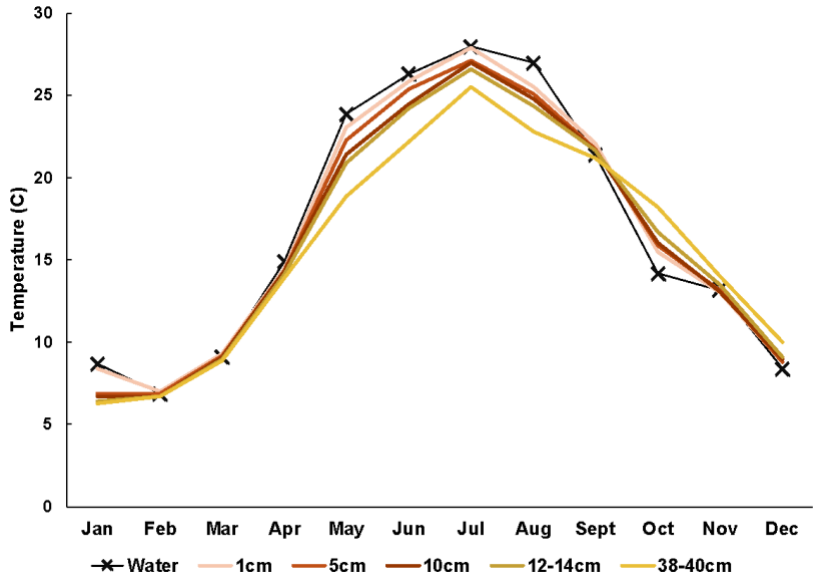

Figure 4.1. Recorded temperature of water and sediment depths over a year. Data presents a lag in sediment depth temperature behind oscillating water temperatures and a preservation of heat within sediment when water cools in fall.

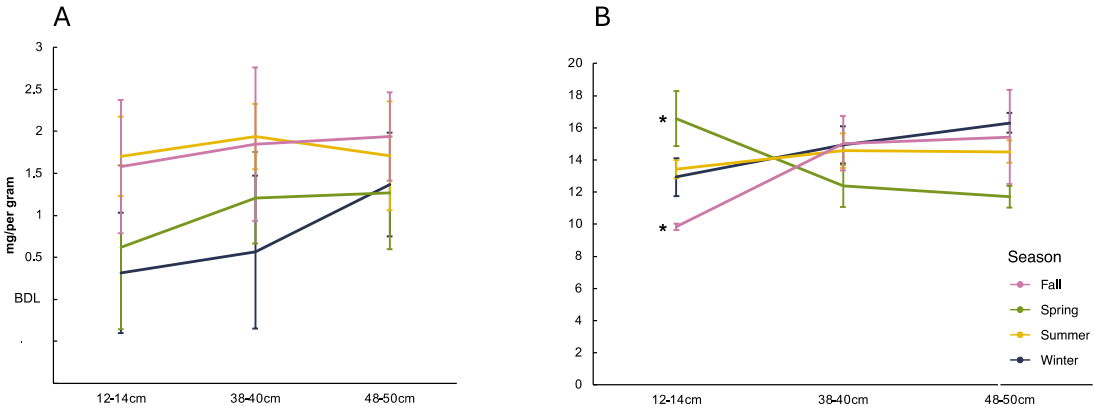

Figure 4.2. Average milligrams of total nitrogen (A) and organic carbon (B) across seasons at different depths with SE bars. Data shows no statistically significant variability in overall total nitrogen across seasons, however and organic carbon exhibits statistically significant variation at depth 12-14cm (p-value = 0.015) between spring and fall sampling (adjusted p-value = 0.009) indicated by black asterisks. Below detection limit (BDL).

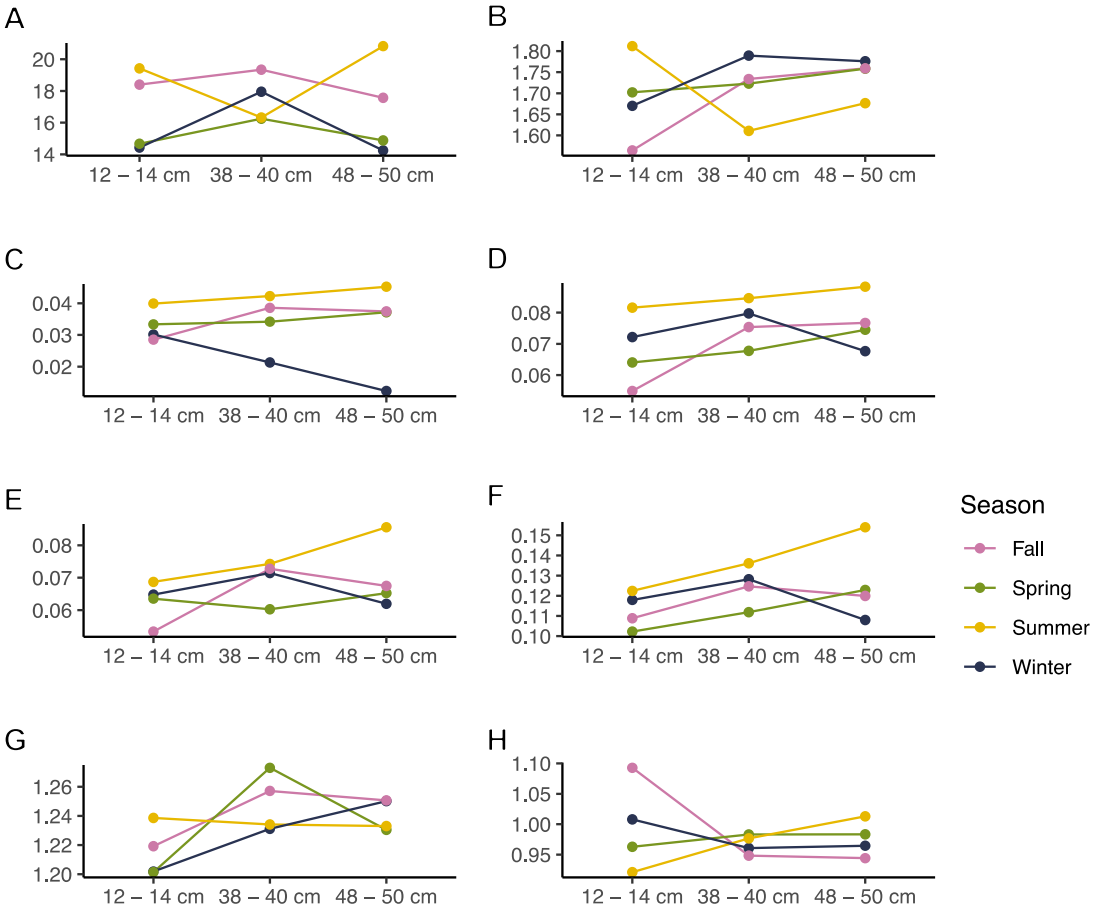

Figure 4.3. Excitation Emission Matrix (EEMs) indices characterizing DOM across depth and seasons. A) Specific ultraviolet absorbance (SUVa254) is used to estimate the percentage of aromatic carbon content of humics, B) humification index (HIX) measures the degree to which C/N organic matter is polycondensation in soil, C) marine-like humics (m), D) humic-like compounds (a), E) tyrosine-like (t) refers to protein-like molecules , F) tryptophan-like (b) refers to amino acids, G) fluorescence index (fi) indicates algal/microbial or terrestrial origins of organic matter, and H) biological activity index (BIX) suggests recent biological activity contribution to DOM.

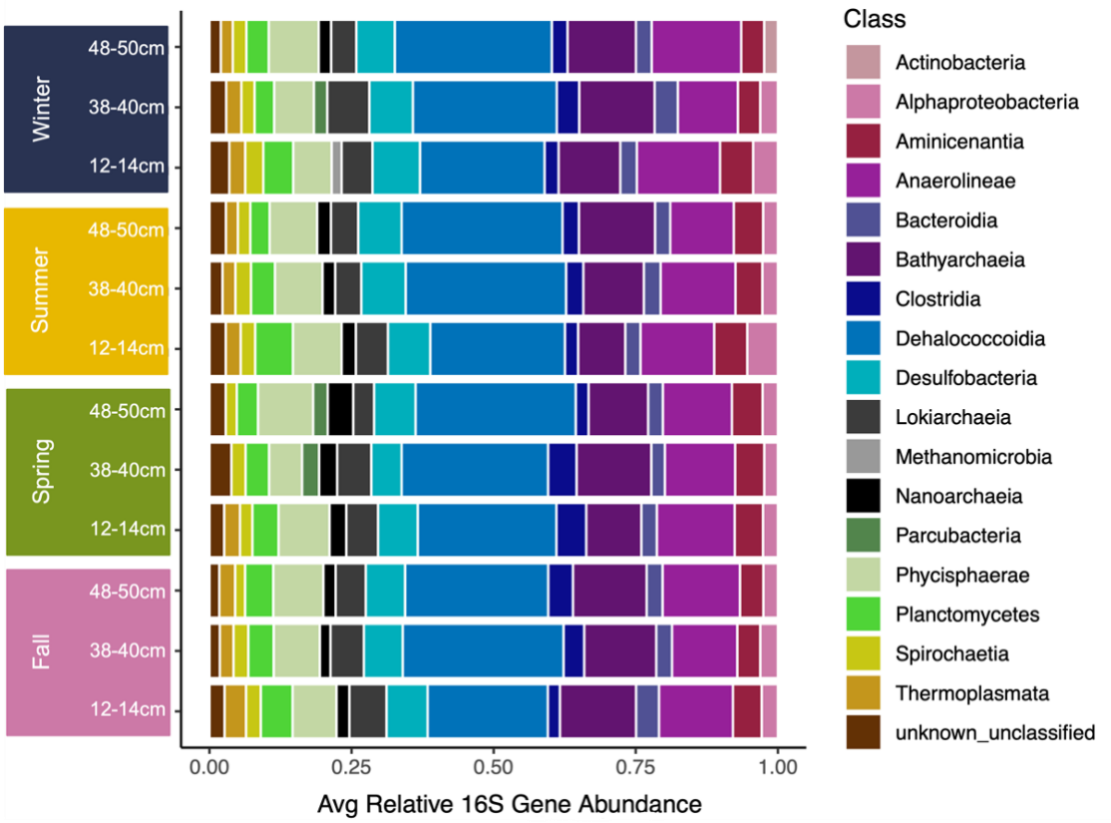

Figure 4.4. Top 15 most abundant microbial Classes based on 16S rRNA gene percent abundance averaged across triplicate samples that have been identified to Class level from the seasonal cores. Data shows the dominant abundance of Dehalococcoidia across seasons and depths and more subtle shifts in less abundant taxa with season and depth. Parcubacteria are not seen in every season and are most abundant at depth in spring.

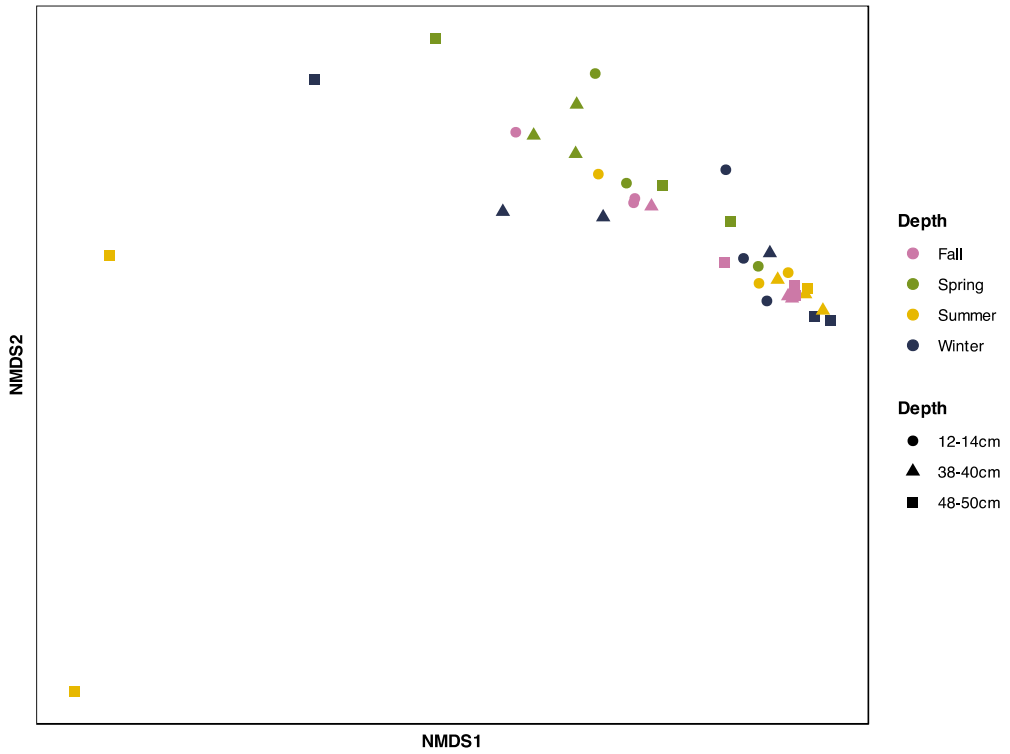

Figure 4.5. Non-metric Dimensional Scaling (NMDS) of a Bray-Curtis similarity matrix from Class-level taxonomic identification of the16S rRNA gene sequences across sediment cores and depths over seasons (Stress 0.04). There is composition variability among season, depth, and triplicate sub-sampling, which is very pronounced for the deepest summer sample.

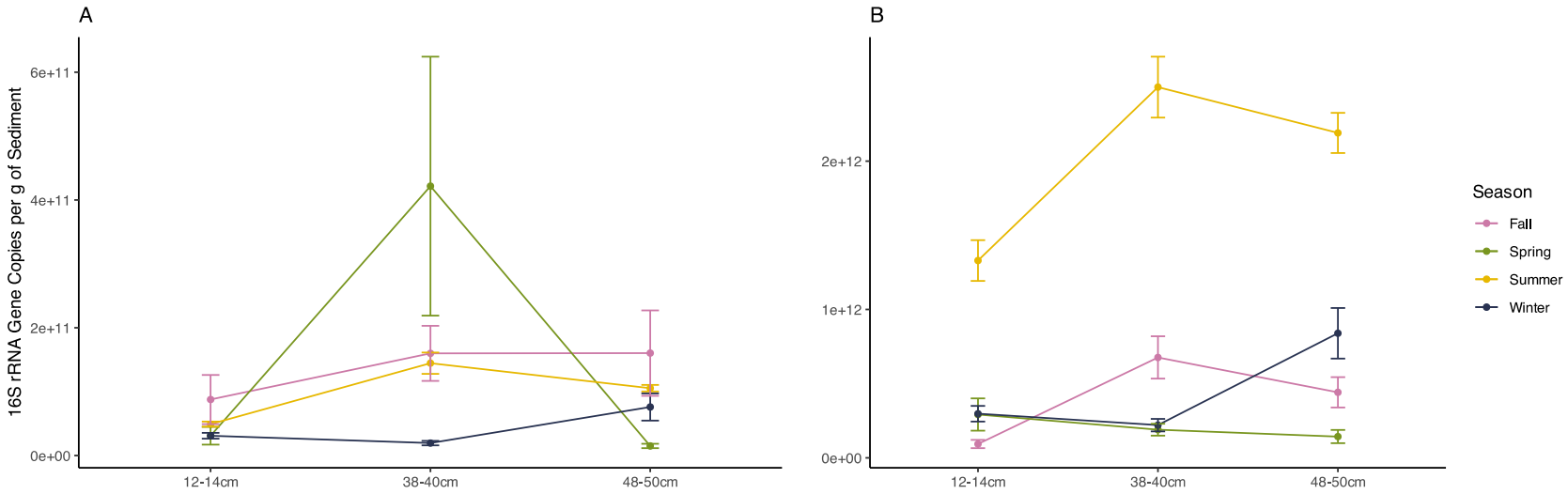

Figure 4.6. Average qPCR 16S rRNA gene abundance per gram of sediment for archaeal (A) and bacterial (B) populations across seasons with SE bars. Archaeal abundance peaks in the Spring core mid-depth while overall bacterial abundance peaks in the Summer core.

Discussion & Conclusion

In this study, we investigated the seasonal variations in both the environment and the microbial community in shallow estuarine sediments over the course of a year. Our results revealed that sediment temperatures mirror the seasonal shifts in water temperature, extending down to depths of 38-40 cm. This finding is particularly significant, as much research has focused on temperature fluctuations within the top 10 cm of shallow estuarine sediments (Douglas et al., 2024). As a result, the influence of temperature on microbial activity, the availability of dissolved organic matter (DOM), and gas-phase changes that occur throughout the seasons in these shallow coastal sediments may be underestimated due to the lack of accurate temperature data at depth. The microbial community observed in the sediments included common anaerobes, facultative anaerobes, and other typical marine sediment microorganisms, many of which are from taxa known to perform processes such as sulfate reduction, methanogenesis, and alkane degradation (Jones, Beeman & Suflita, 1989). While the types of microbes remained relatively consistent across seasons, the abundance of specific taxa varied greatly. This was observed in changes of relative abundance within the averaged top 15 microbial classes that included Parcubacteria only in deep spring core and the mid depth winter core samples. Parcubacteria are considered potential symbionts of Bacteria (Nelson & Stegen, 2015) and have been described with fermentative metabolisms that could produce volatile fatty acids and hydrogen to other organisms (Vigneron et al. 2019; Danczak et al. 2017). While Parcubacteria are often abundant in environments, it is notable that they are only significantly abundant in a minority of our samples,

considering the relative stability of the geochemical measurements. These fermentative microbes could be responding to shifts in usable organic matter and could influence the later shifts recognized in the growth of other taxa during offset seasons. There is also still the possibility that these shifts are due to the heterogeneous nature of sediments, however, we combined three distinct samples per depth and controlled for geochemistry, and none of these samples show any increase in available carbon compared to the other samples. Hence, we interpret the increase in Parcubacteria as significant in these samples.

Total nitrogen (TN) measurements remained consistent across depth and seasons, showing no significant seasonal variation, which is not unexpected in these anoxic sediments (Ogrinc et al., 2005). In deep marine sediments, TN is generally known to decrease with depth (Wakeham, 2002; Burdige, 2007). Total organic carbon (TOC) showed more variation than TN, with a statistically significant variation between spring and fall at the 12-14 cm depth. Previous work has shown that sediments in this location below 6 cm depth have an age over 100 years (Rambo et al. 2019), so little change was anticipated in the TOC at this depth. This variation is bolstered by the apparent differences in the biological index (BIX) and humification index (HIX), in that the fall humification index is higher than spring, and the fall biological index is highest. We interpret this variation to suggest the TOC in the fall core at 12-14cm is biologically derived organic matter. This biologically derived organic matter could potentially be microbial necromass, as the summer core showed much higher abundances of bacteria, without concurrently higher TOC or TN, and the abundance of 16S rRNA genes are

lower in the fall sample. In the summer core, we observed the highest index in tyrosine- and tryptophan-like DOM (b, t) which increases with depth, signatures of microbially-derived amino acids, concurrent with the high abundance of bacteria during this season. This pattern aligns with the warmer temperatures, which we hypothesize stimulates metabolic activity in sediments.

The fluorescence index (FI) derived from EEM spectra provides insight into the origin of the DOM. A FI around 1.2 typically indicates terrestrially derived organic matter, while values approaching 1.8 suggests microbially sourced organic matter (Coble, Lead & Baker, 2014). In our study, archaeal abundance significantly peaked at the 38-40 cm depth in spring, coinciding with an increase in FI, suggesting that microbially derived DOM contributed significantly to the overall DOM at this depth and season. Bacterial abundance also increased throughout the summer, coinciding with the highest measured concentrations of fluorophoric (b,t) DOM, values typically driven by amino acids. The fluorophoric portion of the DOM (m, a) are often described as humic, and these are also higher in the summer core, however, there is no significant change in TN or TOC in the summer core, suggesting that the DOM present in the summer core is of a different nature than the other seasons. The increased fluorophoric abundance (m, a) in summer suggest that we may be measuring microbially derived DOM in the summer core. While bacterial and archaeal "blooms" in marine sediments are not widely accepted due to the perceived lack of bioavailable carbon substrates, our observations challenge this notion. They indicate that microbial communities in these sediments may thrive in response to seasonal

variables such as higher temperature in summer. The observed increase in $SUVA_{254}$ values suggests elevated aromaticity of the dissolved organic matter (DOM) in these samples. However, our values are higher than those typically reported in the literature (D'Andrilli et al., 2022). This enhancement is likely attributable to the presence of colloidal materials in sediments, which can influence the optical properties of DOM (Philippe & Schaumann, 2014). The direct impact of these materials on our excitation-emission matrix EEM-based analyses, however, remains to be fully understood.

If microbial blooms are possible in shallow coastal sediments, this challenges the notion that shallow sediments are sufficient windows into the deep biosphere (Rambo et al. 2019; Petro et al. 2019; Lloyd et al. 2020; Engelen & Cypionka, 2008). While the taxa of microbes found in these locations are similar to the deep sea, the view of microbial history with depth cannot be carried over to shallow sediments, unless the researchers are able to prove that the community is stable subsurface. Additionally, we show that geochemical DOM characterization can assist in assessing the organic matter nature in the subsurface. As use of EEMs in marine sediments continues to expand, future work may introduce the establishment of new spectroscopy identification methods, providing higher resolution in characterizing DOM in marine sediments. Additionally, studies that include the total characterization of inorganic and gas shifts would better elucidate the carbon cycling possible throughout the year in the subsurface.

Our findings emphasize the importance of seasonal and depth-dependent changes in environmental factors, such as temperature, organic matter composition, and microbial community dynamics in estuarine sediments. Temperature fluctuations may have a

significant impact on microbial populations, influencing the character of dissolved organic matter. This study highlights the complex interplay between physical, chemical, and biological factors in shaping the microbial landscape of shallow sediments. Future research should focus on further distinguishing specific changes in organic matter and microbial taxa in response to seasonal succession and how they contribute to the overall function of organic matter degradation and diagenesis in shallow coastal sediments.

REFERENCES

6. Kallmeyer, J., Pockalny, R., Adhikari, R. R., Smith, D. C., & D'Hondt, S. (2012). Global distribution of microbial abundance and biomass in subseafloor sediment. *Proceedings of the National Academy of Sciences*, *109*(40), 16213-16216.

7. Bar-On, Y. M., Phillips, R., & Milo, R. (2018). The biomass distribution on Earth. Proceedings of the National Academy of Sciences, 115(25), 6506-6511.

8. Lloyd, K. G., Bird, J. T., Buongiorno, J., Deas, E., Kevorkian, R., Noordhoek, T., ... & Roy, T. (2020). Evidence for a growth zone for deep-subsurface microbial clades in near-surface anoxic sediments. Applied and Environmental Microbiology, 86(19), e00877-20.

9. Lennon, J. T., & Jones, S. E. (2011). Microbial seed banks: the ecological and evolutionary implications of dormancy. Nature reviews microbiology, 9(2), 119-130.

10. Gattuso, J. P., Frankignoulle, M., & Wollast, R. (1998). Carbon and carbonate metabolism in coastal aquatic ecosystems. Annual Review of Ecology and Systematics, 29(1), 405-434.

11. Yi, J., Lo, L. S. H., & Cheng, J. (2020). Dynamics of microbial community structure and ecological functions in estuarine intertidal sediments. Frontiers in Marine Science, 7, 585970.

12. Crump, B. C., & Bowen, J. L. (2024). The microbial ecology of estuarine ecosystems. Annual Review of Marine Science, 16(1), 335-360.

13. Rice, A. L., Billett, D. S. M., Fry, J., John, A. W. G., Lampitt, R. S., Mantoura, R. F. C., & Morris, R. J. (1986). Seasonal deposition of phytodetritus to the deep-sea floor. Proceedings of the Royal Society of Edinburgh, Section B: Biological Sciences, 88, 265-279.

14. Arndt, S., Jørgensen, B. B., LaRowe, D. E., Middelburg, J. J., Pancost, R. D., & Regnier, P. (2013). Quantifying the degradation of organic matter in marine sediments: A review and synthesis. Earth-science reviews, 123, 53-86.

15. LaRowe, D. E., Arndt, S., Bradley, J. A., Estes, E. R., Hoarfrost, A., Lang, S. Q., ... & Zhao, R. (2020). The fate of organic carbon in marine sediments-New insights from recent data and analysis. Earth-Science Reviews, 204, 103146.

16. Ouyang, T., McKenna, A. M., & Wozniak, A. S. (2024). Storm-driven hydrological, seasonal, and land use/land cover impact on dissolved organic matter dynamics in a mid-Atlantic, USA coastal plain river system characterized by 21 T FT-ICR mass spectrometry. Frontiers in Environmental Science, 12, 1379238.

17. Krom, M. D., & Sholkovitz, E. R. (1977). Nature and reactions of dissolved organic matter in the interstitial waters of marine sediments. Geochimica et Cosmochimica Acta, 41(11), 1565-1574.

18. Burdige, D. J., Kline, S. W., & Chen, W. (2004). Fluorescent dissolved organic matter in marine sediment pore waters. Marine Chemistry, 89(1-4), 289-311.

19. Fischer, H., Wanner, S. C., & Pusch, M. (2002). Bacterial abundance and production in river sediments as related to the biochemical composition of particulate organic matter (POM). Biogeochemistry, 61, 37-55.

20. Ruan, Y., Kuzyakov, Y., Liu, X., Zhang, X., Xu, Q., Guo, J., ... & Ling, N. (2023). Elevated temperature and CO2 strongly affect the growth strategies of soil bacteria. Nature communications, 14(1), 391.

21. Powers, L. C., Luek, J. L., Schmitt-Kopplin, P., Campbell, B. J., Magen, C., Cooper, L. W., & Gonsior, M. (2018). Seasonal changes in dissolved organic matter composition in Delaware Bay, USA in March and August 2014. Organic geochemistry, 122, 87-97.

22. Douglas, E. J., Lam-Gordillo, O., Hailes, S. F., Lohrer, A. M., & Cummings, V. J. (2024). Characterising intertidal sediment temperature gradients in estuarine systems. Estuarine, Coastal and Shelf Science, 309, 108968.

23. Weston, N. B., & Joye, S. B. (2005). Temperature-driven decoupling of key phases of organic matter degradation in marine sediments. Proceedings of the National Academy of Sciences, 102(47), 17036-17040.

24. Engelen, B., & Cypionka, H. (2009). The subsurface of tidal-flat sediments as a model for the deep biosphere. *Ocean Dynamics*, *59*, 385-391.

25. Malinverno, A., & Martinez, E. A. (2015). The effect of temperature on organic carbon degradation in marine sediments. Scientific Reports, 5(1), 17861.

26. Parkes, R. J., Webster, G., Cragg, B. A., Weightman, A. J., Newberry, C. J., Ferdelman, T. G., ... & Fry, J. C. (2005). Deep sub-seafloor prokaryotes stimulated at interfaces over geological time. Nature, 436(7049), 390-394.

27. Schloss, P. D., Westcott, S. L., Ryabin, T., Hall, J. R., Hartmann, M., Hollister, E. B., ... & Weber, C. F. (2009). Introducing mothur: open-source, platform-independent, community-supported software for describing and comparing microbial communities. Applied and environmental microbiology, 75(23), 7537-7541.

28. Gurevich, A., Saveliev, V., Vyahhi, N., & Tesler, G. (2013). QUAST: quality assessment tool for genome assemblies. Bioinformatics, 29(8), 1072-1075.

29. Walters, W., Hyde, E. R., Berg-Lyons, D., Ackermann, G., Humphrey, G., Parada, A., ... & Knight, R. (2016). Improved bacterial 16S rRNA gene (V4 and V4-5) and fungal internal transcribed spacer marker gene primers for microbial community surveys. Msystems, 1(1), 10-1128.

30. Yoshimura, K. M., York, J., & Biddle, J. F. (2018). Impacts of salinity and oxygen on particle-associated microbial communities in the Broadkill River, Lewes DE. *Frontiers in Marine Science*, *5*, 100.

31. Vuillemin, A., Wankel, S. D., Coskun, Ö. K., Magritsch, T., Vargas, S., Estes, E. R., ... & Orsi, W. D. (2019). Archaea dominate oxic subseafloor communities over multimillion-year time scales. Science Advances, 5(6), eaaw4108.

32. Starnawski, P., Bataillon, T., Ettema, T. J., Jochum, L. M., Schreiber, L., Chen, X., ... & Kjeldsen, K. U. (2017). Microbial community assembly and evolution in subseafloor sediment. Proceedings of the National Academy of Sciences, 114(11), 2940-2945.

33. Ogrinc, N., Fontolan, G., Faganeli, J., & Covelli, S. (2005). Carbon and nitrogen isotope compositions of organic matter in coastal marine sediments (the Gulf of Trieste, N Adriatic Sea): indicators of sources and preservation. Marine chemistry, 95(3-4), 163-181.

34. Pucher, M., Wünsch, U., Weigelhofer, G., Murphy, K., Hein, T., & Graeber, D. (2019). staRdom: versatile software for analyzing spectroscopic data of dissolved organic matter in R. Water, 11(11), 2366.

35. Dixon, P. (2003). VEGAN, a package of R functions for community ecology. Journal of vegetation science, 14(6), 927-930.

36. Wickham, H., Averick, M., Bryan, J., Chang, W., McGowan, L. D. A., François, R., ... & Yutani, H. (2019). Welcome to the Tidyverse. Journal of open source software, 4(43), 1686.

37. Petro, C., Zäncker, B., Starnawski, P., Jochum, L. M., Ferdelman, T. G., Jørgensen, B. B., ... & Schramm, A. (2019). Marine deep biosphere microbial communities assemble in near-surface sediments in Aarhus Bay. *Frontiers in Microbiology*, *10*, 758.

38. Rambo, I. M., Marsh, A., & Biddle, J. F. (2019). Cytosine methylation within marine sediment microbial communities: potential epigenetic adaptation to the environment. Frontiers in Microbiology, 10, 1291.

39. Cartaxana, P., Vieira, S., Ribeiro, L., Rocha, R. J., Cruz, S., Calado, R., & da Silva, J. M. (2015). Effects of elevated temperature and CO 2 on intertidal microphytobenthos. BMC ecology, 15, 1-10.

40. Nelson, W. C., & Stegen, J. C. (2015). The reduced genomes of Parcubacteria (OD1) contain signatures of a symbiotic lifestyle. Frontiers in microbiology, 6, 713.

41. Vigneron, A., Cruaud, P., Langlois, V., Lovejoy, C., Culley, A. I., & Vincent, W. F. (2020). Ultra-small and abundant: candidate phyla radiation bacteria are potential catalysts of carbon transformation in a thermokarst lake ecosystem. Limnology and Oceanography Letters, 5(2), 212-220.

42. Danczak, R. E., Johnston, M. D., Kenah, C., Slattery, M., Wrighton, K. C., & Wilkins, M. J. (2017). Members of the Candidate Phyla Radiation are functionally differentiated by carbon-and nitrogen-cycling capabilities. Microbiome, 5, 1-14.

43. Wakeham, S. (2002). Diagenesis of organic matter at the water-sediment interface. In Chemistry of marine water and sediments (pp. 147-164). Berlin, Heidelberg: Springer Berlin Heidelberg.

44. Burdige, D. J. (2007). Preservation of organic matter in marine sediments: controls, mechanisms, and an imbalance in sediment organic carbon budgets?. Chemical reviews, 107(2), 467-485.

45. Coble, P. G., Lead, J., & Baker, A. (Eds.). (2014). Aquatic organic matter fluorescence. Cambridge University Press.

46. Jones, R. E., Beeman, R. E., & Suflita, J. M. (1989). Anaerobic metabolic processes in the deep terrestrial subsurface. Geomicrobiology Journal, 7(1-2), 117-130.

47. Ogrinc, N., Fontolan, G., Faganeli, J., & Covelli, S. (2005). Carbon and nitrogen isotope compositions of organic matter in coastal marine sediments (the Gulf of Trieste, N Adriatic Sea): indicators of sources and preservation. *Marine chemistry*, *95*(3-4), 163-181.

48. D'Andrilli, J., Silverman, V., Buckley, S., & Rosario-Ortiz, F. L. (2022). Inferring ecosystem function from dissolved organic matter optical properties: a critical review. *Environmental science & technology*, *56*(16), 11146-11161.

49. Philippe, A., & Schaumann, G. E. (2014). Interactions of dissolved organic matter with natural and engineered inorganic colloids: a review. *Environmental science & technology*, *48*(16), 8946-8962.

ASSESSING REDOX INFLUENCE ON MICROBIAL COMMUNITIES IN COASTAL SEDIMENTS

Introduction

Marine sediments are thought to harbor 15% of the planet's biomass (Kallmeyer et al., 2012; Bar-On, Phillips & Milo, 2018). Signs of microbial life have been detected at depths of up to 2.5 km below the seafloor surface, demonstrating the remarkable persistence of life under extreme conditions (Roussel et al., 2008). As microbial communities become increasingly buried over geological timescales, the environmental variables that govern their growth, physiology, and metabolic activity such as temperature, pressure, redox potential, and nutrient availability change substantially (Reimers et al., 2013; Cook et al., 2007; Grossart & Gust, 2009). The uppermost 10 cm of marine sediments play a critical role in the deposition and long-term storage of organic matter, serving as a key interface between the water column and subsurface biosphere (Calvert & Pederson, 1992; Wakeham & Canuel, 2005). In particular, coastal sediments often exhibit elevated rates of organic matter burial due to the confluence of high terrestrial and marine productivity, as well as sediment trapping at the land-sea margin (Gonneea, Paytan & Herrera-Silveira, 2004; Calvert & Pederson, 1992; Hutchings, 2020).

Vast quantities of organic matter are deposited and subsequently buried in coastal sediments, initiating the process of diagenesis, a number of physical, chemical, and

biological changes that organic matter undergoes after initial sediment deposition (Van Cappellen, Gaillard & Rabouille, 1993). In shallow sediment layers, microbial metabolisms such as aerobic respiration and nitrification dominate, utilizing oxygen and nitrate, respectively, as terminal electron acceptors to drive the remineralization of organic carbon (Sørensen, Jørgensen & Revsbech, 1979). However, as sediment depth increases and conditions become anoxic, the availability of these high-energy electron acceptors decreases (Reimers et al., 2013). These deeper layers exhibit increased concentrations of reduced sulfur species and C1 compounds such as methane, reflecting the ongoing activity of sulfate-reducing bacteria and methanogenic archaea (Sela-Adler et al., 2017; Maltby et al., 2018). The shift from oxic to anoxic environments creates a shift in redox potential, which serves as a critical regulator of microbial community structure and metabolic function in sedimentary environments (Reimers et al., 2013, Hunter, Wang & Van Cappellen, 1998).

Redox reactions refer to both oxidation and reduction processes, and these processes play a fundamental role in regulating microbial metabolism through terminal electron donors and acceptors (Burgin et al., 2011). In deep marine sediments, the degradation of organic matter becomes energetically unfavorable due to the depletion of high-energy electron acceptors such as oxygen and nitrate (Boetius & Lochte, 1994; Bradley et al., 2022). As a result, microbes are forced to rely on lower-energy metabolic pathways like sulfate reduction and methanogenesis, which dominate low redox potential environments (Burgin et al., 2011; Chiarabelli, Stano & Luisi, 2013). Redox itself is a key environmental variable that shapes the structure, function, and activity of microbial communities in marine sediments (Bradley et al., 2022). Although much is known about redox-driven metabolic processes, a significant portion of microbial diversity in these environments remains uncultured and poorly characterized (Chiarabelli, Stano & Luisi, 2013; Bradley et al., 2022). Many of these uncultivated taxa likely play essential roles in carbon cycling and methane transformation, but their metabolic capabilities and ecological functions are still largely inferred from metagenomic predictions rather than experimental validation (Boetius & Lochte, 1994; Bradley et al., 2022).

Genomic and metagenomic studies have revealed a vast diversity of uncultured microbial taxa across marine sediments; however, progress in isolating and cultivating these organisms has been limited (Ravin, Mardanov & Skryabin, 2015). High-throughput -omics approaches, including metagenomics, metatranscriptomics, and metabolomics, have provided valuable insights into the metabolic potential of these microbial

communities further highlighting pathways such as methane oxidation, sulfate reduction, and metabolite biosynthesis (Wang et al., 2017). For instance, Lokiarchaeota demonstrated the ability to degrade proteins and fatty acids under anoxic conditions, findings that align with prior metagenomic predictions about its role in anaerobic carbon cycling (Spang et al., 2015; Sousa et al., 2016; Dombrowski et al., 2020). While -omics methods are powerful tools for predicting microbial function, they cannot directly characterize the physicochemical conditions such as redox potential, substrate availability, and electron acceptor concentration that influence microbial activity *in situ* (Sun et al., 2020). To bridge this gap, experimental cultivation and physiological testing of uncultured taxa are essential. By doing so, we can validate genomic predictions and gain a more mechanistic and comprehensive understanding of the ecological roles, metabolic constraints, and environmental tolerances of microbes driving biogeochemical processes in estuarine sediments.

In this study, we examined how variations in redox potential and sediment depth influence the composition and activity of anaerobic microbial communities in estuarine sediments from Delaware Bay. Over a six-month incubation period, we monitored methane headspace and microbial community dynamics under a range of controlled low redox conditions using sodium dithionite and titanium (III) citrate. We fed our microcosms volatile fatty acids that are common products of organic matter fermentation. Our findings reveal that while the microbial communities initially reflect the depth-specific characteristics of their source sediments, manipulation of redox potential can drive community convergence, suggesting a strong environmental filtering effect.

Additionally, our results highlight the critical roles of inoculum origin, reductant selection, and redox conditions in shaping anaerobic microbial communities in vitro. These findings provide valuable insights into the environmental factors that govern microbial community structure and function in marine sediment ecosystems.

Methods

Oyster Rocks Preserve is a tidally influenced temperate estuary located along the Broadkill River estuary. A 51cm sediment core was collected below the wrack line at Oyster Rocks Preserve in the Broadkill River estuary, Milton, Delaware USA (38.80214 N, 75.20332 W) in October 2023 using a 1-meter-long polycarbonate tube with a 4cm diameter. The core was collected away from vegetation and potential bioturbated sediments. The core was brought to the lab the same day and sectioned into 2cm slices at 12-14cm, 38-40cm and 48-50cm for sampling and inoculation. Each 2cm section was sampled by collecting 5g of sediment for inoculation and 0.25g in triplicate for DNA extraction while the remaining sediment was stored at -80 C.

Media Preparation and Initial Inoculation

Marine minimal media was prepared by adding KBr (0.09g/L), KCl (0.66g/L), $CaCl_2*H_2O$ (0.30g/L), $MgCl_2*6H_2O$ (3.20g/L), NaCl (18.6g/L) in sterile milli-Q water. Minimal media was autoclaved and degassed using N_2/CO_2. The following solutions were added to the marine minimal media: N_aHCO_3 buffer (1 M, 30mL/L), NH_4CI/KH_2PO_4 buffer (NH_4Cl 5g/L; KH_2PO_4 4g/L, 50mL/L), filter-sterilized vitamin

solution SI10 (DSMZ medium 141) (1mL/L), and filter-sterilized trace element solution TS15v (DSMZ medium 141) (1mL/L). 25mL of the solution was added to each serum bottle then sealed and crimped with rubber stoppers. Serum bottles were then made anaerobic by venting and gassing with N_2 for 10 minutes in the media and 5 minutes in the headspace, followed by venting and gassing with 80% N_2/ 20% CO_2 gas mix for 10 minutes in the media and 5 minutes in the headspace. Concentrations of titanium (Ill) citrate stock solution (100 mM stock solution; 1.7mM, 2.4mM, 3.1mM) and sodium dithionite (143.5 mM stock solution; 8.6 mM, 11.5 mM) were used as reductant agents to achieve set redox potentials. Additional bottles were prepared with the intention of reducing sulfate reduction by using (242.8 mM stock solution; 24.3 mM and 34 mM) concentrations of sodium molybdate (IV) dihydrate. Redox potentials were monitored using the Pinpoint ORP/REDOX probe (American Marine Inc., Ridgefield, CT). Organic acids (acetate, butyrate, and propionate) were added to each enrichment at 5mM concentration. Filter-sterilized antibiotic solution consisting of ampicillin (0.5g/20mL H_2O), rifampicin (0.5g/10mL methanol), tetracycline (0.5/10mL H_2O), vancomycin hydrochloride (0.2g/10mL H_2O), and spectinomycin dihydrochloride pentahydrate (0.5g/10mL H_2O) was added to all microcosms at 2mg/mL final concentration. Serum bottle headspace was filled with 100% CH_4 for 5min.

Inoculation: 5g of sediment from each 2cm sediment section was mixed with 5mL of sterile, anaerobic milli-Q water to create a sediment slurry for inoculation. Serum bottles were each inoculated with 500uL of these sediment slurries, totaling 10 enrichment microcosms for each depth (12-14cm, 38-40cm, 48-50cm). Controls

underwent the same media preparation excluding the addition of a reducing agent. Controls (n=3) were inoculated with 500uL of autoclaved sediment slurry for each depth (12-14cm, 38-40cm, 48-50cm).

Sampling and Analyses: All enrichments were incubated at room temperature in a dark room and sampled over the course of six months. Headspace methane concentrations were measured monthly by gas chromatography using a flame-ionization detector (Agilent 7890B, Wilmington, DE, USA). Methane is separated isothermally within a HP-Plot Q column (Agilent, 30 m x 0.530 µm inner diameter, 40 µm film thickness). We conducted manual injection of 100uL headspace sample using a gastight syringe. Injector temperature was 250° C with a set oven temperature of 60° C and detector temperature of 250° C. Methane peaks were integrated using Agilent ChemStation Data Analysis software version F.01.03. Methane concentrations were determined from a standard curve of equilibrated standards and the ideal gas law. Liquid sample (500uL) was sampled once a month for taxonomic analysis, and DNA was extracted from 250uL of sample using the Qiagen DNeasy PowerSoil Pro kit (Germantown, Maryland). Extracted DNA was sent to the UCONN MARS facility for amplicon sequencing of the 16S rRNA gene targeting the V4 region (primers 515F and 806R) using the Illumina MiSeq paired-end sequencing platform via the v2 2x250 base pair kit (Illumina) following their standard protocol (Parada et al., 2016). Raw forward and reverse sequences were paired, and quality checked; sequences that passed QC were further processed using the 16S rRNA gene analysis pipeline implemented in MOTHUR version 1.46.1 (Schloss et al., 2009). Forward and reverse sequences were aligned and

quality filtered using MOTHUR, yielding amplicons ranging in sizes of 130-200 bp in lengths, where ambiguous nucleotides and homopolymer stretches were removed. We opted against the use of amplicon sequence variants (ASV) considering the amount of available computation and created operational taxonomic units (OTU). OTUs were created with a 3% dissimilarity and were aligned and classified against the Silva SSU database, version 138 (Gurevich et al., 2013). Nontarget OTUs and taxa <1% were removed from representative sequences prior to further downstream analysis. Relative 16S rRNA gene abundance was averaged across triplicate sampling of sediment core samples whereas gene abundance from enrichment samples were not run, sampled, or sequenced in triplicate.

Diversity analyses of enrichments were performed in R using the following packages: VEGAN and tidyverse (Dixon, 2003; Wickham et al., 2019). OTUs were classified to the class level and assigned a taxonomic representative for beta diversity analysis among samples. Indicator species analyses in the indicspecies R package were performed to determine strong statistical associations between microbial groups and treatment variables (i.e. time, redox, depth and reducing agent) (De Daceres, Jansen & De Caceres, 2016). Data has been deposited in the NCBI repository under BioProject number XXXX.

Results

Microbial Analysis of Sediment Core

The microbial community and composition of the initial sediment core consisted of anaerobic and unknown taxa. Abundant microbial phyla from all depths included representatives from *Chloroflexi*, *Crenarcheoata*, *Planctomycetota*, and unclassified bacteria (Figure 5.1). The largest microbial phyla identified in the shallowest depth (12-14cm) were *Chloroflexi*, *Crenarchaeota*, and *Planctomycetota* (Figure 5.1). The shallowest and mid depth had a higher abundance of *Calditrichota* than the deepest depth (Figure 5.1). The middle and deepest depths (38-40cm & 48-50cm) had a higher abundance of *Patescibacteria*, *Nanoarchaeota* and *Verrucomicrobiota* than the shallowest depth (Figure 5.1).

Time Series

After 30-days of incubation, the microbial composition of the enrichments were diverse as determined by amplicon sequencing. The microbial composition at each depth had shifted with an abundance of class *Methanosarcinia* in 12-14 cm and 48-50 cm depth enrichments across redox potentials (Figure 5.2). The microbial composition between 12-14 cm and 48-50 cm began to look more similar than the 38-40 cm depth enrichments. At this time, the microbial composition of samples in the sodium dithionite reducing agent treatments at 12-14cm and 48-50 cm more closely resembled the composition of samples from 38-40 cm depth enrichments. Depth 38-40 cm enrichments experienced an increase in classes *Dehalococcoidia*, *Acetothermia*, *Aminicenantia*, *Desulobacteria*, and *Clostridia* (Figure 5.2).

After 90-days incubation, the diversity of the microbial composition remained varied, presenting more abundant representatives than previously described at the 30-day

sampling (Figure 5.3). In the 12-14 cm enrichments, there was an increase in *Methanosarcinia* across redox conditions (Figure 5.3). In the 38-40 cm enrichments, there was an increase of *Dehalococcoidia* and *Acetothermiia* (Figure 5.3). In the 48-50 cm enrichments, *Methanosarcinia* increased across redox conditions (Figure 5.3).

After 150-days incubation, the microbial composition drastically shifted, and previously less abundant taxa became more abundant across the enrichments (Figure 5.4). In 12-14 cm enrichments, *Bacilli* and *Gammaproteobacteria* increased (Figure 5.4). In the 38-40 cm enrichments, *Halobacteria* abundance increased in half of the enrichments (Figure 5.4). In the 48-50 cm enrichments, where *Methanosarcinia* decreased in relative abundance across samples, *Halobacteria* increased in relative abundance (Figure 5.4).

Methane measurements in the headspace over 150-days were above 4000 µmol concentration until 120-days where they dropped below 2000 µmol in the 12-14 cm and 48 – 50 cm enrichments (Figure 5.5A; Figure 5.5C). Methane concentrations stayed above 1000 µmol in 12-14 cm enrichments containing sodium dithionite as a reductant (Figure 5.5A). Methane measurements in 38-40 cm enrichments stayed above 3000 µmol until 120-days and then began to increase at 150-days across most redox conditions (Figure 5.5B). Methane concentrations stayed above 3500 µmol in 38-40 cm enrichments containing sodium dithionite as a reductant (Figure 5.5B). One 38-40 cm enrichment sample containing sodium dithionite experienced a headspace leak at 30-days as shown on the figure (Figure 5.3B). Methane concentrations stayed above 1000 µmol in 48-50 cm enrichments containing sodium dithionite as a reductant (Figure 5.5C). Headspace

methane in controls did not drop below 3500 µmol concentration over 150-days (Figure 5.6).

Indicator Species Analyses

Indicator species analyses identified *Bacilli* (p-value = 0.002) and *Methanosarcinia* (p-value = 0.0111) to be significantly associated with 30-days post inoculation, *Halobacteria* (p-value = 0.0001 to be significantly associated with 90-days post inoculation, and *Desulfobacteria* (p-value = 0.0001), *Phycisphaerae* (p-value = 0.0001), *Anaerolineae* (p-value = 0.0001), *Aminicencenantia* (p-value = 0.0003), and *Nanoarchaeia* (p-value = 0.0017) to be significantly associated with 150-days post inoculation. Further analyses identified *Methanosarcinia* (p-value = 0.0010), *Dehalococcoidia* (p-value = 0.0026), and *Bathyarchaeia* (p-value = 0.0058) to be significantly associated with inoculation and 30- and 150-days post inoculation.

The analyses showed that Bacilli (p-value = 0.0068) was significantly associated with 12-14 cm depth, *Nanoarchaeia* (p-value = 0.0002), *Desulfobacteria* (p-value = 0.0105), Clostridia (p-value = 0.0446), *Omnitrophia* (p-value = 0.0409), and *Lokiarchaeia* (p-value = 0.0111) was significantly associated with 38-40 cm depth. *Methanosarcinia* (p-value = 0.0250) was significantly associated with 12-14 cm and 48-50 cm depth.

Bacilli (p-value = 0.0278) was significantly associated with the -380 mV redox and *Methanomicrobia* (p-value = 0.0004) was significantly associated with the -570 mV redox. *Methanosarcinia* (p-value = 0.0101), whereas *Dehalococcoidia* (p-value = 0.0252), and *Bathyarchaeia* (p-value = 0.0251) were significantly associated with -380

mV and -570 mV redoxes. *Halobacteria* (p-value = 0.0123), *Calditrichia* (p-value = 0.0235), and *Actinobacteria* (p-value = 0.0314) were significantly associated with sodium dithionite as a reducing agent, whereas *Methanosarcinia* (p-value = 0.0006), *Methanomicrobia* (p-value = 0.0001), Dehalococcoidia (p-value = 0.0090), Bathyarchaeia (p-value = 0.0135), and *Desulfarculia* (p-value = 0.0484) were significantly associated with titanium(III) citrate as a reducing agent.

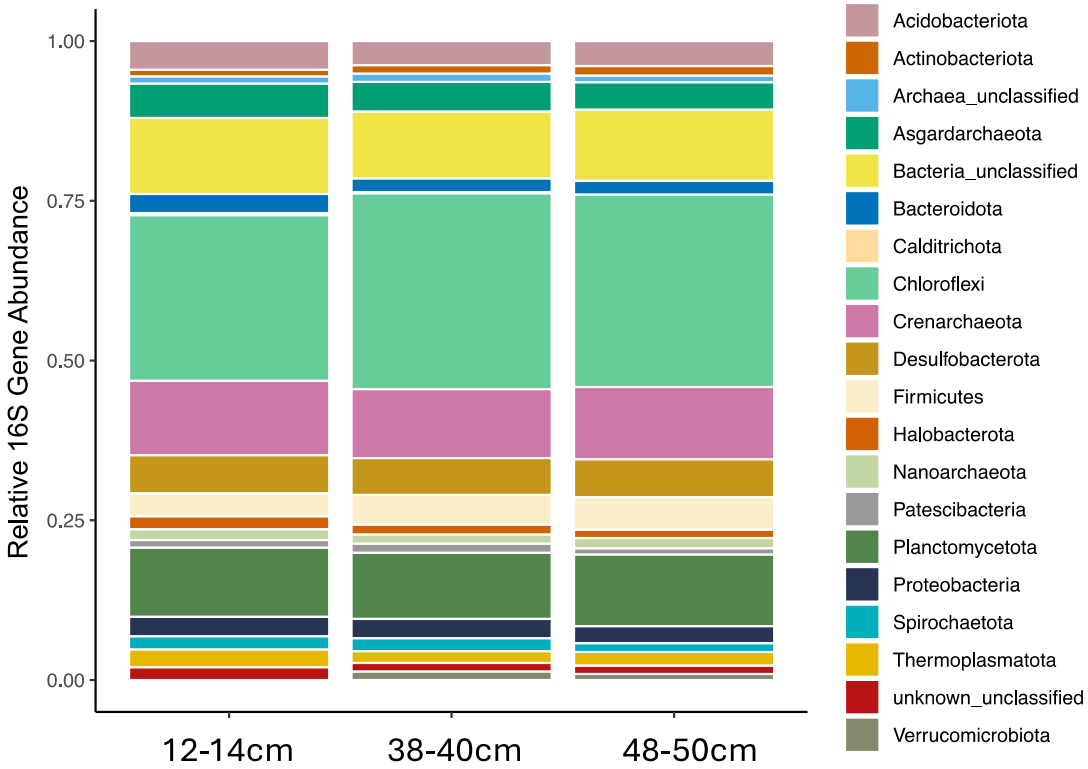

Figure 5.1. Abundant microbial taxa based on relative 16S rRNA gene percent abundance averaged across triplicate samples that have been identified to Phyla level from the initial October core prior to incubation. Data shows the dominant abundance of *Chloroflexi, Crenarchaeota*, and Unclassified Bacteria across depths.

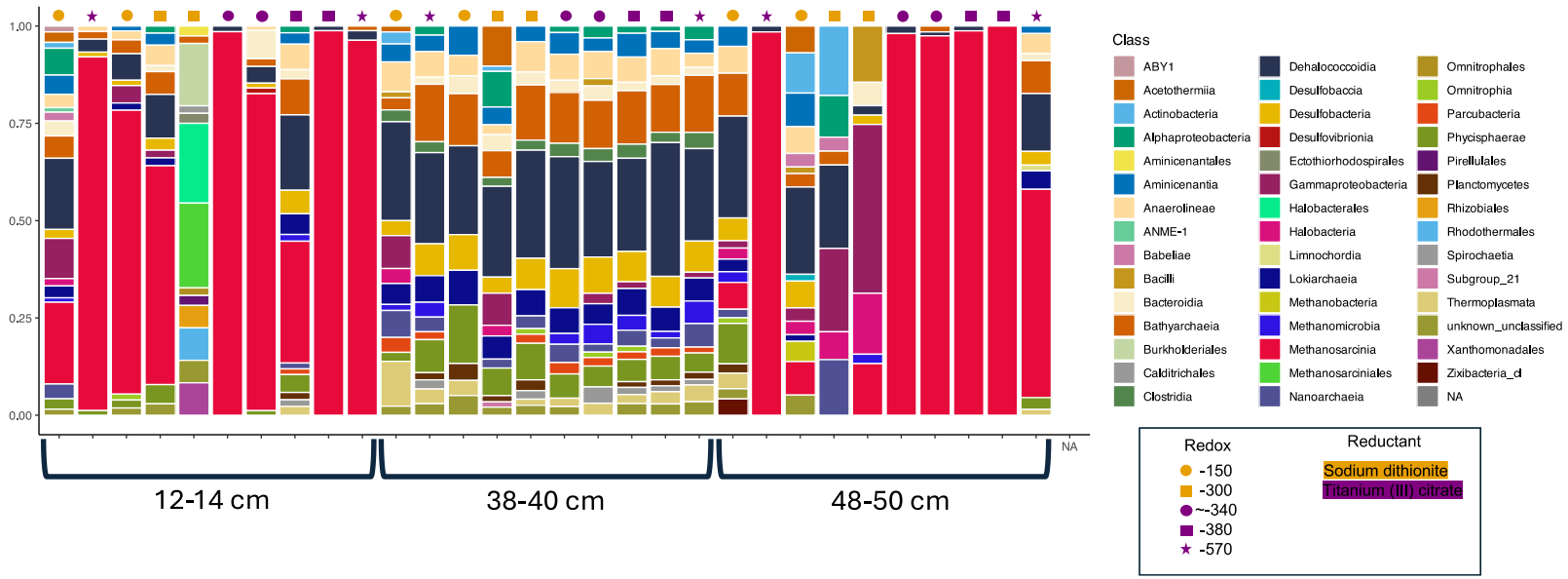

Figure 5.2. Abundant microbial taxa based on relative 16S rRNA gene percent abundance that have been identified to Class level at 30-days incubation. Data shows the dominant abundance of *Methanosarcinia* across samples in the 12-14cm and 48-50cm depth and an abundance of *Dehalococcodia* at the 38-40cm depth.

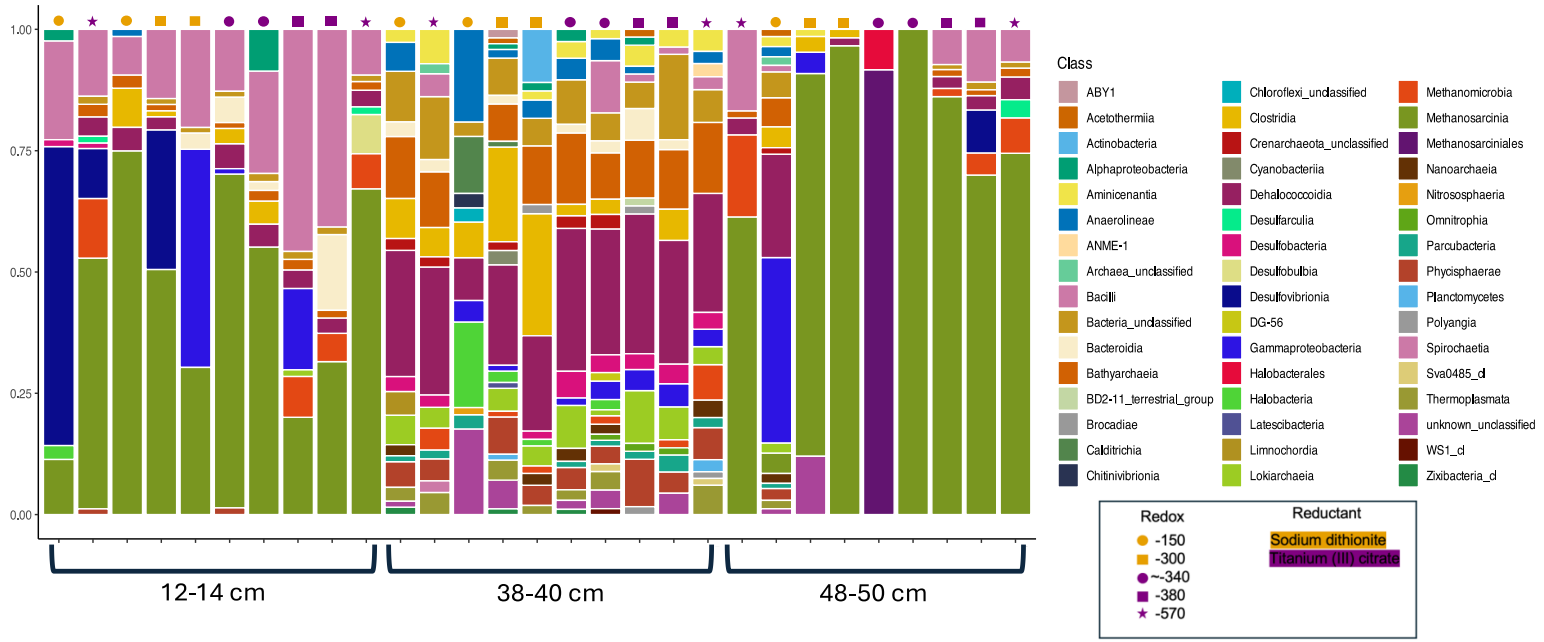

Figure 5.3. Abundant microbial taxa based on relative 16S rRNA gene percent abundance that have been identified to Class level at 90-days incubation. Data shows the dominant abundance of *Methanosarcinia* across samples in the 12-14cm and 48-50cm depth and an abundance of *Dehalococcoidia* at the 38-40cm depth.

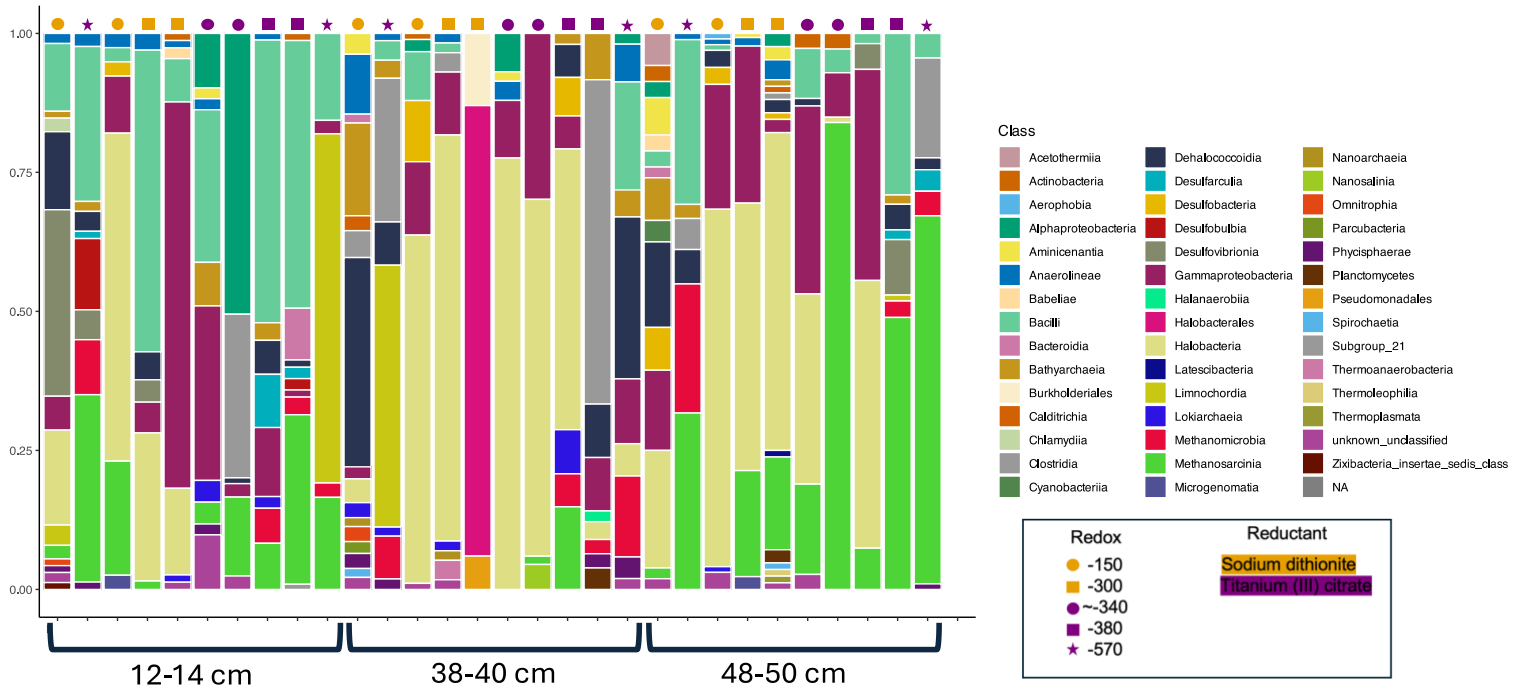

Figure 5.4. Abundant microbial taxa based on relative 16S rRNA gene percent abundance that have been identified to Class level at 150-days incubation. Data shows the increase of Bacilli in the 12-14cm, *Halobacteria* in the 38-40cm depth, *Halobacteria* in the 48-50cm depth.

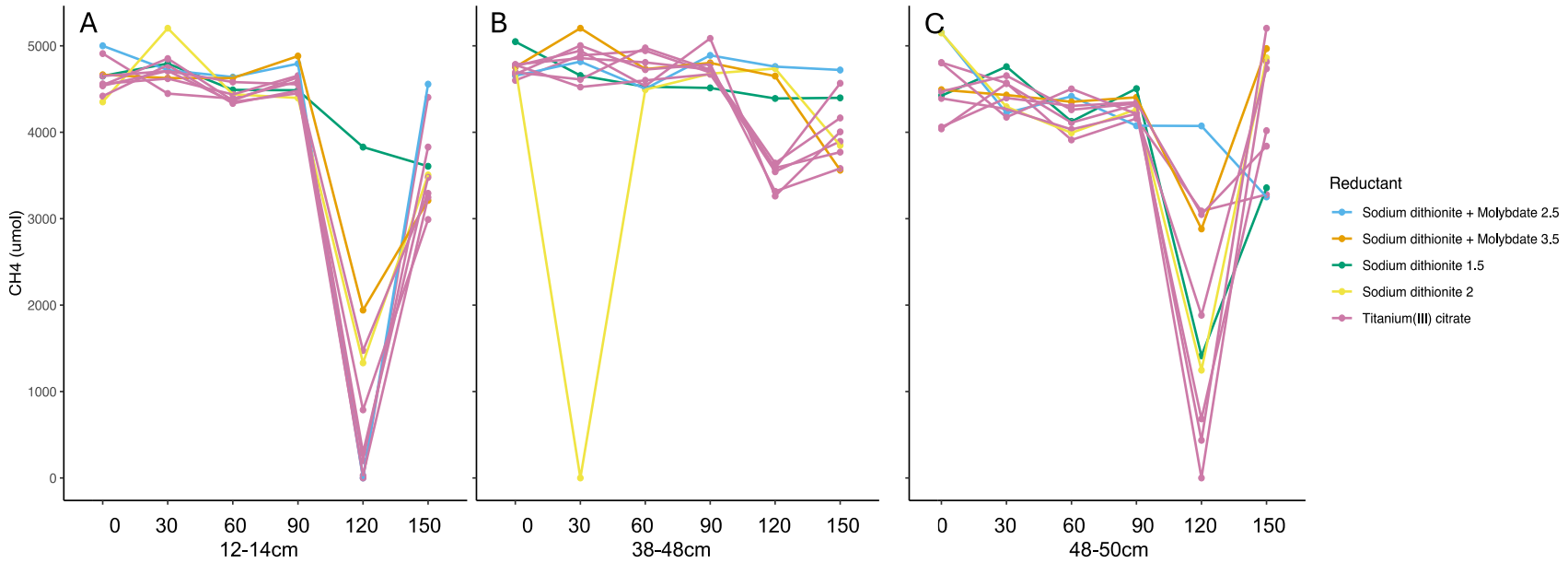

Figure 5.5. Headspace measurements for methane over 150-days for enrichments from 12-14 cm (A), 38-40 cm (B) and 48-50cm (C) depth sediment. The sudden drop in sodium dithionite 2 (panel B) at day 30 was due to a bottle leak, not microbial activity.

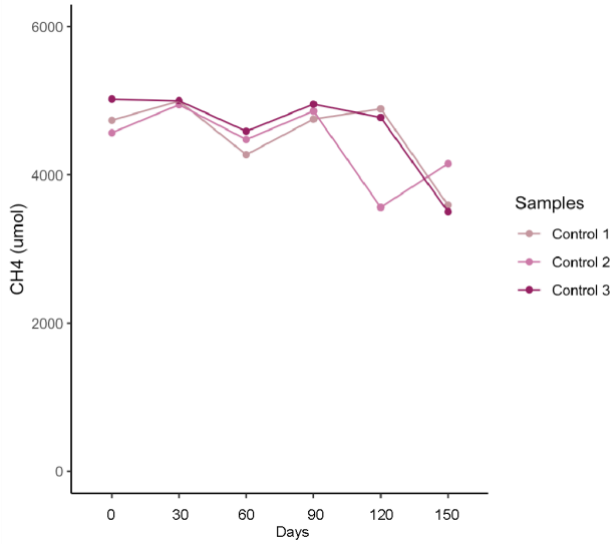

Figure 5.6. Headspace measurements for methane over 150-days for enrichments from controls used for each depth. Controls do not drop below 3500 µmol methane.

Discussion & Conclusion

In this study, we investigated how redox potentials shape microbial communities in anaerobic marine sediments using different reducing agents at varied redox potentials. Although both reductants maintained different long-term reduced redox conditions, they both enable similar anaerobic respiration metabolisms (Boyd, 1995). Our findings revealed that the chemical nature of the reductant significantly influences community composition. Specifically, sodium dithionite (-300 mV) treatments favored Halobacteria, Babeliae, Calditrichia, and Actinobacteria, while titanium(III) citrate (-340 mV)

treatments promoted Methanosarcinia, Methanomicrobia, Dehalococcoidia, and Bathyarchaeia. This differentiation indicates that reductant-specific chemistry, not just redox potential, is a critical factor in determining microbial assembly.

We examined reducing agents considering the majority of anaerobic cultivation currently uses sodium sulfide as a reducing agent, which typically holds reducing conditions around -200 - -350 mV. However, sodium sulfide is suspected to be potentially toxic to many anaerobes, suggesting alternative reducing agents need to be strongly considered (Yekta et al., 2023). Titanium(III) citrate, known for establishing more strongly reduced conditions, as low as -700 mV, has been shown to suppress facultative anaerobes (Mariotto et al., 1989). Sodium dithionite maintains moderately reduced conditions, as low as ~ –600 mV, though we utilized concentrations promoting -150 and -300 mV redox potentials promoting metabolic diversity that allow a mix of anaerobic pathways to thrive (Sudha et al., 2022). This reflects our observations: titanium citrate led to narrower, highly reduced niches supporting presumed methanogenic and dehalogenating taxa, while dithionite allowed broader microbial diversity. Under matched redox potentials, the identity of the reductant played a decisive role in steering microbial succession. We hypothesize this is due to the chemical make-up of the reductant, beyond just the suppression of oxygen and electron transfer. This highlights the crucial importance of redox chemistry, beyond potential or inoculum alone, in shaping anaerobic microbial ecology.

We further observed that cultures inoculated from 12–14 cm and 48–50 cm sediment depths converged over the incubation period, underscoring the influence

of redox potential and culture conditions over initial inoculum in shaping anaerobic microbial communities. This microbial community convergence mirrors findings in controlled bioreactors, where redox-driven thermodynamic constraints drive similar metabolic outcomes regardless of inocula differences (George, Wang, and Maslov, 2023; Favale et al., 2025). By maintaining constant redox potentials, we promoted select lineages adapted to energetically limited conditions, such as Methanosarcinia and Bathyarchaeia, highlighting the power of redox control in selecting for specific taxa.

Our long-term data provide strong evidence that precisely tuning culture parameters (i.e. redox potential and reducing agent choice) can effectively limit metabolic pathways *in-vitro* and enrich for anaerobes often only detected through sequencing. Similar studies using redox-controlled Winogradsky columns have shown depth-dependent community shifts controlled by redox gradients (Toshchakov et al., 2018). By contrast, in our microcosms, redox potential remained the overriding selection pressure, driving community progression more than inoculum history or depth alone.

This work contributes to emerging literature on redox potential effects in highly reduced anaerobic sediments. Despite different starting communities, culture conditions narrowed ecological outcomes, producing predictable successional trajectories defined by redox chemistry and microbial metabolism. The reproducible convergence of communities across sediment depths demonstrates that tight control of redox and the reductant enables predictable microbial outcomes, facilitating targeted enrichment of functionally desired taxa. Future investigations could leverage these insights to isolate

specific anaerobic representatives capable of methanogenesis or anaerobic methane oxidation with fine-tuned redox regimes and reductant specificity. This will refine strategies for microbial isolation and increase repeatability in linking microbial assemblages to biogeochemical functions in reduced sedimentary environments.

REFERENCES

1. Kallmeyer, Jens, et al. "Global distribution of microbial abundance and biomass in subseafloor sediment." *Proceedings of the National Academy of Sciences* 109.40 (2012): 16213-16216.

2. Bar-On, Y. M., Phillips, R., & Milo, R. (2018). The biomass distribution on Earth. *Proceedings of the National Academy of Sciences*, *115*(25), 6506-6511.

3. Roussel, E. G., Bonavita, M. A. C., Querellou, J., Cragg, B. A., Webster, G., Prieur, D., & Parkes, R. J. (2008). Extending the sub-sea-floor biosphere. *Science*, *320*(5879), 1046-1046.

4. Grossart, H. P., & Gust, G. (2009). Hydrostatic pressure affects physiology and community structure of marine bacteria during settling to 4000 m: an experimental approach. *Marine Ecology Progress Series*, *390*, 97-104.

5. Calvert, S. E., & Pedersen, T. F. (1992). Organic carbon accumulation and preservation in marine sediments: how important is anoxia. *Productivity, accumulation and preservation of organic matter in recent and ancient sediments*, 231-263.

6. Wakeham, S. G., & Canuel, E. A. (2005). Degradation and preservation of organic matter in marine sediments. *Marine organic matter: biomarkers, isotopes and DNA*, 295-321.

7. Gonneea, M. E., Paytan, A., & Herrera-Silveira, J. A. (2004). Tracing organic matter sources and carbon burial in mangrove sediments over the past 160 years. *Estuarine, Coastal and Shelf Science*, *61*(2), 211-227.

8. Hutchings, J. A., Bianchi, T. S., Najjar, R. G., Herrmann, M., Kemp, W. M., Hinson, A. L., & Feagin, R. A. (2020). Carbon deposition and burial in estuarine sediments of the contiguous United States. *Global Biogeochemical Cycles*, *34*(2), e2019GB006376.

9. Van Cappellen, P., Gaillard, J. F., & Rabouille, C. (1993). Biogeochemical transformations in sediments: kinetic models of early diagenesis. In *Interactions of C, N, P and S biogeochemical cycles and global change* (pp. 401-445). Berlin, Heidelberg: Springer Berlin Heidelberg.

10. Sørensen, J., Jørgensen, B. B., & Revsbech, N. P. (1979). A comparison of oxygen, nitrate, and sulfate respiration in coastal marine sediments. *Microbial Ecology*, *5*, 105-115.

11. Reimers, C. E., Alleau, Y., Bauer, J. E., Delaney, J., Girguis, P. R., Schrader, P. S., & Stecher III, H. A. (2013). Redox effects on the microbial degradation of refractory organic matter in marine sediments. *Geochimica et Cosmochimica Acta*, *121*, 582-598.

12. Sela-Adler, M., Ronen, Z., Herut, B., Antler, G., Vigderovich, H., Eckert, W., & Sivan, O. (2017). Co-existence of methanogenesis and sulfate reduction with common substrates in sulfate-rich estuarine sediments. *Frontiers in microbiology*, *8*, 766.

13. Maltby, J., Steinle, L., Löscher, C. R., Bange, H. W., Fischer, M. A., Schmidt, M., & Treude, T. (2018). Microbial methanogenesis in the sulfate-reducing zone of sediments in the Eckernförde Bay, SW Baltic Sea. *Biogeosciences*, *15*(1), 137-157.

14. Reimers, C. E., Alleau, Y., Bauer, J. E., Delaney, J., Girguis, P. R., Schrader, P. S., & Stecher III, H. A. (2013). Redox effects on the microbial degradation of refractory organic matter in marine sediments. *Geochimica et Cosmochimica Acta*, *121*, 582-598.

15. Hunter, K. S., Wang, Y., & Van Cappellen, P. (1998). Kinetic modeling of microbially-driven redox chemistry of subsurface environments: coupling transport, microbial metabolism and geochemistry. *Journal of hydrology*, *209*(1-4), 53-80.

16. De Caceres, M., Jansen, F., & De Caceres, M. M. (2016). Package 'indicspecies'. *indicators*, *8*(1).

17. Burgin, A. J., Yang, W. H., Hamilton, S. K., & Silver, W. L. (2011). Beyond carbon and nitrogen: how the microbial energy economy couples elemental cycles in diverse ecosystems. *Frontiers in Ecology and the Environment*, *9*(1), 44-52.

18. Bradley, J. A., Arndt, S., Amend, J. P., Burwicz-Galerne, E., & LaRowe, D. E. (2022). Sources and fluxes of organic carbon and energy to microorganisms in global marine sediments. *Frontiers in microbiology*, *13*, 910694.

19. Boetius, A., & Lochte, K. (1994). Regulation of microbial enzymatic degradation of organic matter in deep-sea sediments. *Marine Ecology Progress Series*, 299-307.

20. Chiarabelli, C., Stano, P., & Luisi, P. L. (2013). Chemical synthetic biology: a mini-review. *Frontiers in microbiology*, *4*, 285.

21. Ravin, N. V., Mardanov, A. V., & Skryabin, K. G. (2015). Metagenomics as a tool for the investigation of uncultured microorganisms. *Russian Journal of Genetics*, *51*, 431-439.

22. Sun, Y., Liu, Y., Pan, J., Wang, F., & Li, M. (2020). Perspectives on cultivation strategies of archaea. *Microbial ecology*, *79*, 770-784.

23. Wang, Y., Zhang, R., He, Z., Van Nostrand, J. D., Zheng, Q., Zhou, J., & Jiao, N. (2017). Functional gene diversity and metabolic potential of the microbial community in an estuary-shelf environment. *Frontiers in microbiology*, *8*, 1153.

24. Spang, A., Saw, J. H., Jørgensen, S. L., Zaremba-Niedzwiedzka, K., Martijn, J., Lind, A. E., ... & Ettema, T. J. (2015). Complex archaea that bridge the gap between prokaryotes and eukaryotes. *Nature*, *521*(7551), 173-179.

25. Sousa, F. L., Neukirchen, S., Allen, J. F., Lane, N., & Martin, W. F. (2016). Lokiarchaeon is hydrogen dependent. *Nature Microbiology*, *1*(5), 1-3.

26. Dombrowski, N., Williams, T. A., Sun, J., Woodcroft, B. J., Lee, J. H., Minh, B. Q., ... & Spang, A. (2020). Undinarchaeota illuminate DPANN phylogeny and the impact of gene transfer on archaeal evolution. *Nature Communications*, *11*(1), 3939.

27. Boyd, C. E., & Boyd, C. E. (1995). Soil organic matter, anaerobic respiration, and oxidation—reduction. *Bottom soils, sediment, and pond aquaculture*, 194-218.

28. Mariotto, C., Loubière, P., Goma, G., & Lindley, N. D. (1989). Influence of various reducing agents on methylotrophic growth and organic acid production of Eubacterium limosum. *Applied microbiology and biotechnology*, *32*, 193-198.

29. Sudha, N. R., Varaprasad, D., Riazunnisa, K., Prasanna, V. A., Reddy, P. R., & Chandrasekhar, T. (2022). Effects of oxygen scavengers (Sodium sulfite, sodium bisulfite, sodium dithionite, and sodium metabisulfite) on growth and accumulation of biomass in the green alga Asterarcys quadricellulare. *J. Appl. Biol. Biotechnol*, *10*(4), 136-140.

30. George, A. B., Wang, T., & Maslov, S. (2023). Functional convergence in slow-growing microbial communities arises from thermodynamic constraints. *The ISME Journal*, *17*(9), 1482-1494.

31. Favale, N., Costa, S., Summa, D., Sabbioni, S., Mamolini, E., Tamburini, E., & Scapoli, C. (2025). Comparison of microbiome community structure and dynamics during anaerobic digestion of different renewable solid wastes. *Current Research in Microbial Sciences*, *8*, 100383.

32. Toshchakov, S. V., Lebedinsky, A. V., Sokolova, T. G., Zavarzina, D. G., Korzhenkov, A. A., Teplyuk, A. V., ... & Gavrilov, S. N. (2018). Genomic insights into energy metabolism of Carboxydocella thermautotrophica coupling hydrogenogenic CO oxidation with the reduction of Fe (III) minerals. *Frontiers in Microbiology*, *9*, 1759.

33. Yekta, S. S., Svensson, B. H., Skyllberg, U., & Schnürer, A. (2023). Sulfide in engineered methanogenic systems–Friend or foe?. *Biotechnology Advances*, *69*, 108249

APPENDIX A

A REPRINT PERMISSIONS CHAPTER 2

Publication: Bowen, M., Main, C. R., Farag, I. F., & Biddle, J. F. (2024). Identifying potential introduced and natural sources of pollution in Delaware watersheds. *Applied and Environmental Microbiology*, *90*(12), e01958-24. https://doi.org/10.1128/aem.01958-24

ASM Permission Policy: "ASM also grants authors the right to republish discrete portions of their article in any other publication (including print, CD-ROM, and other electronic formats) provided that proper credit is given to the original ASM publication. ASM authors also retain the right to reuse the full article in their dissertation or thesis. "Proper credit" means the copyright notice shown on the initial page of the article (https://journals.asm.org/author-self-archiving-permissions)."

All available supplemental data is accessible through published data found at the publication's ASM supplemental material.

APPENDIX B

B SUPPLEMENTAL DATA FOR CHAPTER 3

Table B.1 Sample information for caprellids collected

Sample ID	Collection Date	Site	Species	Sex
1	9/18/24	MOB	Caprella equilibra	Male
2	9/18/24	MOB	Caprella laeviuscula	Male
3	9/18/24	MOB	Caprella mutica	Female
4	9/18/24	MOB	Caprella laeviuscula	Male
5	9/18/24	MOB	Caprella mutica	Female
6	9/18/24	MOB	Caprella laeviuscula	Male
7	9/18/24	MOB	Caprella linearis	Male
8	9/18/24	MOB	Caprella mutica	Female
9	9/18/24	PEL	Caprella mutica	Male
10	9/18/24	PEL	Caprella mutica	Male
11	9/18/24	PEL	Caprella scaura	Female
12	9/18/24	PEL	Caprella scaura	Female
13	9/18/24	PEL	Caprella scaura	Female
14	9/18/24	PEL	Caprella scaura	Male
15	9/18/24	PEL	Caprella scaura	Female
16	9/18/24	PEL	Caprella scaura	Female
17	9/18/24	PEL	Caprella mutica	Male
18	9/18/24	PEL	Caprella mutica	Female
19	9/18/24	PEL	Caprella linearis	Male
20	9/18/24	PEL	Caprella mutica	Male
21	9/18/24	PEL	Caprella scaura	Female
22	9/18/24	PEL	Caprella scaura	Male
23	9/18/24	PEL	Caprella equilibria	Male
24	9/18/24	PEL	Caprella scaura	Male
25	9/18/24	PEL	Caprella scaura	Female
26	9/18/24	PEL	Caprella mutica	Male
27	9/18/24	PEL	Caprella scaura	Male
28	9/18/24	PEL	Caprella linearis	Male
29	9/18/24	PEL	Caprella mutica	Female
30	9/18/24	PEL	Caprella mutica	Male
31	9/18/24	PEL	Caprella scaura	Male
32	9/18/24	PEL	Caprella mutica	Female
33	9/18/24	PEL	Caprella mutica	Female
34	9/18/24	PEL	Caprella mutica	Male
35	9/18/24	PEL	Caprella mutica	Male
36	9/18/24	PEL	Caprella mutica	Female
37	9/18/24	PEL	Caprella scaura	Female
38	9/18/24	PEL	Caprella scaura	Male
39	9/18/24	PEL	Caprella mutica	Male
40	9/18/24	PEL	Caprella mutica	Male
A1	6/22/23	MOB	Caprella equilibra	Female
A2	6/22/23	MOB	Caprella equilibra	Female
A3	6/22/23	MOB	Caprella equilibra	Female (Pregnant)
A4	6/22/23	MOB	Caprella penantis	Female
A5	6/22/23	MOB	Caprella penantis	Female (Pregnant)
A6	6/22/23	MOB	Caprella penantis	Female (Pregnant)
A7	6/22/23	MOB	Caprella penantis	Female (Pregnant)
A8	6/22/23	MOB	Caprella penantis	Female
B1	6/23/23	PEL	Caprella equilibra	Female (Pregnant)
B10	6/23/23	PEL	Caprella equilibra	Female (Pregnant)
B11	6/22/23	MOB	Control of Seawater	
B12	6/27/23	MOB	Control of Seawater	
B13	7/7/23	PEL	Control of Seawater	
B14	7/24/23	PEL	Control of Seawater	

B2	6/23/23	PEL	Caprella equilibra	Female
B3	6/23/23	PEL	Caprella equilibra	Male
B4	6/23/23	PEL	Caprella equilibra	Male
B5	6/23/23	PEL	Caprella equilibra	Male
B6	6/23/23	PEL	Caprella equilibra	Male
B7	6/23/23	PEL	Caprella laeviuscula	Female (Pregnant)
B8	6/23/23	PEL	Caprella equilibra	Male
B9	6/23/23	PEL	Caprella equilibra	Female (Pregnant)
C1	6/27/23	MOB	Caprella equilibra	Male
C10	6/27/23	MOB	Caprella laeviuscula	Male
C11	6/27/23	MOB	Caprella equilibra	Female (Pregnant)
C12	6/27/23	MOB	Caprella linearis	Male
C13	6/27/23	MOB	Caprella equilibra	Female
C2	6/27/23	MOB	Caprella equilibra	Male
C3	6/27/23	MOB	Caprella equilibra	Male
C4	6/27/23	MOB	Caprella penantis	Male
C5	6/27/23	MOB	Caprella penantis	Male
C6	6/27/23	MOB	Caprella penantis	Female
C7	6/27/23	MOB	Caprella equilibra	Male
C8	6/27/23	MOB	Caprella equilibra	Female (Pregnant)
C9	6/27/23	MOB	Caprella equilibra	Female (Pregnant)
E1	7/7/23	PEL	Caprella equilibra	Female
E10	7/7/23	PEL	Caprella equilibra	Male
E11	7/7/23	PEL	Caprella penantis	Female (Pregnant)
E12	7/7/23	PEL	Caprella equilibra	Female (Pregnant)
E13	7/7/23	PEL	Caprella scaura	Male
E14	7/7/23	PEL	Caprella penantis	Female
E15	7/7/23	PEL	Caprella scaura	Male
E16	7/7/23	PEL	Caprella penantis	Female (Pregnant)
E18	7/7/23	PEL	Caprella scaura	Male
E2	7/7/23	PEL	Caprella equilibra	Male
E20	7/7/23	PEL	Caprella equilibra	Female
E21	7/7/23	PEL	Caprella scaura	Male
E22	7/7/23	PEL	Caprella penantis	Male
E24	7/7/23	PEL	Caprella penantis	Male
E25	7/7/23	PEL	Caprella penantis	Male
E26	7/7/23	PEL	Caprella penantis	Female
E27	7/7/23	PEL	Caprella equilibra	Female
E28	7/7/23	PEL	Caprella equilibra	Female
E29	7/7/23	PEL	Caprella equilibra	Male
E3	7/7/23	PEL	Caprella equilibra	Female
E30	7/7/23	PEL	Caprella equilibra	Male
E31	7/11/23	PEL	Caprella equilibra	Male
E33	7/11/23	PEL	Caprella equilibra	Male
E34	7/11/23	PEL	Caprella equilibra	Male
E35	7/11/23	PEL	Caprella equilibra	Female
E36	7/11/23	PEL	Caprella equilibra	Male
E38	7/11/23	PEL	Caprella equilibra	Male
E39	7/11/23	PEL	Caprella scaura	Female
E4	7/7/23	PEL	Caprella equilibra	Male
E40	7/11/23	PEL	Caprella equilibra	Male
E5	7/7/23	PEL	Caprella penantis	Male
E6	7/7/23	PEL	Caprella penantis	Male
E7	7/7/23	PEL	Caprella scaura	Male
E8	7/7/23	PEL	Caprella penantis	Male
E9	7/7/23	PEL	Caprella scaura	Male
MS1	6/21/23	MOB	Caprella equilibra	Male
MS10	6/21/23	MOB	Caprella equilibra	Male
MS11	6/21/23	MOB	Caprella equilibra	Male
MS12	6/21/23	MOB	Caprella penantis	Male
MS13	6/21/23	MOB	Caprella penantis	Male
MS14	6/21/23	MOB	Caprella penantis	Female
MS15	6/21/23	MOB	Caprella mutica	Female
MS2	6/21/23	MOB	Caprella equilibra	Male
MS3	6/21/23	MOB	Caprella equilibra	Male
MS4	6/21/23	MOB	Caprella equilibra	Male
MS5	6/21/23	MOB	Caprella equilibra	Male
MS6	6/21/23	MOB	Caprella equilibra	Male
MS7	6/21/23	MOB	Caprella equilibra	Male
MS8	6/21/23	MOB	Caprella equilibra	Male
MS9	6/21/23	MOB	Caprella equilibra	Male
O1	7/24/23	MOB	Caprella equilibra	Male
O10	7/24/23	MOB	Caprella equilibra	Male ?
O11	7/24/23	MOB	Caprella equilibra	Male ?
O12	7/24/23	PEL	Caprella linearis	Male ?
O13	7/24/23	PEL	Caprella linearis	Male ?
O14	7/24/23	PEL	Caprella equilibra	Female (Pregnant)
O15	7/24/23	PEL	Caprella equilibra	Female (Pregnant)
O16	7/24/23	PEL	Caprella linearis	Female
O17	7/24/23	PEL	Caprella linearis	Male
O18	7/24/23	PEL	Caprella linearis	Male
O19	7/24/23	PEL	Caprella linearis	Male
O2	7/24/23	MOB	Caprella equilibra	Male
O20	7/24/23	PEL	Caprella penantis	Male
O21	7/24/23	PEL	Caprella linearis	Male
O22	7/24/23	PEL	Caprella linearis	Female?
O23	7/24/23	PEL	Caprella linearis	Male ?
O24	7/24/23	PEL	Caprella equilibra	Male ?
O26	7/24/23	PEL	Caprella equilibra	Male
O3	7/24/23	MOB	Caprella equilibra	Male
O4	7/24/23	MOB	Caprella penantis	Male
O5	7/24/23	MOB	Caprella penantis	Male
O6	7/24/23	MOB	Caprella linearis	Male ?
O7	7/24/23	MOB	Caprella penantis	Male ?
O8	7/24/23	MOB	Caprella penantis	Male ?
O9	7/24/23	MOB	Caprella penantis	Male ?
P1	7/24/23	PEL	Caprella linearis	Male
P2	7/24/23	PEL	Caprella equilibra	Male
P4	7/24/23	PEL	Caprella equilibra	Male
P5	7/24/23	PEL	Caprella linearis	Male

Table B.2 16S rRNA amplicon abundance identified to the Order level of caprella guts.

Row Labels	Arenicellales	Bacteroidales	Burkholderiales	Cddilineales	Campylobacterales	Cauloba cterales	Chitinophagales	Corynebacteriales	Cytophagales	Desulfobulbales	Desulfuromonadales	Ectothiorhodospirales	Enterobacterales	Flavobacteriales	Frankiales	Lachnospirales	Lactobacillales	Micrococcales	Microtrichales	Peptostreptococcales-Tissierellales
A1	0	0	0	1271	0	0	0	0	0	0	0	817	15444	0	0	0	0	0	0	654
A2	0	0	0	0	0	0	0	0	0	0	0	0	7708	0	0	0	0	0	0	0
A3	0	0	3094	0	0	0	0	0	0	0	0	0	0	0	0	0	2285	0	0	0
A4	0	0	0	0	0	0	0	0	0	0	0	0	98483	0	0	0	0	0	0	0
A5	0	572	0	0	15881	0	0	0	0	0	0	0	26815	0	0	0	0	0	0	1383
A6	0	0	0	0	0	0	0	0	544	0	0	0	26374	0	0	0	0	443	0	0
A7	0	0	0	0	0	0	0	0	0	1358	0	1443	27188	0	0	0	0	0	0	0
A8	0	0	0	0	1051	0	3819	0	0	0	0	0	25916	0	0	0	840	0	0	0
MS1	0	828	0	410	0	0	0	944	0	587	0	0	2894	0	0	0	1674	0	465	905
MS2	0	0	0	0	0	0	0	0	0	0	0	0	642	0	0	0	0	0	0	0
MS3	0	1768	1757	0	0	0	0	0	0	0	0	0	17788	0	0	2709	0	0	0	0
MS4	0	0	0	0	0	0	0	0	0	0	0	0	0	0	0	0	0	0	0	496
MS5	0	2538	0	1211	0	0	0	2907	0	1246	0	0	6648	0	0	0	4309	0	0	1437
MS6	903	0	0	0	0	0	770	0	0	0	0	0	1729	0	0	0	0	0	949	0
MS7	0	0	0	0	0	0	0	0	0	0	0	0	0	0	0	0	0	0	0	0
MS8	0	0	0	0	0	0	0	336	0	0	0	0	3489	0	0	0	0	0	0	0
MS9	0	0	0	0	0	1875	3265	0	0	0	0	0	0	1383	889	0	0	2180	0	940
MS10	0	0	2239	0	9310	0	0	0	0	0	0	0	74223	0	0	0	0	0	0	7932
MS11	0	0	0	0	0	0	0	0	0	0	0	0	14586	0	0	0	0	0	0	0
MS12	0	0	1701	0	0	0	2331	0	0	1761	0	0	35616	0	0	0	2724	0	3084	0
MS13	0	0	0	0	0	0	23932	0	0	0	0	0	0	2923	0	0	0	0	7627	0
MS14	0	0	0	0	0	0	1006	0	0	0	0	0	0	0	0	0	0	0	0	0
MS15	0	0	0	0	0	0	0	0	0	0	1091	0	51124	0	0	0	0	0	0	0

Pirellulales	Planctomycetales	Polyangiales	Pseudomonadales	Rhizobiales	Rhodobacterales	Rickettsiales	SAR11_clade	Solirubrobacterales	Sphingomonadales	Staphylococcales	Thermoanaerobaculales	Thiotrichales	Tistrellales	uncultured	Verrucomicrobiales
0	0	0	1219	0	0	0	0	0	0	642	0	0	0	0	0
0	0	0	4998	0	0	0	0	0	0	5159	0	0	0	0	5324
0	0	0	0	0	0	0	0	0	0	0	0	0	0	0	0
0	0	0	3831	0	0	0	0	0	0	0	0	0	0	0	8746
0	0	0	7656	0	0	0	0	0	0	0	0	0	0	0	0
0	0	0	4668	0	1393	0	0	0	0	0	0	0	0	0	0
2935	0	0	5626	0	0	0	0	0	0	0	0	0	0	0	0
0	0	0	0	0	0	0	924	0	0	0	0	6204	0	0	1951
904	1659	0	6856	3863	0	0	0	0	3495	3090	478	0	0	0	489
0	0	0	1167	0	0	0	0	583	0	2250	0	0	0	0	0
0	0	0	22535	0	0	0	0	0	0	0	0	2289	0	0	0
0	0	0	0	0	0	0	0	0	0	0	0	0	0	0	0
1971	5656	0	14496	9242	0	0	0	0	7920	7418	1039	0	0	0	0
0	0	0	0	0	953	0	0	0	0	0	0	707	0	0	0
0	0	0	0	0	0	0	0	0	0	7196	0	0	0	0	0
2479	0	0	0	0	0	1456	0	0	0	7646	0	0	0	0	0
0	1465	2197	3479	686	563	0	0	686	0	1173	0	0	562	580	2336
0	0	0	3253	0	15073	0	0	0	0	0	0	0	0	0	0
0	0	0	9440	0	0	0	0	0	0	0	0	0	0	0	0
7645	1699	0	11834	0	2461	0	0	0	0	0	2529	0	0	0	4741
0	0	0	2404	0	7307	0	0	0	0	0	0	28172	0	0	18451
0	0	0	0	0	0	0	0	0	0	0	0	0	0	0	2165
0	0	0	3672	716	1009	0	0	0	0	0	0	0	0	0	0

Table B.3 Sulfur related taxa from our study on caprellids and other marine invertebrates.

Host	Order	Abundance
T. gratilla elatensis	Fusobacteriota	0.35
T. gratilla elatensis	Clostridiales	0.2
T. gratilla elatensis	Z Not Sulfur Related	0.45
A. marisindica	Xanthomonadales	0.03
A. marisindica	Sulfurovum	0.22
A. marisindica	Enterobacterales	0.003
A. marisindica	Z Not Sulfur Related	0.75
C. penantis	Burkholderiales	0.00961168
C. penantis	Desulfobulbales	0.0062521
C. penantis	Desulfuromonadales	0
C. penantis	Enterobacterales	0.53228884
C. penantis	Lachnospirales	0
C. penantis	Microtrichales	0.02147044
C. penantis	Rhodobacterales	0.022372
C. penantis	Thiotrichales	0.068907
C. penantis	Z Not Sulfur Related	0.33
C. equilibra	Burkholderiales	0.011738
C. equilibra	Desulfobulbales	0.005384
C. equilibra	Desulfuromonadales	0
C. equilibra	Enterobacterales	0.358356
C. equilibra	Lachnospirales	0.007957
C. equilibra	Microtrichales	0.004153
C. equilibra	Rhodobacterales	0.048728
C. equilibra	Thiotrichales	0.0088
C. equilibra	Z Not Sulfur Related	0.56
O. mirabilis	Altermondales	0.045
O. mirabilis	Bacillales	0.02
O. mirabilis	Cryomorphaceae	0.005
O. mirabilis	Desulfobacterales	0.02
O. mirabilis	Eubacteriales	0.02
O. mirabilis	Flavobacteriales	0.05
O. mirabilis	Fusobacteriales	0.01
O. mirabilis	Oceanospirillales	0.005
O. mirabilis	Rhodobacterales	0.05
O. mirabilis	Spirochaetales	0.015
O. mirabilis	Thiotrichales	0.005
O. mirabilis	Vibrionales	0.01
O. mirabilis	Woeseiales	0.02
O. mirabilis	Z Not Sulfur Related	0.73
O. kinbergi	Altermondales	0.05
O. kinbergi	Bacillales	0.02
O. kinbergi	Cryomorphaceae	0.005
O. kinbergi	Desulfobacterales	0.02
O. kinbergi	Eubacteriales	0.02
O. kinbergi	Flavobacteriales	0.055
O. kinbergi	Fusobacteriales	0.01
O. kinbergi	Oceanospirillales	0.005
O. kinbergi	Rhodobacterales	0.07
O. kinbergi	Spirochaetales	0.01
O. kinbergi	Thiotrichales	0.01
O. kinbergi	Vibrionales	0.01
O. kinbergi	Woeseiales	0.02
O. kinbergi	Z Not Sulfur Related	0.7
S. sladenii	Altermondales	0.03
S. sladenii	Bacillales	0.015
S. sladenii	Cryomorphaceae	0.005
S. sladenii	Desulfobacterales	0.015
S. sladenii	Eubacteriales	0.015
S. sladenii	Flavobacteriales	0.045
S. sladenii	Fusobacteriales	0.005
S. sladenii	Oceanospirillales	0.01
S. sladenii	Rhodobacterales	0.06
S. sladenii	Spirochaetales	0.005
S. sladenii	Thiotrichales	0.01
S. sladenii	Vibrionales	0.01
S. sladenii	Woeseiales	0.02
S. sladenii	Z Not Sulfur Related	0.76
O. sarsii vadicola	Altermondales	0.05
O. sarsii vadicola	Bacillales	0.02
O. sarsii vadicola	Cryomorphaceae	0.005
O. sarsii vadicola	Desulfobacterales	0.02
O. sarsii vadicola	Eubacteriales	0.02
O. sarsii vadicola	Flavobacteriales	0.05
O. sarsii vadicola	Fusobacteriales	0.015
O. sarsii vadicola	Oceanospirillales	0.02
O. sarsii vadicola	Rhodobacterales	0.025
O. sarsii vadicola	Spirochaetales	0.01
O. sarsii vadicola	Thiotrichales	0.01
O. sarsii vadicola	Vibrionales	0.01
O. sarsii vadicola	Woeseiales	0.02
O. sarsii vadicola	Z Not Sulfur Related	0.73

APPENDIX C

C SUPPLEMENTAL DATA FOR CHAPTER 4

Table C.1 Measured sediment and water temperature in 2024

Month	Water	1cm	5cm	10cm	12-14cm	38-40cm
Jan	8.7 C	8.4 C	6.9 C	6.7 C	6.4 C	6.3 C
Feb	6.9 C	7 C	6.9 C	6.7 C	6.7 C	6.7 C
Mar	9.1 C	9.3 C	9.2 C	9.1 C	9 C	8.9 C
Apr	14.9 C	14.5 C	14.3 C	14.3 C	14.1 C	13.9 C
May	23.9 C	23.1 C	22.3 C	21.4 C	20.9 C	18.9 C
Jun	26.3 C	25.9 C	25.4 C	24.5 C	24.2 C	22.2 C
Jul	28 C	27.9 C	27.1 C	27 C	26.6 C	25.5 C
Aug	27 C	25.5 C	25.1 C	24.8 C	24.4 C	22.8 C
Sept	21.4 C	22.1 C	21.8 C	21.7 C	21.7 C	21.2 C
Oct	14.2 C	15.5 C	15.9 C	16.1 C	16.7 C	18.2 C
Nov	13.2 C	13 C	13.2 C	13.1 C	13.5 C	14 C
Dec	8.4 C	8.8 C	8.8 C	9 C	9.1 C	10 C

Table C.2 Measured organic nitrogen and total organic carbon in seasonal sediment cores

Sample ID	Depth	Season	mg of C/g of Sediment	mg of N/g of Sediment
Fall 12-14	12-14cm	Fall	9.677012678	1.013040564
Fall 12-14	12-14cm	Fall	10.20371612	1.205622865
Fall 12-14	12-14cm	Fall	9.57193266	2.519555591
Fall 38-40	38-40cm	Fall	13.57600423	1.384104761
Fall 38-40	38-40cm	Fall	13.10544727	1.548172412
Fall 38-40	38-40cm	Fall	18.392253	2.615130489
Fall 48-50	48-50cm	Fall	12.68548865	1.171186005
Fall 48-50	48-50cm	Fall	12.29492195	1.413231887
Fall 48-50	48-50cm	Fall	21.29752692	3.233434658
Spring 12-14	12-14cm	Spring	13.66313313	Below Detection Limit
Spring 12-14	12-14cm	Spring	16.4566601	2.240223333
Spring 12-14	12-14cm	Spring	19.61231277	0.739853909
Spring 38-40	38-40cm	Spring	12.51086364	0.649159107
Spring 38-40	38-40cm	Spring	10.03505498	2.29723771
Spring 38-40	38-40cm	Spring	14.62472721	0.68047787
Spring 48-50	48-50cm	Spring	10.50915996	0.554021902
Spring 48-50	48-50cm	Spring	11.80237223	2.612098708
Spring 48-50	48-50cm	Spring	12.83746741	0.636948174
Summer 12-14	12-14cm	Summer	14.37791257	0.878368399
Summer 12-14	12-14cm	Summer	12.45612457	0.940848273
Summer 12-14	12-14cm	Summer	13.3878108	3.277896657
Summer 38-40	38-40cm	Summer	13.85116972	0.885588464
Summer 38-40	38-40cm	Summer	13.21694417	1.167229916
Summer 38-40	38-40cm	Summer	16.71163658	3.758195429
Summer 48-50	48-50cm	Summer	14.04255839	1.029203885
Summer 48-50	48-50cm	Summer	13.58033216	1.350880566
Summer 48-50	48-50cm	Summer	15.8836917	2.747236448
Winter 12-14	12-14cm	Winter	11.95724777	0.528709275
Winter 12-14	12-14cm	Winter	11.5630047	Below Detection Limit
Winter 12-14	12-14cm	Winter	15.24509026	1.438126905
Winter 38-40	38-40cm	Winter	14.12304003	Below Detection Limit
Winter 38-40	38-40cm	Winter	13.47248389	0.669368271
Winter 38-40	38-40cm	Winter	17.19703457	2.088216793
Winter 48-50	48-50cm	Winter	15.38198744	0.647626478
Winter 48-50	48-50cm	Winter	16.02038027	0.857973122
Winter 48-50	48-50cm	Winter	17.52103084	2.594093893

Table C.3 Calculated EEMs intensities.

Depth	Season	sample	bix	fi	hix	b	t	a	m	c	Integrated_Intensity	percent_b	percent_t	percent_a	percent_m	percent_c	C/M ratio	C/T ratio
12 - 14 cm	Fall	B1S10S10	1.23373212	1.28302307	1.51551889	0.13401268	0.05761342	0.05845194	0.03349738	0.0248695	417.5634985	0.03209396	0.01379752	0.01399834	0.0080221	0.00595586	0.74243119	0.43166159
38 - 40 cm	Fall	B1S11S11	0.97560853	1.24172009	1.71291934	0.1621028	0.09255563	0.0928619	0.04736868	0.04309587	551.200658	0.02940904	0.01679164	0.0168472	0.00859373	0.00781854	0.90979677	0.46562129
48 - 50 cm	Fall	B1S12S12	0.95681059	1.23940238	1.75524335	0.14586451	0.08149092	0.09093472	0.04434928	0.04099561	504.5805554	0.02890807	0.01615023	0.01802184	0.00878934	0.00812469	0.92438047	0.50306966
12 - 14 cm	Winter	B1S13S13	1.06988002	1.19662619	1.7238879	0.07169619	0.0325805	0.04239923	0.02020066	0.01675277	244.8502975	0.02928164	0.01330629	0.01731639	0.00825021	0.00684205	0.82931791	0.51419635
38 - 40 cm	Winter	B1S14S14	0.93920598	1.21737088	1.73676288	0.0767134	0.042759	0.04743645	0.02505611	0.02152538	271.4980408	0.0282556	0.01574928	0.01747211	0.00922884	0.00792837	0.85908693	0.50341172
48 - 50 cm	Winter	B1S15S15	0.94835874	1.20698534	1.82798892	0.06725132	0.03324466	0.04083807	0.02103803	0.01857543	231.9771045	0.0289905	0.01433101	0.01760436	0.00906901	0.00800744	0.88294537	0.55874935
12 - 14 cm	Spring	B1S16S16	0.98791145	1.21212374	1.73537316	0.06871036	0.03514391	0.03932185	0.01947602	0.01743381	236.2424828	0.02908468	0.0148762	0.0166447	0.00824408	0.00737962	0.89514225	0.49606908
38 - 40 cm	Spring	B1S17S17	1.01234118	1.33964743	1.63661109	0.0654942	0.03110698	0.03648708	0.01809167	0.01636144	217.2843514	0.03014216	0.01431625	0.01679232	0.00832626	0.00752997	0.90436327	0.52597332
48 - 50 cm	Spring	B1S18S18	1.00037665	1.26412061	1.70290549	0.07519082	0.03660927	0.04485498	0.02293087	0.01957447	260.2760197	0.02888888	0.01406556	0.01723362	0.00881021	0.00752066	0.85362939	0.53468604
12 - 14 cm	Summer	B1S19S19	0.91423074	1.29236552	1.82017209	0.06394545	0.03050747	0.0399102	0.01987491	0.01830895	225.531198	0.02835326	0.01352694	0.01769609	0.00881249	0.00811815	0.92120925	0.60014643
12 - 14 cm	Winter	B1S1S1	1.0023276	1.2149928	1.7210502	0.14363429	0.07310079	0.08285667	0.04051778	0.03463604	505.3304461	0.02842383	0.01446594	0.01639653	0.00801808	0.00685414	0.85483564	0.47381221
38 - 40 cm	Summer	B1S20S20	0.99980557	1.29016888	1.69469038	0.08669539	0.04750752	0.05262994	0.02534647	0.02261108	298.0985815	0.02908279	0.01593685	0.01765521	0.00850271	0.0075851	0.89208002	0.47594735
48 - 50 cm	Summer	B1S21S21	1.03081376	1.23984478	1.67073393	0.0979474	0.05185599	0.05647074	0.02782173	0.02289425	327.0917215	0.02994493	0.01585365	0.0172645	0.00850579	0.00699934	0.82289109	0.44149676
12 - 14 cm	Fall	B1S22S22	1.040308	1.21663529	1.59564488	0.07135454	0.03580441	0.03840506	0.01873296	0.01567544	237.3899018	0.03005795	0.01508253	0.01617805	0.00789122	0.00660325	0.83678381	0.43780745
38 - 40 cm	Fall	B1S23S23	0.98220221	1.33646691	1.73334425	0.08343314	0.04422038	0.04689828	0.02364479	0.02251809	291.8987628	0.0285829	0.01514922	0.01606663	0.00810034	0.00771435	0.95234861	0.50922416
48 - 50 cm	Fall	B1S24S24	0.90916814	1.32073487	1.75253839	0.07136265	0.03956001	0.04771975	0.02104192	0.01997912	244.6836433	0.02916527	0.01616782	0.01950263	0.00859964	0.00816529	0.94949136	0.50503319
38 - 40 cm	Winter	B1S2S2	0.97245747	1.24846081	1.84280723	0.14881649	0.08123975	0.09122825	0.04604636	0.04178512	519.6915082	0.02863554	0.0156323	0.01755431	0.00886033	0.00804037	0.90745767	0.51434337
48 - 50 cm	Winter	B1S3S3	0.97694054	1.29290916	1.83286627	0.13021296	0.07231909	0.07964252	0.04120614	0.03701512	452.0386979	0.02880571	0.01599843	0.01761852	0.00911562	0.00818848	0.89829135	0.51183057
12 - 14 cm	Spring	B1S4S4	1.04898208	1.21176305	1.51240119	0.1359973	0.09098169	0.07910963	0.04234538	0.03420655	470.5310787	0.02890294	0.01933596	0.01681284	0.00899949	0.00726977	0.80779893	0.37597181
38 - 40 cm	Spring	B1S5S5	0.9413507	1.25092245	1.81462915	0.1318091	0.07248528	0.08389341	0.04103487	0.03747262	462.3193011	0.0285104	0.01567862	0.01814621	0.00887587	0.00810535	0.91318961	0.51696862
48 - 50 cm	Spring	B1S6S6	0.9859628	1.25337904	1.76434146	0.140363	0.07298628	0.08279214	0.04030775	0.0354516	488.9020546	0.02870984	0.01492861	0.0169343	0.00824455	0.00725127	0.87952319	0.48572971
12 - 14 cm	Summer	B1S7S7	0.89264317	1.23768348	1.83349588	0.13317372	0.07539828	0.09170562	0.04452273	0.04158066	482.4409437	0.02760415	0.0156285	0.01900867	0.00922864	0.00861881	0.93391972	0.5514802
38 - 40 cm	Summer	B1S8S8	1.01629207	1.22574946	1.34938314	0.16229001	0.07810114	0.09225424	0.04651764	0.04031347	560.3422974	0.02896266	0.01393811	0.01646391	0.00830165	0.00719444	0.86662753	0.51617008
48 - 50 cm	Summer	B1S9S9	1.02870326	1.25178726	1.6979872	0.19222026	0.10160542	0.1038069	0.05373482	0.04564645	643.1933994	0.0298853	0.01579703	0.0161393	0.00835438	0.00709685	0.84947606	0.44925206
12 - 14 cm	Fall	B1S10S10	1.004166	1.15788391	1.58150865	0.12111973	0.06679892	0.06777338	0.03333491	0.02961949	410.3935002	0.02951307	0.0162768	0.01651424	0.00812267	0.00721734	0.88854269	0.44341269
38 - 40 cm	Fall	B1S11S11	0.88679722	1.19318164	1.7550596	0.12846632	0.08149549	0.0862978	0.04462117	0.04118899	453.6490936	0.02831843	0.01796443	0.01902303	0.00983606	0.00907948	0.92308173	0.50541433
48 - 50 cm	Fall	B1S12S12	0.9664626	1.19166337	1.76922603	0.14253667	0.08139882	0.0914321	0.04686081	0.04085319	504.0843838	0.02827635	0.01614786	0.01813825	0.00929622	0.00810444	0.87179877	0.50188927
12 - 14 cm	Winter	B1S1S1	0.95149156	1.19400607	1.56541367	0.13846383	0.08869915	0.09119778	0.04680041	0.04107138	484.1230383	0.02860096	0.01832161	0.01883773	0.00966705	0.00848367	0.87758594	0.46304141
38 - 40 cm	Winter	B1S2S2	0.97056872	1.22764469	1.78832806	0.15912556	0.09031048	0.10053826	0.05212701	0.0456076	555.3930889	0.02865098	0.01626064	0.01810218	0.00938561	0.00821177	0.87493216	0.50500888
48 - 50 cm	Winter	B1S3S3	0.96856255	1.25039357	1.6672768	0.12651978	0.08031352	0.08247214	0.04197055	0.03796828	436.9437398	0.02895562	0.01838075	0.01887477	0.00960548	0.00868951	0.90464102	0.47275076
12 - 14 cm	Spring	B1S4S4	0.85157349	1.18037756	1.8586027	0.1019581	0.06454822	0.07368611	0.03817348	0.03475944	363.9486742	0.02801442	0.01773553	0.02024629	0.0104887	0.00955064	0.91056502	0.53850344
38 - 40 cm	Spring	B1S5S5	0.99576368	1.22828818	1.71726604	0.13833863	0.07728554	0.08286193	0.04345447	0.03789224	480.4494149	0.02879359	0.01608609	0.01724675	0.00904455	0.00788683	0.87199867	0.4902889
48 - 50 cm	Spring	B1S6S6	0.96355877	1.17372168	1.80761277	0.1530871	0.08618433	0.09583925	0.04818106	0.04345112	542.6309919	0.02821201	0.01588268	0.01766196	0.00887916	0.00800749	0.90182977	0.50416494
12 - 14 cm	Summer	B1S7S7	0.95647087	1.18574725	1.78169984	0.17011579	0.10022724	0.11311998	0.05532805	0.04925277	603.9281965	0.02816822	0.01659589	0.0187307	0.00916136	0.0081554	0.89019528	0.49141105
38 - 40 cm	Summer	B1S8S8	0.91404387	1.18649781	1.78797616	0.15931666	0.09713597	0.10899658	0.05490063	0.04954755	560.3086077	0.02843373	0.01733616	0.01945295	0.00979828	0.0088429	0.90249523	0.51008449
48 - 50 cm	Summer	B1S9S9	0.97922499	1.20745694	1.66098609	0.17183354	0.10314694	0.10461372	0.05408306	0.04656114	587.2639382	0.02926002	0.01756398	0.01781375	0.00920933	0.00792849	0.86091908	0.45140587

Table C.4 DOC measurements coupled with DOC adjusted EEMs measurements.

Sample ID	[DOC]	NPOCuM	DOC_ppm	DOC_uM	Season	Depth	TOC	TON	a254	a300	m	a	t	b	hix	fi	bix	SUVA254
Winter A	0.26611307	22.1557799	0.53222614	44.3115598	Winter	12 - 14 cm	11.9572478	0.52870928	17.6799657	9.1956642	0.03013783	0.07215123	0.06479348	0.11793144	1.67011726	1.20187502	1.00789973	14.4241847
Winter B	0.24135837	20.0947771	0.48271674	40.1895542	Winter	38 - 40 cm	14.12304	-1.0621313	19.957085	10.3518014	0.02131979	0.07973432	0.07143641	0.12821848	1.78929939	1.23115879	0.96074405	17.9519162
Winter C	0.24671495	20.5407504	0.49342991	41.0815008	Winter	48 - 50 cm	15.3819874	0.64762648	16.1856255	8.42481928	0.01230899	0.06765091	0.06195909	0.10799469	1.776044	1.25009602	0.96462061	14.2432823
Spring A	0.21826785	18.1723291	0.43653569	36.3446583	Spring	12 - 14 cm	13.6631331	-1.121859	14.7485173	7.59035181	0.03333163	0.0640392	0.06355794	0.10222192	1.70212568	1.20142145	0.96282234	14.6701538
Spring B	0.22695279	18.895412	0.45390559	37.7908241	Spring	38 - 40 cm	12.5108636	0.64915911	16.9884947	8.7699986	0.03419367	0.06774747	0.0602926	0.11188065	1.72283543	1.27295269	0.98315185	16.251574
Spring C	0.28577122	23.7924586	0.57154244	47.5849171	Spring	48 - 50 cm	10.50916	0.5540219	19.58238	10.2791722	0.0371399	0.07449546	0.06525996	0.12288031	1.75828657	1.23040711	0.9832994	14.8772634
Summer A	0.20823075	17.3366704	0.4164615	34.6733409	Summer	12 - 14 cm	14.3779126	0.8783684	18.631933	9.4928407	0.03990857	0.0815786	0.068711	0.12241166	1.81178927	1.23859875	0.92111493	19.4262566
Summer B	0.28369099	23.619265	0.56738198	47.2385301	Summer	38 - 40 cm	13.8511697	0.88558846	21.3288117	11.0472795	0.04225491	0.08462692	0.07424821	0.13610068	1.61068323	1.23413872	0.97671384	16.3228948
Summer C	0.25560792	21.2811527	0.51121585	42.5623053	Summer	48 - 50 cm	14.0425584	1.02920389	24.5254412	12.7483041	0.0452132	0.08829712	0.08553612	0.1540004	1.67656907	1.23302966	1.012914	20.8314059
Fall A	0.20495439	17.0638907	0.40990878	34.1277813	Fall	12 - 14 cm	9.67701268	1.01304056	17.3717044	9.01266136	0.02852175	0.05487679	0.05340558	0.10882898	1.56422414	1.21918075	1.09273538	18.4018409
Fall B	0.22466454	18.7048992	0.44932909	37.4097983	Fall	38 - 40 cm	13.5760042	1.38410476	20.0193628	10.2628533	0.03854488	0.07535266	0.07275717	0.12466742	1.7337744	1.25712288	0.94820265	19.3460265
Fall C	0.22648474	18.8564435	0.45296949	37.712887	Fall	48 - 50 cm	12.6854887	1.17118601	18.3269422	9.46480749	0.03741734	0.07669553	0.06748325	0.11992128	1.75900259	1.25060021	0.94414711	17.5681943

Table C.5 16S rRNA amplicon abundance of all samples identified down to microbial class.

Row Labels	ABY1	Acetothermia	Acidimicrobiia	Acidobacteriae	Actinobacteria	Actinobacteriota_unc	Aenigmarchaeia	Aerophobia	Alphaproteobacteria	Aminicenantia	Anaerolineae	AncK6_cl	ANME-1	Armatimonadota_unclassified	Asgardarchaeota_cl	Asgardarchaeota_unclassified	AT-S3-28	Babeliae	Bacilli	Bacteroidia	Bathyarchaeia	BD2-11_terrestrial_group
Spring 1A	0	0	0	0	0	0	10	0	66	73	235	0	0	0	0	0	0	58	30	22	205	0
Spring 1B	61	160	14	11	47	0	22	23	345	622	1707	11	64	0	0	0	0	74	221	394	1131	40
Spring 1C	0	33	0	0	11	0	0	0	44	169	440	0	15	13	0	0	0	26	18	58	349	0
Spring 2A	0	0	0	0	16	0	0	0	73	99	223	0	13	0	0	0	0	17	32	41	262	0
Spring 2B	0	24	0	0	0	0	0	0	37	95	234	0	0	0	0	0	0	20	15	48	260	0
Spring 2C	0	36	0	0	0	0	0	0	41	129	325	0	13	0	0	0	0	18	20	61	309	0
Spring 3A	0	14	0	0	0	0	0	0	38	111	170	0	0	0	0	0	0	0	0	0	140	0
Spring 3B	0	45	0	0	20	0	0	0	113	281	588	0	0	0	0	0	0	49	42	127	432	0
Spring 3C	13	36	0	14	75	0	14	10	238	388	999	0	10	0	0	0	0	108	46	245	945	11
Winter 1A	14	60	0	0	58	0	23	0	273	420	712	28	24	0	14	0	0	78	188	152	671	0
Winter 1B	28	114	19	21	54	15	0	26	647	803	2573	14	51	0	0	17	0	100	184	489	1827	21
Winter 1C	29	149	0	0	60	0	20	25	579	780	1758	19	22	0	0	0	0	36	120	361	1247	11
Winter 2A	21	0	0	0	145	0	0	16	176	108	187	0	0	0	0	0	0	28	207	232	274	0
Winter 2B	23	17	0	13	0	0	0	0	89	187	481	0	26	10	0	0	0	24	24	90	543	10
Winter 2C	21	45	0	0	42	0	32	13	268	385	1156	0	43	51	0	0	0	130	69	383	1472	17
Winter 3A	0	0	0	0	1755	0	0	0	13	20	17	0	0	0	0	0	0	0	197	31	55	0
Winter 3B	240	580	16	41	94	25	40	81	735	1794	8393	54	263	38	0	30	12	342	162	1495	5993	46
Winter 3C	84	246	18	22	97	19	38	36	553	1459	4322	17	263	24	10	0	0	201	140	707	3690	26
Summer 1A	40	163	11	0	72	0	20	15	694	731	1526	0	23	0	12	0	0	140	98	339	1031	13
Summer 1B	0	29	0	0	14	0	0	0	126	125	323	0	0	0	0	0	0	24	14	70	227	0
Summer 1C	46	144	24	14	77	0	12	25	611	693	1607	0	40	0	10	0	0	140	93	297	955	21
Summer 2A	126	281	436	591	746	11	28	14	659	1242	3657	0	88	10	11	0	0	284	175	970	3203	29
Summer 2B	69	101	133	165	197	12	26	0	359	489	1639	0	40	10	0	0	0	109	114	334	1075	13
Summer 2C	84	117	150	183	216	14	31	14	613	1105	2595	0	99	0	0	13	0	220	137	467	2108	43
Summer 3A	0	0	0	0	0	0	0	0	0	0	0	0	0	0	0	0	0	0	1	0	0	0
Summer 3B	71	120	22	18	108	15	50	16	577	1149	2497	13	72	22	12	0	0	333	192	594	2989	33
Summer 3C	0	1	0	0	0	0	0	0	0	1	3	0	0	0	0	0	0	0	0	1	3	0
Fall 1A	0	18	0	0	11	0	0	0	70	102	291	0	11	0	0	0	0	11	0	92	257	0
Fall 1B	13	47	0	0	15	0	0	0	115	228	558	0	60	0	0	0	0	28	41	170	618	0
Fall 1C	6.5	32.5	0	0	13	0	0	0	92.5	165	424.5	0	35.5	0	0	0	0	19.5	20.5	131	437.5	0
Fall 2A	12	53	0	0	39	0	0	0	143	223	484	0	15	0	0	0	0	48	32	151	580	0
Fall 2B	73	287	17	10	77	0	19	21	675	850	2560	0	101	11	15	0	0	151	146	588	2782	13
Fall 2C	42.5	170	8.5	5	53.5	0	9.5	10.5	409	536.5	1522	0	58	5.5	7.5	0	0	98.5	89	369.5	1681	6.5
Fall 3A	48	209	24	23	103	0	45	23	477	756	2816	11	68	12	17	0	0	135	104	499	2613	21
Fall 3B	20	113	29	17	35	0	0	22	314	514	1601	10	70	0	0	0	0	49	80	367	1401	14
Fall 3C	34	161	26.5	20	67.5	0	22.5	22.5	395.5	635	2108.5	10.5	69	6	8.5	0	0	92	92	433	2007	17.5

Bdellovibrionia	BH60-139_cl	Brocadiae	Calditrichia	Campylobacteria	Chthonivirionia	Chlamydiae	Chloroflexi_unclassified	CK-2C2-2_cl	Clostridia	Coriobacteriia	Crenarchaeota_unclassified	Cyanobacteria	Dadabacteria	Dehalococcoidia	Desulfitobacterii	Desulfobaccia	Desulfobacteria	Desulfobacterota_unclassified	Desulfobulbia	Desulfomonilia	Desulfonatronumbellia	Desulfuromonadia
0	0	0	13	0	0	0	24	0	140	0	16	0	0	303	0	0	79	0	0	0	0	0
0	0	46	98	0	20	32	136	0	686	0	127	42	0	3053	0	36	906	18	28	11	0	0
0	0	16	28	0	0	18	23	0	86	0	30	11	0	883	0	0	230	0	0	0	0	14
0	0	0	29	0	0	0	31	0	151	0	0	52	0	467	0	0	115	0	0	0	0	0
0	0	11	18	0	0	0	17	0	73	0	17	0	0	485	0	0	124	0	0	0	0	0
0	0	31	21	0	0	0	26	0	92	0	21	0	0	676	0	0	98	0	0	0	0	0
0	0	0	0	0	0	12	23	0	22	0	0	0	0	184	0	19	61	0	0	0	0	0
0	0	24	26	0	0	24	50	0	106	0	41	14	0	1425	10	25	334	0	0	0	0	0
0	19	77	40	0	0	45	54	0	196	0	71	41	0	2458	0	69	663	0	0	11	13	0
0	0	12	20	0	0	61	30	0	158	0	116	45	0	1104	0	0	645	0	26	0	0	55
0	0	98	190	56	0	34	140	0	448	0	382	72	0	3612	31	100	1247	21	22	22	0	23
0	0	29	107	0	10	39	130	0	240	0	249	41	0	2835	0	0	989	17	12	19	0	12
0	0	0	13	11	0	0	0	0	243	0	30	20	0	427	0	0	209	0	0	0	0	10
0	0	0	47	0	0	0	28	0	103	0	69	0	0	1222	12	16	254	0	0	0	0	0
0	0	55	115	24	0	39	52	0	333	0	198	23	0	2721	15	66	858	13	15	0	0	0
0	0	0	0	0	0	0	0	0	345	41	0	0	0	94	0	0	40	0	0	0	0	0
10	13	252	572	10	58	95	549	27	1211	0	794	88	0	13860	36	142	3405	44	19	50	16	32
0	13	140	228	17	13	79	372	15	662	10	472	105	0	8398	32	58	2026	29	0	56	17	53
0	0	44	118	17	0	64	70	0	272	0	192	63	0	2897	11	46	928	0	11	25	0	29
0	0	11	29	0	0	11	13	0	47	0	36	23	0	500	0	0	192	0	0	0	0	0
0	13	68	114	22	0	38	77	0	294	12	181	29	0	2863	16	35	865	15	0	20	10	18
0	22	143	270	18	15	96	301	0	824	0	531	80	0	7935	20	78	2307	52	15	32	13	27
0	12	78	112	0	0	51	153	0	408	0	144	33	0	3573	13	50	859	17	19	19	10	35
0	0	86	156	13	0	86	211	0	576	0	288	63	0	5412	0	133	1521	24	16	41	18	19
0	0	0	0	0	0	0	0	0	0	0	0	0	0	0	0	0	0	0	0	0	0	0
0	15	74	216	0	0	121	192	0	641	0	463	52	12	6319	28	107	1706	20	11	55	10	27
0	0	0	0	0	0	0	0	0	0	0	1	0	0	2	0	0	1	0	0	0	0	0
0	0	0	29	0	0	0	0	0	41	0	36	0	0	385	0	0	159	0	0	0	0	0
0	0	25	38	0	0	0	35	0	97	0	110	12	0	994	0	0	314	0	10	0	0	0
0	0	12.5	33.5	0	0	0	17.5	0	69	0	73	6	0	689.5	0	0	236.5	0	5	0	0	0
0	0	22	68	0	0	0	26	0	121	0	60	12	0	1339	0	17	384	0	0	13	0	0
0	11	104	153	0	0	55	169	0	836	0	345	66	0	6186	10	52	1431	25	10	28	0	15
0	5.5	63	110.5	0	0	27.5	97.5	0	478.5	0	202.5	39	0	3752.5	5	34.5	907.5	12.5	5	20.5	0	7.5
0	0	74	177	19	0	53	185	0	641	0	395	35	0	5188	18	53	1364	14	20	49	16	31
0	0	33	98	0	0	34	95	0	701	0	208	0	0	2609	0	33	779	10	15	20	0	0
0	0	53.5	137.5	9.5	0	43.5	140	0	671	0	301.5	17.5	0	3898.5	9	43	1071.5	12	17.5	34.5	8	15.5

D2-56	Dissulfuribacteria	Elusimicrobia	Elusimicrobiota_unclassified	Endomicrobia	Fibrobacteria	Firmicutes_unclassified	Gammaproteobacteria	GN01_cl	Gracilibacteria	Hadarchaeia	Halamaericbia	Halobacteria	Helmidalbacteria	Hydrogenedentia	JS1	KD4-96	Kiritimatiellae	Kladobacteria	Latescibacteria	Latescibacteria_cl	LCA-59_cl	Leptospirae	Limnochordia	Lokiarchaeia	MBNT15_cl	MD2902-B12	Methanobacteria	Methanosarcinia	Methanomicrobia
0	0	0	0	0	0	29	134	13	0	0	0	0	0	0	23	0	0	0	0	0	0	20	72	0	0	0	0	0	19
24	0	19	0	0	0	61	178	12	0	0	0	0	0	0	116	0	19	0	61	0	13	11	45	680	11	16	38	0	151
11	0	0	0	0	0	0	30	18	0	0	0	0	0	0	49	0	0	0	11	0	0	0	30	219	0	0	11	0	24
16	0	0	0	0	0	0	55	0	0	0	11	0	0	0	43	0	0	0	0	0	0	0	64	177	0	0	11	0	13
0	0	0	0	0	0	13	13	0	0	0	0	0	0	0	20	0	0	0	0	0	0	0	25	108	0	0	0	0	14
0	0	0	0	0	0	31	27	0	0	0	0	0	0	0	27	0	0	0	14	0	0	0	20	135	0	0	0	0	18
0	0	0	0	0	0	0	23	0	0	0	0	0	0	0	50	0	0	0	0	0	0	0	0	0	0	0	0	0	0
15	0	0	0	0	0	12	49	11	0	0	0	0	0	0	71	0	0	0	22	0	11	0	20	171	0	0	12	0	13
45	0	0	0	0	0	35	63	0	0	0	0	0	25	0	122	0	0	0	29	0	0	0	44	352	0	0	21	15	42
0	0	0	0	0	0	18	199	0	0	0	0	16	0	0	43	0	0	0	0	0	0	0	19	246	15	0	0	0	83
63	16	0	22	0	15	72	294	60	0	0	32	15	0	35	12	197	0	29	0	71	13	0	19	71	1909	0	0	16	398
61	0	19	0	0	0	17	210	39	0	16	0	0	85	0	187	0	0	10	70	0	0	19	28	615	0	0	0	0	168
0	0	0	0	0	0	0	137	0	0	0	0	0	36	0	34	0	125	0	0	0	0	0	0	105	0	0	0	0	0
0	0	0	0	0	0	12	30	12	0	0	0	0	11	0	51	0	0	0	0	0	0	0	31	290	0	0	0	0	55
63	0	0	0	0	0	219	196	90	0	0	33	12	37	0	79	15	0	0	16	33	0	0	12	48	883	10	0	0	147
0	0	0	0	0	0	0	19	0	0	0	0	0	0	0	0	0	0	0	0	0	0	0	0	25	0	0	0	0	0
262	29	45	12	0	10	333	200	77	0	22	50	24	91	29	470	0	0	12	150	0	14	42	145	2143	11	21	62	31	447
140	22	62	0	0	0	89	217	62	15	12	28	45	61	14	275	12	0	10	107	0	14	59	156	1416	0	23	49	36	195
32	0	13	0	0	24	52	192	28	20	0	10	0	45	15	196	0	25	0	71	13	0	0	96	721	0	0	20	14	67
0	0	0	0	0	0	0	39	0	0	0	0	0	19	0	27	0	0	0	15	0	0	0	0	134	0	0	0	0	18
48	0	0	0	0	19	39	174	41	0	0	0	0	59	21	134	0	0	0	72	0	21	0	63	644	0	0	16	0	71
167	0	0	0	0	10	113	284	75	14	17	43	33	47	14	194	14	18	13	123	0	13	24	645	1324	14	30	27	16	221
58	0	0	16	0	0	101	127	15	0	10	19	0	16	12	104	0	12	0	57	0	0	0	87	468	0	13	21	0	82
53	0	0	11	13	10	73	245	53	0	17	28	71	46	0	221	0	10	0	107	0	17	0	87	996	12	25	40	0	94
0	0	0	0	0	0	0	0	0	0	0	0	0	0	0	0	0	0	0	0	0	0	0	0	0	0	0	0	0	0
169	0	0	0	13	0	89	229	48	0	16	47	21	46	13	179	0	0	0	97	0	0	22	112	1062	0	22	42	0	134
0	0	0	0	0	0	0	0	0	0	0	0	0	0	0	0	0	0	0	0	0	0	0	0	0	0	0	0	0	0
0	0	0	0	0	0	16	34	0	0	0	0	0	12	0	11	0	0	0	0	0	0	0	67	119	0	0	0	0	12
17	0	0	0	0	0	19	93	19	0	0	0	0	27	0	45	0	0	0	13	0	0	0	14	307	0	0	0	0	81
8.5	0	0	0	0	0	13	42	9.5	0	0	0	0	19.5	0	28	0	0	0	6.5	0	0	0	40.5	213	0	0	0	0	36.5
13	0	0	0	0	0	62	60	10	0	0	0	0	12	0	20	0	0	0	0	0	0	0	79	260	0	0	15	0	59
42	0	17	14	0	11	73	186	42	10	0	19	13	22	11	133	0	0	0	72	0	14	16	210	1291	13	21	42	16	272
27.5	0	8.5	7	0	5.5	67.5	123	28	5	0	9.5	6.5	17	5.5	81.5	0	0	0	36	0	7	8	144	778	6.5	10.5	28.5	8	165.5
48	0	0	24	0	30	101	213	60	17	0	13	23	34	0	197	0	0	0	74	0	0	9	165	1093	0	14	26	0	238
33	0	11	14	0	0	38	82	16	0	0	0	0	22	0	41	13	116	11	0	0	0	11	109	588	0	14	11	0	48
49.5	0	5.5	19	0	15	69.5	147.5	38	8.5	0	6.5	23	27.5	6.5	156.5	5.5	0	0	59	0	8	5.5	162	820.5	0	14	18.5	0	143

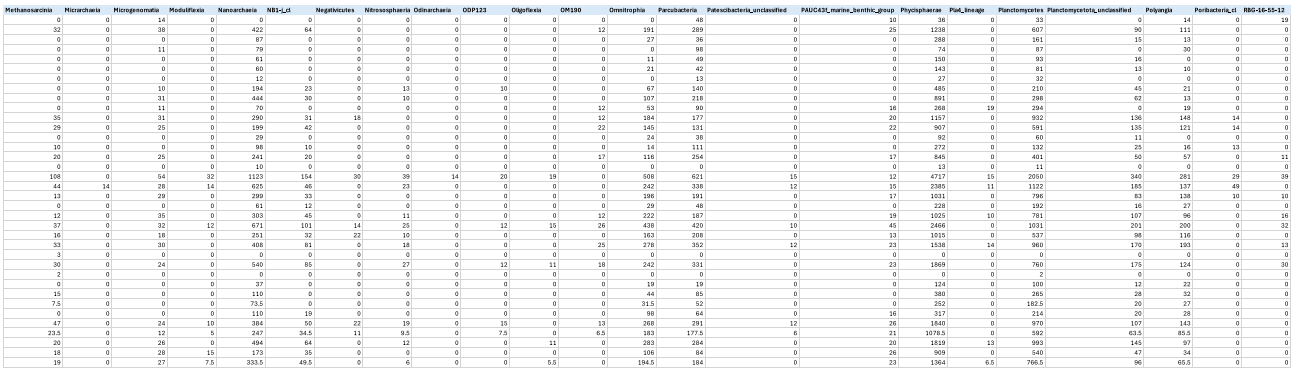

Table C.6 Averaged bacterial and archaeal qPCR results coupled with calculated standard deviation and standard error.

Bacterial					Archaeal			
Sample	std	avg	error		Sample	std	avg	error
Apr 12-14	3.08E+11	2.92E+11	1.09E+11		Apr 12-14	41577258641	3.10E+10	13859086214
Apr 38-40	1.06E+11	1.89186E+11	40145642167		Apr 38-40	6.07827E+11	4.22E+11	2.02609E+11
Apr 48-50	1.19E+11	1.43136E+11	44824521237		Apr 48-50	10438462464	1.50E+10	3479487488
Jan 12-14	1.39E+11	2.97071E+11	52571088896		Jan 12-14	13674840036	3.09E+10	4558280012
Jan 38-40	1.32E+11	2.2033E+11	41888768184		Jan 38-40	10569929044	1.95E+10	3523309681
Jan 48-50	5.40E+11	8.396E+11	1.70711E+11		Jan 48-50	64014908767	7.60E+10	21338302922
July 12-14	4.12E+11	1.33E+12	1.37277E+11		July 12-14	11882655427	4.91E+10	3960885142
July 38-40	6.16E+11	2.49889E+12	2.05172E+11		July 38-40	50104659907	1.45E+11	16701553302
July 48-50	4.06E+11	2.19E+12	1.35421E+11		July 48-50	15410286968	1.05E+11	5.14E+09
Oct 12-14	7.38E+10	9.28E+10	27900229341		Oct 12-14	1.15286E+11	8.77E+10	38428710621
Oct 38-40	3.78E+11	6.76371E+11	1.42785E+11		Oct 38-40	1.29429E+11	1.60E+11	43143027991
Oct 48-50	2.70E+11	4.41571E+11	1.02055E+11		Oct 48-50	2.00608E+11	1.60E+11	66869254861

APPENDIX D

D SUPPLEMENTAL DATA FOR CHAPTER 5

Table D.1 16S rRNA amplicon abundance identified to the Phyla level of October sediment core.

Sample	Phyla	Avg Total
O 12-14	Chloroflexi	1136
O 12-14	Bacteria_unclassified	521.5
O 12-14	Crenarchaeota	510.5
O 12-14	Planctomycetota	475
O 12-14	Desulfobacterota	260.5
O 12-14	Asgardarchaeota	236
O 12-14	Acidobacteriota	198
O 12-14	Firmicutes	159
O 12-14	Proteobacteria	134.5
O 12-14	Bacteroidota	131
O 12-14	Thermoplasmatota	124
O 12-14	Spirochaetota	88.5
O 12-14	Halobacterota	88
O 12-14	unknown_unclassified	86
O 12-14	Nanoarchaeota	73.5
O 12-14	Patescibacteria	52
O 12-14	Archaea_unclassified	49.5
O 12-14	Actinobacteriota	44
O 12-14	Calditrichota	14.5
O 38-40	Chloroflexi	5376
O 38-40	Crenarchaeota	1893.5
O 38-40	Bacteria_unclassified	1844
O 38-40	Planctomycetota	1819.5
O 38-40	Desulfobacterota	1010.5
O 38-40	Firmicutes	816.5
O 38-40	Asgardarchaeota	807.5
O 38-40	Acidobacteriota	667
O 38-40	Proteobacteria	532
O 38-40	Bacteroidota	369.5
O 38-40	Spirochaetota	353.5
O 38-40	Thermoplasmatota	321
O 38-40	Halobacterota	272.5
O 38-40	Patescibacteria	248
O 38-40	Nanoarchaeota	247
O 38-40	unknown_unclassified	240.5
O 38-40	Archaea_unclassified	230
O 38-40	Verrucomicrobiota	228
O 38-40	Actinobacteriota	227.5
O 38-40	Calditrichota	34
O 48-50	Chloroflexi	6161
O 48-50	Crenarchaeota	2319
O 48-50	Planctomycetota	2299.5
O 48-50	Bacteria_unclassified	2281
O 48-50	Desulfobacterota	1212.5
O 48-50	Firmicutes	1038.5
O 48-50	Asgardarchaeota	877.5
O 48-50	Acidobacteriota	801
O 48-50	Proteobacteria	543.5
O 48-50	Thermoplasmatota	439
O 48-50	Bacteroidota	433
O 48-50	Nanoarchaeota	333.5
O 48-50	Actinobacteriota	309.5
O 48-50	Spirochaetota	279.5
O 48-50	unknown_unclassified	267
O 48-50	Halobacterota	263
O 48-50	Archaea_unclassified	205.5
O 48-50	Verrucomicrobiota	190.5
O 48-50	Patescibacteria	190

Table D.2 16S rRNA amplicon abundance identified to the Class level of post 30, 90, and 150-days inoculation coupled with depth, reductant, redox, and time.

Row Labels	ABY1	Acetothermia	Acidobacteriota	Actinobacteria	Actinobacteriota	Aerophobia	Alphaproteobacteria	Aminicenantales	Aminicenantia	Anaerolineae	ANME-1	Archaea_unclassified	Asgardarchaeota	Babeliae	Bacilli	Bacteria_unclassified	Bacteroidia	Bacteroidota	Bathyarchaeia	Burkholderiales	Calditrichales	Calditrichia	Calditrichota	Chlamydiia
120_DA1	0	0	0	0	0	0	0	0	0	0	0	0	0	0	0	0	0	0	0	0	0	0	0	0
120_DA10	0	0	0	0	0	0	0	0	0	0	0	0	116	0	0	0	0	0	0	0	0	0	0	0
120_DA2	0	0	0	0	0	0	0	0	0	0	0	0	0	0	0	0	0	0	0	0	0	0	0	0
120_DA3	0	0	0	0	0	0	0	0	0	0	0	0	0	0	0	0	0	0	0	0	0	0	0	0
120_DA4	0	0	0	0	0	0	0	0	0	0	0	0	0	0	0	0	0	3	0	0	0	0	0	0
120_DA5	0	0	0	0	0	0	0	0	0	0	0	0	0	0	0	0	0	115	0	0	0	0	0	0
120_DA6	0	0	0	0	0	0	0	0	0	0	0	0	0	0	0	0	0	138	0	0	0	0	0	0
120_DA7	0	0	0	0	0	0	0	0	0	0	0	0	137	0	0	0	0	0	0	0	0	0	0	0
120_DA8	0	0	0	0	0	0	0	0	0	0	0	0	0	0	0	0	0	2508	0	0	0	0	0	0
120_DA9	0	0	0	0	0	0	0	0	0	0	0	0	0	0	0	0	0	0	0	0	0	0	0	0
120_DB1	0	0	128	0	0	0	0	0	0	0	0	0	311	0	0	0	0	136	0	0	0	0	0	0
120_DB10	0	0	48	0	0	0	0	0	0	0	0	0	33	0	0	0	0	17	0	0	0	0	0	0
120_DB2	0	0	0	0	0	0	0	0	0	0	0	0	0	0	0	0	0	0	0	0	0	0	8	0
120_DB3	0	0	0	0	6	0	0	0	0	0	0	0	8	0	0	0	0	0	0	0	0	0	0	0
120_DB4	0	0	15	0	59	0	0	0	0	0	0	0	22	0	0	0	0	0	0	0	0	0	0	0
120_DB5	0	0	49	0	0	0	0	0	0	0	0	0	110	0	0	0	0	0	0	0	0	0	0	0
120_DB6	0	0	0	0	0	0	0	0	0	0	0	0	0	0	0	0	0	0	0	0	0	0	0	0
120_DB7	0	0	0	0	0	0	0	0	0	0	0	0	20	0	0	0	0	12	0	0	0	0	0	0
120_DB8	0	0	20	0	0	0	0	0	0	0	0	0	37	0	0	0	0	0	0	0	0	0	0	0
120_DB9	0	0	37	0	0	0	0	0	0	0	0	0	27	0	0	0	0	0	0	0	0	0	0	0
120_DC1	0	0	0	0	0	0	0	0	0	0	0	0	0	0	0	0	0	0	0	0	0	0	0	0
120_DC10	0	0	0	0	0	0	0	0	0	0	0	0	0	0	0	0	0	0	0	0	0	0	0	0
120_DC2	0	0	38	0	0	0	0	0	0	0	0	0	32	0	0	0	0	0	0	0	0	0	0	0
120_DC3	0	0	9	0	0	0	0	0	0	0	0	0	0	0	0	0	0	0	0	0	0	0	0	0
120_DC4	0	0	0	0	0	0	0	0	0	0	0	0	0	0	0	0	0	0	0	0	0	0	0	0
120_DC5	0	0	0	0	0	0	0	0	0	0	0	0	0	0	0	0	0	0	0	0	0	0	0	0
120_DC6	0	0	0	0	0	0	0	0	0	0	0	0	12	0	0	0	0	0	0	0	0	0	0	0
120_DC7	0	0	0	0	0	0	0	0	0	0	0	0	0	0	0	0	0	0	0	0	0	0	0	0
120_DC8	0	0	0	0	0	0	0	0	0	0	0	0	0	0	0	0	0	0	0	0	0	0	0	0
120_DC9	0	0	0	0	0	0	0	0	0	0	0	0	0	0	0	0	0	0	0	0	0	0	0	0
180_DA1	0	0	0	0	0	0	0	0	0	3	0	0	0	0	0	20	0	0	2	0	0	0	0	4
180_DA10	0	0	0	0	0	0	0	0	0	25	0	0	0	0	0	296	0	0	19	0	0	0	0	0
180_DA2	0	0	0	0	0	0	0	0	0	1	0	0	0	0	0	1	0	0	0	0	0	0	0	0
180_DA3	0	0	0	0	0	0	0	0	0	6	0	0	0	0	0	108	0	0	0	0	0	0	0	0
180_DA4	0	0	0	2	0	0	0	0	0	2	0	0	0	3	12	0	0	0	0	0	0	0	0	0
180_DA5	0	0	0	0	0	0	5	0	1	1	0	0	0	0	14	0	0	4	0	0	0	0	0	0
180_DA6	0	0	0	0	0	0	146	0	0	0	0	0	0	0	0	0	0	0	0	0	0	0	0	0
180_DA7	0	0	0	0	0	0	0	0	0	75	0	0	0	0	3161	0	0	198	0	0	0	0	0	0
180_DA8	0	0	0	7	0	0	0	0	0	0	0	0	0	0	259	0	50	0	0	0	0	0	0	0
180_DA9	0	0	0	0	0	0	0	0	0	0	0	0	0	0	308	0	0	0	0	0	0	0	0	0
180_DB1	0	0	0	0	0	0	0	0	7	20	0	0	0	0	0	0	3	31	0	0	5	0	0	0
180_DB10	0	0	0	0	0	0	0	0	0	78	0	0	0	0	206	0	0	192	0	0	0	0	0	0
180_DB2	0	0	0	1	0	0	2	0	0	0	0	0	0	0	8	0	0	0	0	0	0	0	0	0
180_DB3	0	0	0	0	0	0	0	0	0	2	0	0	0	0	2	0	0	0	0	0	0	0	0	0
180_DB4	0	0	0	0	0	0	0	0	0	0	0	0	0	0	0	0	0	0	13	0	0	0	0	0
180_DB5	0	0	0	0	0	0	4	0	1	2	0	0	0	0	0	0	0	0	0	0	0	0	0	0
180_DB6	0	0	0	0	0	0	0	0	0	0	0	0	0	0	0	0	0	0	0	0	0	0	0	0
180_DB7	0	0	0	0	0	0	0	0	0	0	0	0	0	0	0	0	0	2	0	0	0	0	0	0
180_DB8	0	0	0	0	0	0	0	0	0	0	0	0	0	0	0	0	0	13	0	0	0	0	0	0
180_DB9	0	0	0	0	0	0	2	0	0	7	0	0	0	0	20	0	0	0	5	0	0	0	0	0
180_DC1	0	6	0	3	0	0	3	0	7	0	0	0	0	3	3	0	2	8	0	0	0	0	0	0
180_DC10	0	0	0	0	0	0	0	0	0	53	0	0	0	0	1389	0	0	119	0	0	0	0	0	0
180_DC2	0	0	0	0	1	0	0	0	0	1	0	0	0	0	1	0	0	0	0	0	0	0	0	0
180_DC3	0	0	0	0	0	0	0	0	1	2	0	0	0	0	0	0	0	0	0	0	0	0	0	0
180_DC4	0	0	0	0	0	0	2	0	2	3	0	0	0	0	0	0	0	1	0	0	1	0	0	0
180_DC5	0	0	0	8	0	0	0	0	0	0	0	0	0	0	20	0	0	0	0	0	0	0	0	0
180_DC6	0	0	0	6	0	0	0	0	0	0	0	0	0	0	9	0	0	0	0	0	0	0	0	0
180_DC7	0	0	0	0	0	0	0	0	0	0	0	0	0	0	2	0	0	0	0	0	0	0	0	0
180_DC8	0	0	0	0	0	0	0	0	0	0	0	0	0	0	755	0	0	43	0	0	0	0	0	0
180_DC9	0	0	0	0	0	0	0	0	0	0	0	0	0	0	31	0	0	0	0	0	0	0	0	0
30_DA1	4	7	0	4	0	0	18	0	13	9	3	0	0	6	0	0	10	15	0	0	0	0	0	0
30_DA10	0	0	0	0	0	0	0	0	0	106	0	0	0	0	0	0	0	142	0	0	0	0	0	0
30_DA2	0	0	0	0	0	0	0	0	11	20	0	0	0	0	0	0	0	31	0	0	0	0	0	0
30_DA3	0	0	0	0	0	0	12	0	20	34	0	0	0	0	0	0	10	38	0	0	0	0	0	0
30_DA4	0	0	0	0	0	0	0	4	0	0	0	0	0	0	0	0	0	3	25	3	0	0	0	0
30_DA5	0	0	0	0	0	0	0	0	0	0	0	0	0	0	0	0	0	0	0	0	0	0	0	0
30_DA6	0	0	0	0	0	0	0	0	0	124	0	0	0	0	0	0	812	218	0	0	0	0	0	0
30_DA7	0	0	0	0	0	0	115	0	194	436	0	0	0	0	0	0	196	614	0	0	0	0	0	0
30_DA8	0	0	0	0	0	0	0	0	0	0	0	0	0	0	0	0	0	0	0	0	0	0	0	0
30_DA9	0	0	0	0	0	0	0	0	0	0	0	0	0	0	0	0	0	137	0	0	0	0	0	0
30_DB1	0	2	0	4	0	0	0	0	6	10	0	0	0	0	2	0	0	4	0	0	0	0	0	0
30_DB10	0	0	0	0	0	0	131	0	239	368	0	0	0	0	0	0	100	829	0	0	0	0	20	0
30_DB2	0	0	0	0	0	0	0	0	64	45	0	0	0	0	0	0	39	114	0	0	0	0	0	0
30_DB3	0	45	0	6	0	0	40	0	20	11	0	0	0	0	0	0	18	30	0	0	0	0	0	0
30_DB4	0	0	0	0	0	0	0	0	103	200	0	0	0	0	0	0	86	364	0	0	0	0	10	0
30_DB5	0	0	0	0	0	0	69	0	228	273	0	0	0	0	0	0	129	534	0	0	0	0	0	0
30_DB6	0	0	0	0	0	0	31	0	35	70	0	0	0	0	19	0	37	125	0	0	0	0	0	0
30_DB7	0	0	0	0	0	0	128	0	429	445	0	0	0	0	0	0	150	942	0	0	0	0	0	0
30_DB8	0	0	0	0	0	0	30	0	94	150	0	0	0	0	0	0	47	262	0	0	0	0	0	0
30_DB9	0	0	0	0	0	0	70	0	68	72	0	0	0	0	0	0	40	289	0	0	0	0	0	0
30_DC1	0	0	0	0	0	0	0	0	50	66	0	0	0	0	0	0	0	155	0	0	0	0	0	0
30_DC10	0	0	0	0	0	0	0	0	0	0	0	0	0	0	0	0	0	0	0	0	0	0	0	0
30_DC2	0	4	0	6	0	0	0	0	5	4	0	0	0	2	1	0	0	2	0	0	0	0	0	0
30_DC3	0	0	0	5	0	0	3	0	0	0	0	0	0	1	0	0	0	1	0	0	0	0	0	0
30_DC4	0	0	0	0	0	0	0	0	0	0	0	0	0	0	12	0	5	0	0	0	0	0	0	0
30_DC5	0	0	0	0	0	0	0	0	0	0	0	0	0	0	0	0	0	0	0	0	0	0	0	0
30_DC6	0	0	0	0	0	0	0	0	0	0	0	0	0	0	0	0	0	12	0	0	0	0	0	0
30_DC7	0	0	0	0	0	0	0	0	0	0	0	0	0	0	0	0	0	0	0	0	0	0	0	0
30_DC8	0	0	0	0	0	0	0	0	0	0	0	0	0	0	0	0	0	0	0	0	0	0	0	0
30_DC9	0	0	0	0	0	0	0	0	171	455	0	0	0	0	0	0	168	751	0	0	0	0	0	0

Chloroflexi	Clostridia	Crenarchaeota	Crenarchaeota_unclassified	Cyanobacteria	Cyanobacteria	Dehalococcoidia	Desulfarculia	Desulfobaccia	Desulfobacteria	Desulfobacterota	Desulfobulbia	Desulfovibrionia	Ectothiorhodospirales	Fibrobacterota	Firmicutes	Gammaproteobacteria	Halanaerobiia	Halobacterales	Halobacteria
0	0	0	0	0	0	0	0	0	0	133	0	0	0	0	43	0	0	0	0
503	0	326	0	0	0	0	0	0	0	1391	0	0	0	0	1501	0	0	0	0
79	0	38	0	0	0	0	0	0	0	0	0	0	0	0	199	0	0	0	0
568	0	259	0	0	0	0	0	0	0	4463	0	0	0	0	2388	0	0	0	0
0	0	0	0	0	0	0	0	0	0	0	0	0	0	0	18	0	0	0	0
136	0	41	0	0	0	0	0	0	0	0	0	0	0	0	356	0	0	0	0
416	0	212	0	0	0	0	0	0	0	197	0	0	0	0	1975	0	0	0	0
453	0	255	0	0	0	0	0	0	0	128	0	0	0	0	4541	0	0	0	0
657	0	310	0	0	0	0	0	0	0	192	0	0	0	0	6592	0	0	0	0
632	0	304	0	0	0	0	0	0	0	1479	0	0	0	0	1342	0	0	0	0
1470	0	689	0	0	0	0	0	0	0	142	0	0	0	0	622	0	0	0	0
189	0	92	0	0	0	0	0	0	0	0	0	0	0	0	73	0	0	0	0
21	0	1	0	0	0	0	0	0	0	0	0	0	0	2	5	0	0	0	0
39	0	16	0	5	0	0	0	0	0	0	0	0	0	0	33	0	0	0	0
124	0	70	0	0	0	0	0	0	0	0	0	0	0	0	134	0	0	0	0
414	0	207	0	0	0	0	0	0	0	72	0	0	0	0	39	0	0	0	0
175	0	72	0	0	0	0	0	0	0	21	0	0	0	0	80	0	0	0	0
58	0	23	0	0	0	0	0	0	0	6	0	0	0	0	0	0	0	0	0
139	0	70	0	0	0	0	0	0	0	22	0	0	0	0	47	0	0	0	0
200	0	114	0	0	0	0	0	0	0	37	0	0	0	0	0	0	0	0	0
0	0	0	0	0	0	0	0	0	0	0	0	0	0	0	0	0	0	0	0
568	0	194	0	0	0	0	0	0	0	0	0	0	0	0	2106	0	0	0	0
344	0	105	0	0	0	0	0	0	0	0	0	0	0	0	83	0	0	0	0
0	0	0	0	0	0	0	0	0	0	0	0	0	0	0	20	0	0	0	0
115	0	72	0	0	0	0	0	0	0	0	0	0	0	0	120	0	0	0	0
0	0	0	0	0	0	0	0	0	0	0	0	0	0	0	2	0	0	0	0
45	0	33	0	0	0	0	0	0	0	0	0	0	0	0	95	0	0	0	0
219	0	111	0	0	0	0	0	0	0	0	0	0	0	0	513	0	0	0	0
430	0	164	0	0	0	0	0	0	0	1097	0	0	0	0	1276	0	0	0	0
708	0	268	0	0	0	0	0	0	0	567	0	0	0	0	936	0	0	0	0
0	0	0	0	0	0	23	0	0	0	0	0	55	0	0	0	10	0	0	28
0	0	0	0	0	0	38	14	0	0	0	136	57	0	0	0	0	0	0	0
0	0	0	0	0	0	0	0	0	1	0	0	0	0	0	0	4	0	0	23
0	0	0	0	0	0	10	0	0	0	0	0	8	0	0	0	11	0	0	53
0	0	0	0	0	0	0	0	0	0	0	0	0	0	0	0	107	0	0	24
0	0	0	0	0	0	0	0	0	0	0	0	0	0	0	0	16	0	0	0
0	85	0	0	0	0	3	0	0	0	0	0	0	0	0	0	7	0	0	0
0	0	0	0	0	0	379	596	0	0	0	0	0	0	0	0	772	0	0	0
0	0	0	0	0	0	7	11	0	0	0	11	0	0	0	0	7	0	0	0
0	0	0	0	0	0	0	0	0	0	0	0	0	0	0	0	48	0	0	0
0	9	0	0	0	0	70	0	0	0	0	0	0	0	0	0	4	0	0	8
0	1524	0	0	0	0	458	0	0	0	0	0	0	0	0	0	0	0	0	0
0	0	0	0	0	0	0	0	0	10	0	0	0	0	0	0	12	0	0	57
0	4	0	0	0	0	0	0	0	0	0	0	0	0	0	0	13	0	0	84
0	0	0	0	0	0	0	0	0	0	0	0	0	0	0	0	0	0	81	0
0	0	0	0	0	0	0	0	0	0	0	0	0	0	0	0	6	0	0	45
0	0	0	0	0	0	0	0	0	0	0	0	0	0	0	0	20	0	0	43
0	0	0	0	0	0	6	0	0	7	0	0	0	0	0	0	6	0	0	51
0	91	0	0	0	0	15	0	0	0	0	0	0	0	0	0	15	3	0	5
0	0	0	0	0	0	30	0	0	0	0	0	0	0	0	0	12	0	0	6
0	0	0	0	0	4	16	0	0	8	0	0	0	0	0	0	15	0	0	22
0	262	0	0	0	0	290	0	0	0	0	0	0	0	0	0	0	0	0	0
0	0	0	0	0	0	3	0	0	3	0	0	0	0	0	0	22	0	0	63
0	0	0	0	0	0	0	0	0	0	0	0	0	0	0	0	37	0	0	63
0	1	0	0	0	0	2	0	0	1	0	0	0	0	0	0	2	0	0	48
0	0	0	0	0	0	3	0	0	0	0	0	0	0	0	0	75	0	0	76
0	0	0	0	0	0	0	0	0	0	0	0	0	0	0	0	17	0	0	2
0	0	0	0	0	0	0	0	0	0	0	0	5	0	0	0	41	0	0	52
0	0	0	0	0	0	120	45	0	0	0	0	259	0	0	0	0	0	0	0
0	126	0	0	0	0	15	27	0	0	0	0	0	0	0	0	0	0	0	0
0	0	0	0	0	0	48	0	0	6	0	0	0	0	0	0	27	0	0	5
0	0	0	0	0	0	246	0	0	90	0	0	0	0	0	0	0	0	0	0
0	0	0	0	0	0	59	0	0	12	0	0	0	0	0	0	39	0	0	0
0	0	0	0	0	0	73	0	0	20	0	0	0	0	0	0	13	0	0	0
0	0	0	0	0	0	0	0	0	0	0	0	0	4	0	0	0	0	32	0
0	0	0	0	0	0	164	0	0	0	0	0	0	0	0	0	0	0	0	0
0	0	0	0	0	0	475	0	0	143	0	0	158	0	0	0	0	0	0	0
0	0	0	0	0	0	1285	0	0	402	0	0	0	0	0	0	0	0	0	0
0	0	0	0	0	0	84	0	0	0	0	0	0	0	0	0	0	0	0	0
0	0	0	0	0	0	278	0	0	0	0	0	0	0	0	0	0	0	0	0
0	4	0	0	0	0	33	0	0	5	0	0	0	0	0	0	11	0	0	5
0	156	0	0	0	0	1314	0	0	458	0	0	0	0	0	0	0	0	0	0
0	0	0	0	0	0	194	0	0	78	0	0	0	0	0	0	0	0	0	0
0	10	0	0	0	0	102	0	0	18	0	0	0	0	0	0	36	0	0	12
0	66	0	0	0	0	713	0	0	207	0	0	0	0	0	0	0	0	0	0
0	141	0	0	0	0	1177	0	0	411	0	0	0	0	0	0	0	0	0	0
0	33	0	0	0	0	247	0	0	94	0	0	0	0	0	0	27	0	0	0
0	250	0	0	0	0	1643	0	0	536	0	0	0	0	0	0	119	0	0	0
0	57	0	0	0	0	734	0	0	169	0	0	0	0	0	0	0	0	0	0
0	82	0	0	0	0	468	0	0	158	0	0	0	0	0	0	29	0	0	0
0	0	0	0	0	0	250	0	0	56	0	0	0	0	0	0	18	0	0	27
0	0	0	0	0	0	154	0	0	0	0	0	0	0	0	0	0	0	0	0
0	0	0	0	0	0	13	0	1	4	0	0	0	0	0	0	2	0	0	2
0	0	0	0	0	0	6	0	0	0	0	0	0	0	0	0	6	0	0	2
0	0	0	0	0	0	2	0	0	2	0	0	0	0	0	0	36	0	0	13
0	0	0	0	0	0	63	0	0	0	0	0	0	0	0	0	0	0	0	0
0	0	0	0	0	0	8	0	0	0	0	0	0	0	0	0	0	0	0	0
0	0	0	0	0	0	112	0	0	0	0	0	0	0	0	0	0	0	0	0
0	0	0	0	0	0	0	0	0	0	0	0	0	0	0	0	0	0	0	0
0	0	0	0	0	0	1320	0	0	314	0	0	0	0	0	0	0	0	0	0

Halobacteriota	Latescibacteria	Limnochordia	Lokiarchaeia	Methanobacteria	Methanomicrobia	Methanosarcinia	Methanosarcinales	Microgenomatia	Nanoarchaeia	Nanoarchaeota	Nanosalinia	Omnitropholes	Omnitrophia	Parcubacteria	Patescibacteria	Phycisphaerae	Pirellulales	Planctomycetes	Planctomycetota	Proteobacteria	Pseudomonadales	Rhizobiales	Rhodothermales	Spirochaetia	Subgroup_21	Thermoanaerobacteria	Thermoleophilia
30	0	0	0	0	0	0	0	0	0	0	0	0	0	0	0	0	0	0	0	5	0	0	0	0	0	0	0
6709	0	0	0	0	0	0	0	0	0	0	0	0	0	0	0	0	0	0	174	0	0	0	0	0	0	0	0
936	0	0	0	0	0	0	0	0	0	0	0	0	0	0	0	0	0	0	0	0	0	0	0	0	0	0	0
7759	0	0	0	0	0	0	0	0	0	0	0	0	0	0	0	0	0	0	0	0	0	0	0	0	0	0	0
27	0	0	0	0	0	0	0	0	0	0	0	0	0	0	0	0	0	0	0	40	0	0	0	0	0	0	0
1513	0	0	0	0	0	0	0	0	0	0	0	0	0	0	0	0	0	0	27	24	0	0	0	0	0	0	0
4239	0	0	0	0	0	0	0	0	0	0	0	0	0	0	0	0	0	0	0	665	0	0	0	0	0	0	0
2821	0	0	0	0	0	0	0	0	0	0	0	0	0	0	0	0	0	0	0	1688	0	0	0	0	0	0	0
6032	0	0	0	0	0	0	0	0	0	0	0	0	0	0	0	0	0	0	0	0	0	0	0	0	0	0	0
10485	0	0	0	0	0	0	0	0	0	0	0	0	0	0	0	0	0	0	0	0	0	0	0	0	0	0	0
9	0	0	0	0	0	0	0	0	0	0	0	0	0	0	0	0	0	0	304	0	0	0	0	0	0	0	0
37	0	0	0	0	0	0	0	0	0	0	0	0	0	0	0	0	0	0	41	0	0	0	0	0	0	0	0
12	0	0	0	0	0	0	0	0	0	0	0	0	0	0	0	0	0	0	0	3	0	0	0	0	0	0	0
7	0	0	0	0	0	0	0	0	0	0	0	0	0	0	0	0	0	0	17	0	0	0	0	0	0	0	0
20	0	0	0	0	0	0	0	0	0	0	13	0	0	0	0	0	0	0	37	0	0	0	0	0	0	0	0
0	0	0	0	0	0	0	0	0	0	0	32	0	0	0	0	0	0	0	79	48	0	0	0	0	0	0	0
26	0	0	0	0	0	0	0	0	0	0	0	0	0	0	0	0	0	0	26	27	0	0	0	0	0	0	0
4	0	0	0	0	0	0	0	0	0	0	0	0	0	0	0	0	0	0	21	11	0	0	0	0	0	0	0
0	0	0	0	0	0	0	0	0	0	0	0	0	0	0	0	0	0	0	31	28	0	0	0	0	0	0	0
79	0	0	0	0	0	0	0	0	0	0	0	0	0	0	0	0	0	0	66	33	0	0	0	0	0	0	0
5	0	0	0	0	0	0	0	0	0	0	0	0	0	0	0	0	0	0	0	0	0	0	0	0	0	0	0
9612	0	0	0	0	0	0	0	0	0	0	0	0	0	0	0	0	0	0	0	0	0	0	0	0	0	0	0
81	0	0	0	0	0	0	0	0	0	0	29	0	0	0	0	0	0	0	50	159	0	0	0	0	0	0	0
488	0	0	0	0	0	0	0	0	0	0	0	0	0	0	0	0	0	0	0	27	0	0	0	0	0	0	0
6416	0	0	0	0	0	0	0	0	0	0	0	0	0	0	0	0	0	0	0	0	0	0	0	0	0	0	0
60	0	0	0	0	0	0	0	0	0	0	0	0	0	0	0	0	0	0	0	0	0	0	0	0	0	0	0
699	0	0	0	0	0	0	0	0	0	0	0	0	0	0	0	0	0	0	21	0	0	0	0	0	0	0	0
6077	0	0	0	0	0	0	0	0	0	0	0	0	0	0	0	0	0	0	0	0	0	0	0	0	0	0	0
8664	0	0	0	0	0	0	0	0	0	0	0	0	0	0	0	0	0	0	0	0	0	0	0	0	0	0	0
10899	0	0	0	0	0	0	0	0	0	0	0	0	0	0	0	0	0	0	0	0	0	0	0	0	0	0	0
0	0	6	0	0	0	4	0	0	0	0	0	0	2	0	0	2	0	0	0	0	0	0	0	0	0	0	0
0	0	0	0	0	105	358	0	0	0	0	0	0	0	0	0	14	0	0	0	0	0	0	0	0	0	0	0
0	0	0	0	0	0	8	0	1	0	0	0	0	0	0	0	0	0	0	0	0	0	0	0	0	0	0	0
0	0	0	0	0	0	3	0	0	0	0	0	0	0	0	0	0	0	0	0	0	0	0	0	0	0	0	0
0	0	0	2	0	0	0	0	0	0	0	0	0	0	0	0	0	0	0	0	0	0	0	0	0	0	0	0
0	0	0	2	0	0	2	0	0	0	0	0	0	0	0	0	1	0	0	0	0	0	0	0	0	0	0	0
0	0	0	0	0	0	41	0	0	0	0	0	0	0	0	0	0	0	0	0	0	0	0	0	0	0	0	0
0	0	0	190	0	392	516	0	0	0	0	0	0	0	0	0	0	0	0	0	0	0	0	0	0	0	0	0
0	0	0	0	0	17	164	0	0	0	0	0	0	0	0	0	0	0	0	0	0	0	0	0	0	5	0	0
0	0	1237	0	0	51	326	0	0	0	0	0	0	0	0	0	0	0	0	0	0	0	0	0	0	0	0	0
0	0	0	5	0	0	0	0	0	3	0	0	0	5	4	0	5	0	0	0	0	0	0	0	3	0	0	0
0	0	2776	97	0	453	0	0	0	0	0	0	0	0	0	0	111	0	0	0	0	0	0	0	0	0	0	0
0	0	0	0	0	0	0	0	0	0	0	0	0	0	0	0	0	0	0	0	0	0	0	0	0	0	0	0
0	0	0	2	0	0	0	0	0	2	0	0	0	0	0	0	0	0	0	0	0	0	0	0	0	0	4	0
0	0	0	0	0	0	0	0	0	0	0	0	0	0	0	0	0	0	0	0	0	0	6	0	0	0	0	0
0	0	0	0	0	0	0	0	0	0	0	0	0	0	0	0	0	0	0	0	0	0	0	0	0	0	0	0
0	0	0	0	0	0	1	0	0	0	0	3	0	0	0	0	0	0	0	0	0	0	0	0	0	0	0	0
0	0	0	8	0	6	15	0	0	0	0	0	0	0	0	0	0	0	0	0	0	0	0	0	0	0	0	0
0	0	0	0	0	4	0	0	0	0	0	0	0	0	0	0	4	0	0	6	0	0	0	0	0	0	0	0
0	0	0	0	0	15	0	0	0	0	0	0	0	0	0	0	4	0	0	0	0	0	0	0	0	0	0	0
0	0	0	0	0	0	2	0	0	0	0	0	0	0	0	0	0	0	0	0	0	0	0	0	0	0	0	0
0	0	0	0	0	1088	1487	0	0	0	0	0	0	0	0	0	0	0	0	0	0	0	0	0	0	0	0	0
0	0	0	1	0	0	0	0	0	0	0	0	0	0	0	0	0	0	0	0	0	0	0	0	0	0	0	0
0	0	0	0	0	0	25	0	3	0	0	0	0	0	0	0	0	0	0	0	0	0	0	0	0	0	0	0
0	1	0	0	0	0	14	0	0	0	0	0	0	0	0	0	0	0	0	2	0	0	0	0	1	0	0	1
0	0	0	0	0	0	38	0	0	0	0	0	0	0	0	0	0	0	0	0	0	0	0	0	0	0	0	0
0	0	0	0	0	0	178	0	0	0	0	0	0	0	0	0	0	0	0	0	0	0	0	0	0	0	0	0
0	0	0	0	0	0	8	0	0	0	0	0	0	0	0	0	0	0	0	0	0	0	0	0	0	0	0	0
0	0	28	0	0	77	1270	0	0	0	0	0	0	0	0	0	0	0	0	0	0	0	0	0	0	0	0	0
0	0	0	0	0	31	464	0	0	0	0	0	0	0	0	0	7	0	0	0	0	0	0	0	0	0	0	0
0	0	0	8	0	3	55	0	0	10	0	0	0	0	0	0	7	0	0	0	0	0	0	0	0	0	0	0
0	0	0	0	0	0	6671	0	0	0	0	0	0	0	0	0	88	0	0	0	0	0	0	0	0	0	0	0
0	0	16	16	0	0	634	0	0	0	0	0	0	13	0	0	18	0	0	0	0	0	0	0	0	0	0	0
0	0	0	13	0	0	365	0	0	0	0	0	0	0	0	0	32	0	0	0	0	0	0	0	0	0	0	0
0	0	0	0	0	0	0	34	0	0	0	0	3	0	0	0	0	4	0	0	0	0	0	9	13	0	0	0
0	0	0	0	0	0	11153	0	0	0	0	0	0	0	0	0	0	0	0	0	0	0	0	0	0	0	0	0
0	0	0	0	0	0	9648	0	0	0	0	0	0	0	0	0	127	0	0	0	0	0	0	0	0	0	0	0
0	0	0	353	0	114	2677	0	0	101	0	0	0	0	0	96	0	304	0	126	0	0	0	0	0	114	0	0
0	0	0	0	0	0	6952	0	0	0	0	0	0	0	0	0	0	0	0	0	0	0	0	0	0	0	0	0
0	0	0	0	0	0	10959	0	0	0	0	0	0	0	0	0	0	0	0	0	0	0	0	0	0	0	0	0
0	0	0	7	0	2	0	0	0	0	0	0	0	0	0	5	0	3	0	0	0	0	0	0	0	0	0	0
0	0	0	384	0	212	0	0	0	213	0	0	0	0	113	0	476	0	103	0	0	0	0	0	0	131	0	0
0	0	0	76	0	0	0	0	0	0	0	0	0	0	0	0	128	0	37	0	0	0	0	0	0	0	0	0
0	0	0	26	0	0	0	0	0	10	0	0	0	0	0	0	31	0	7	0	0	0	0	0	0	6	0	0
0	0	0	173	0	0	0	0	0	84	0	0	0	37	60	0	241	0	71	0	0	0	0	0	56	0	0	0
0	0	0	270	0	113	0	0	0	193	0	0	0	0	119	0	255	0	0	0	0	0	0	0	0	0	0	0
0	0	0	53	0	51	0	0	0	23	0	0	0	14	22	0	54	0	0	0	0	0	0	0	42	0	0	0
0	0	0	473	0	282	0	0	0	283	0	0	0	100	131	0	395	0	101	0	0	0	0	0	125	0	0	0
0	0	0	133	0	36	0	0	0	54	0	0	0	0	47	0	129	0	33	0	0	0	0	0	32	0	0	0
0	0	0	117	0	114	0	0	0	119	0	0	0	0	30	0	97	0	37	0	0	0	0	0	28	0	0	0
0	0	0	31	0	26	66	0	0	21	0	0	0	14	0	0	99	0	23	0	0	0	0	0	0	0	0	0
0	0	0	0	0	0	9676	0	0	0	0	0	0	0	0	0	0	0	0	0	0	0	0	0	0	0	0	0
0	0	0	1	3	0	5	0	0	0	0	0	0	0	0	0	0	0	0	0	0	0	0	0	0	0	0	0
0	0	0	0	0	0	0	0	0	4	0	0	0	0	0	0	0	0	0	0	0	0	0	0	0	0	4	0
0	0	0	0	0	2	11	0	0	0	0	0	0	0	0	0	0	0	0	0	0	0	0	0	0	0	0	0
0	0	0	0	0	0	3176	0	0	0	0	0	0	0	0	0	0	0	0	0	0	0	0	0	0	0	0	0
0	0	0	0	0	0	768	0	0	0	0	0	0	0	0	0	0	0	0	0	0	0	0	0	0	0	0	0
0	0	0	0	0	0	8642	0	0	0	0	0	0	0	0	0	0	0	0	0	0	0	0	0	0	0	0	0
0	0	0	0	0	0	7870	0	0	0	0	0	0	0	0	0	0	0	0	0	0	0	0	0	0	0	0	0
0	0	133	420	0	0	4760	0	0	0	0	0	0	0	0	0	271	0	0	0	0	0	0	0	0	0	0	0

Thermoplasmata	Thermoplasmatota	unknown_unclassified	WCHB1-81	Xanthomonadales	Zixibacteria_cl	Zixibacteria_insertae_sedis_class	Reductant	Day	Redox	Depth
0	0	0	0	0	0	0	Sodium dithionite	90	-150	12-14cm
0	0	0	0	0	0	0	Titanium(III) citrate	90	-570	12-14cm
0	0	0	0	0	0	0	Sodium dithionite	90	-150	12-14cm
0	0	0	0	0	0	0	Sodium dithionite	90	-300	12-14cm
0	0	0	0	0	0	0	Sodium dithionite	90	-300	12-14cm
0	0	0	0	0	0	0	Titanium(III) citrate	90	~340	12-14cm
0	0	0	0	0	0	0	Titanium(III) citrate	90	~340	12-14cm
0	0	0	0	0	0	0	Titanium(III) citrate	90	-380	12-14cm
0	0	0	0	0	0	0	Titanium(III) citrate	90	-380	12-14cm
0	0	0	0	0	0	0	Titanium(III) citrate	90	-570	12-14cm
0	131	0	0	0	0	0	Sodium dithionite	90	-150	38-40cm
0	31	0	0	0	0	0	Titanium(III) citrate	90	-570	38-40cm
0	0	12	0	0	0	0	Sodium dithionite	90	-150	38-40cm
0	7	10	0	0	0	0	Sodium dithionite	90	-300	38-40cm
0	0	0	0	0	0	0	Sodium dithionite	90	-300	38-40cm
0	0	0	0	0	0	0	Titanium(III) citrate	90	~340	38-40cm
0	22	22	0	0	0	0	Titanium(III) citrate	90	~340	38-40cm
0	0	0	0	0	0	0	Titanium(III) citrate	90	-380	38-40cm
0	0	24	0	0	0	0	Titanium(III) citrate	90	-380	38-40cm
0	44	0	0	0	0	0	Titanium(III) citrate	90	-570	38-40cm
0	0	0	0	0	0	0	Sodium dithionite	90	-150	48-50cm
0	0	0	0	0	0	0	Titanium(III) citrate	90	-570	48-50cm
0	0	0	0	0	0	0	Sodium dithionite	90	-150	48-50cm
0	0	74	0	0	0	0	Sodium dithionite	90	-300	48-50cm
0	0	0	0	0	0	0	Sodium dithionite	90	-300	48-50cm
0	0	1	0	0	0	0	Titanium(III) citrate	90	~340	48-50cm
0	0	0	0	0	0	0	Titanium(III) citrate	90	~340	48-50cm
0	0	0	0	0	0	0	Titanium(III) citrate	90	-380	48-50cm
0	0	0	0	0	0	0	Titanium(III) citrate	90	-380	48-50cm
0	0	0	0	0	0	0	Titanium(III) citrate	90	-570	48-50cm
0	0	3	0	0	0	2	Sodium dithionite	180	-150	12-14cm
0	0	0	0	0	0	0	Titanium(III) citrate	180	-570	12-14cm
0	0	0	0	0	0	0	Sodium dithionite	180	-150	12-14cm
0	0	0	0	0	0	0	Sodium dithionite	180	-300	12-14cm
0	0	2	0	0	0	0	Sodium dithionite	180	-300	12-14cm
0	0	5	0	0	0	0	Titanium(III) citrate	180	~340	12-14cm
0	0	7	0	0	0	0	Titanium(III) citrate	180	~340	12-14cm
0	0	0	0	0	0	0	Titanium(III) citrate	180	-380	12-14cm
0	0	0	0	0	0	0	Titanium(III) citrate	180	-380	12-14cm
0	0	0	0	0	0	0	Titanium(III) citrate	180	-570	12-14cm
0	0	4	0	0	0	0	Sodium dithionite	180	-150	38-40cm
0	0	0	0	0	0	0	Titanium(III) citrate	180	-570	38-40cm
0	0	1	0	0	0	0	Sodium dithionite	180	-150	38-40cm
0	0	2	0	0	0	0	Sodium dithionite	180	-300	38-40cm
0	0	0	0	0	0	0	Sodium dithionite	180	-300	38-40cm
0	0	0	0	0	0	0	Titanium(III) citrate	180	~340	38-40cm
0	0	0	0	0	0	0	Titanium(III) citrate	180	~340	38-40cm
0	0	0	0	0	0	0	Titanium(III) citrate	180	-380	38-40cm
0	0	0	0	0	0	0	Titanium(III) citrate	180	-380	38-40cm
0	0	2	0	0	0	0	Titanium(III) citrate	180	-570	38-40cm
0	0	2	0	0	0	0	Sodium dithionite	180	-150	48-50cm
0	0	0	0	0	0	0	Titanium(III) citrate	180	-570	48-50cm
0	0	3	0	0	0	0	Sodium dithionite	180	-150	48-50cm
0	0	0	0	0	0	0	Sodium dithionite	180	-300	48-50cm
1	0	1	0	0	0	0	Sodium dithionite	180	-300	48-50cm
0	0	6	0	0	0	0	Titanium(III) citrate	180	~340	48-50cm
0	0	0	0	0	0	0	Titanium(III) citrate	180	~340	48-50cm
0	0	0	0	0	0	0	Titanium(III) citrate	180	-380	48-50cm
0	0	0	0	0	0	0	Titanium(III) citrate	180	-380	48-50cm
0	0	0	0	0	0	0	Titanium(III) citrate	180	-570	48-50cm
0	0	4	0	0	0	0	Sodium dithionite	30	-150	12-14cm
0	0	0	0	0	0	0	Titanium(III) citrate	30	-570	12-14cm
0	0	16	0	0	0	0	Sodium dithionite	30	-150	12-14cm
0	0	19	0	0	0	0	Sodium dithionite	30	-300	12-14cm
0	0	9	0	13	0	0	Sodium dithionite	30	-300	12-14cm
0	0	0	0	0	0	0	Titanium(III) citrate	30	~340	12-14cm
0	0	0	0	0	0	0	Titanium(III) citrate	30	~340	12-14cm
149	0	0	0	0	0	0	Titanium(III) citrate	30	-380	12-14cm
0	0	0	0	0	0	0	Titanium(III) citrate	30	-380	12-14cm
0	0	0	0	0	0	0	Titanium(III) citrate	30	-570	12-14cm
15	0	3	0	0	0	0	Sodium dithionite	30	-150	38-40cm
212	0	166	0	0	0	0	Titanium(III) citrate	30	-570	38-40cm
33	0	43	0	0	0	0	Sodium dithionite	30	-150	38-40cm
0	0	9	0	0	0	0	Sodium dithionite	30	-300	38-40cm
41	0	65	0	0	0	0	Sodium dithionite	30	-300	38-40cm
88	0	91	0	0	0	0	Titanium(III) citrate	30	~340	38-40cm
31	0	0	0	0	0	0	Titanium(III) citrate	30	~340	38-40cm
161	0	204	0	0	0	0	Titanium(III) citrate	30	-380	38-40cm
67	0	62	0	0	0	0	Titanium(III) citrate	30	-380	38-40cm
85	0	68	0	0	0	0	Titanium(III) citrate	30	-570	38-40cm
38	0	25	0	0	40	0	Sodium dithionite	30	-150	48-50cm
0	0	0	0	0	0	0	Titanium(III) citrate	30	-570	48-50cm
0	0	3	0	0	0	0	Sodium dithionite	30	-150	48-50cm
0	0	0	0	0	0	0	Sodium dithionite	30	-300	48-50cm
0	0	0	0	0	0	0	Sodium dithionite	30	-300	48-50cm
0	0	0	0	0	0	0	Titanium(III) citrate	30	~340	48-50cm
0	0	0	0	0	0	0	Titanium(III) citrate	30	~340	48-50cm
0	0	0	0	0	0	0	Titanium(III) citrate	30	-380	48-50cm
0	0	0	0	0	0	0	Titanium(III) citrate	30	-380	48-50cm
132	0	0	0	0	0	0	Titanium(III) citrate	30	-570	48-50cm

Table D.3 Gas headspace measurements (µmol) for methane across the manipulation series.

12-14cm								
Sample_ID	0	30	60	90	120	150	Redox (mV)	Additive
Control	4735.39538	4995.85286	4270.21503	4751.33237	4889.63274	3591.17622	N/A	N/A
DA1	4727.46623	4875.03359	4563.87241	4558.57175	3887.18945	3660.09206	-150	Sodium dithionite
DA2	5085.06858	4796.9881	4714.94546	4873.64534	-26.837259	4631.52104	-150	Sodium dithionite
DA3	4421.40774	5292.99659	4512.09523	4467.58927	1333.95466	3556.90248	-300	Sodium dithionite
DA4	4742.41989	4703.84238	4703.55395	4963.96661	1958.73321	3255.62099	-300	Sodium dithionite
DA5	4728.51988	4787.18212	4656.40281	4629.33191	1480.56442	3340.22042	-300--340	Titanium(III) citrate
DA6	4611.91913	4788.61817	4421.17641	4522.66271	778.292155	3029.89328	-300--340	Titanium(III) citrate
DA7	4635.04047	4696.90757	4508.41638	4732.22403	272.446308	3528.6296	-380	Titanium(III) citrate
DA8	4489.65011	4856.24842	4402.48175	4554.60266	3.6427895	3292.31695	-380	Titanium(III) citrate
DA9	4619.18988	4933.86608	4437.88601	4713.36463	176.898959	3887.3046	-570	Titanium(III) citrate
DA10	4993.00632	4520.31843	4460.42682	4663.46115	-26.837259	4475.21308	-570	Titanium(III) citrate
38-40cm								
Sample_ID	0	30	60	90	120	150	Redox (mV)	Additive
Control	4566.1847	4946.25161	4475.49031	4860.04228	3561.41672	4150.5964	N/A	N/A
DB1	5047.6356	4656.122	4526.56503	4513.04876	4390.49463	4397.60696	-150	Sodium dithionite
DB2	4654.27243	4816.66736	4502.76318	4890.20104	4759.45522	4720.01693	-150	Sodium dithionite
DB3	4761.53547	0	4492.74654	4677.09571	4737.42698	3847.85385	-300	Sodium dithionite
DB4	4753.88456	5203.48158	4731.61215	4802.87966	4649.62425	3561.10706	-300	Sodium dithionite
DB5	4766.94054	4943.21304	4535.47013	5086.08346	3261.39238	4004.22781	-300--340	Titanium(III) citrate
DB6	4694.35557	4610.62473	4976.05962	4724.21531	3587.22894	3769.27819	-300--340	Titanium(III) citrate
DB7	4784.34238	4856.66949	4807.51322	4722.79983	3643.07931	4165.09789	-380	Titanium(III) citrate
DB8	4671.08777	5003.0864	4724.42737	4786.48809	3316.14404	3580.39229	-380	Titanium(III) citrate
DB9	4780.33005	4523.01252	4600.8652	4670.8634	3584.15977	4566.49191	-570	Titanium(III) citrate
DB10	4600.04928	4888.31679	4943.45418	4691.15401	3543.321878	3894.33716	-570	Titanium(III) citrate
48-50cm								
Sample_ID	0	30	60	90	120	150	Redox (mV)	Additive
Control	5022.8274	4999.86574	4587.21259	4954.3284	4774.03432	3503.06174	N/A	N/A
DC1	4782.16834	5066.28025	4531.42148	4851.68929	2243.65515	3883.38577	-150	Sodium dithionite
DC2	5400.06247	4613.33021	4776.31965	4489.53249	4487.53249	3794.23388	-150	Sodium dithionite
DC3	5395.70271	4674.25383	4419.93801	4650.53017	2104.13623	5151.83328	-300	Sodium dithionite
DC4	4840.99217	4789.16808	4722.98882	4767.04593	3482.34803	5242.15282	-300	Sodium dithionite
DC5	4458.8264	4900.25795	4520.40892	4695.81426	1419.18336	5441.20104	-300--340	Titanium(III) citrate
DC6	4822.60423	4978.08976	4645.45736	4706.19807	1051.79516	5113.5211	-300--340	Titanium(III) citrate
DC7	4756.53738	4653.11473	4453.81926	4606.7444	1628.22399	4441.21214	-380	Titanium(III) citrate
DC8	5103.2534	4572.74014	4848.97897	4605.51019	2639.68049	5046.1127	-380	Titanium(III) citrate
DC9	4477.29794	4760.61852	4683.40752	4718.15126	3623.11273	4290.02516	-570	Titanium(III) citrate
DC10	5106.56661	4906.25397	4350.76766	4560.42119	3656.84997	3817.53231	-570	Titanium(III) citrate

APPENDIX E

E MICROBIAL ENRICHMENT FROM ANAEROBIC SEDIMENTS

Introduction

Enrichments from Chapter 5 were further manipulated and transferred under varied media conditions. These conditions further constrained carbon substrates and redox in an attempt to enrich and isolate potential anaerobic methane oxidizers from anaerobic sediments.

Methods

Media Preparation and Initial Inoculation

Marine minimal media was prepared by adding KBr (0.09g/L), KCl (0.66g/L), $CaCl_2*H_2O$ (0.30g/L), $MgCl_2*6H_2O$ (3.20g/L), NaCl (18.6g/L) in sterile milli-Q water. Minimal media was autoclaved and degassed using N_2/CO_2. The following solutions were added to the marine minimal media: N_aHCO_3 buffer (1 M, 30mL/L), NH_4CI/KH_2PO_4 buffer (NH_4Cl 5g/L; KH_2PO_4 4g/L, 50mL/L), filter-sterilized vitamin solution SI10 (DSMZ medium 141) (1mL/L), and filter-sterilized trace element solution TS15v (DSMZ medium 141) (1mL/L). 25mL of the solution was added to each serum bottle then sealed and crimped with rubber stoppers. Serum bottles were then made anaerobic by venting and gassing with N_2 for 10 minutes in the media and 5 minutes in

the headspace, followed by venting and gassing with 80% N_2/ 20% CO_2 gas mix for 10 minutes in the media and 5 minutes in the headspace. Concentrations of titanium (Ill) citrate stock solution (100 mM stock solution; 1.7mM, 2.4mM, 3.1mM) and sodium dithionite (143.5 mM stock solution; 8.6 mM, 11.5 mM) were used as reductant agents to achieve set redox potentials. Additional bottles were prepared with the intention of reducing sulfate reduction by using (242.8 mM stock solution; 24.3 mM and 34 mM) concentrations of sodium molybdate (IV) dihydrate. Redox potentials were monitored using the Pinpoint ORP/REDOX probe (American Marine Inc., Ridgefield, CT). Filter-sterilized antibiotic solution consisting of ampicillin (0.5g/20mL H_2O), rifampicin (0.5g/10mL methanol), tetracycline (0.5/10mL H_2O), vancomycin hydrochloride (0.2g/10mL H_2O), and spectinomycin dihydrochloride pentahydrate (0.5g/10mL H_2O) was added to all microcosms at 2mg/mL final concentration. Serum bottle headspace was filled with 100% CH_4 for 5min.

Transfer 1: Select enrichments from the 12-14 cm and 48-50 cm depth manipulation series outlined in Chapter 5 were used as inoculum for a 100 µL transfer into new marine minimal media, respective of their previous redox conditions, including the reductant and redox potential. Organic acids (acetate, butyrate, and propionate) were added to each enrichment at 5mM concentration. All enrichments were incubated at room temperature in a dark room and maintained over the course of three months. 500 µL was collected during the enrichment series and stored at -80 C until extraction.

Transfer 2A: Marine minimal media was prepared for inoculation using 100 µL from select Transfer 1 enrichments. Concentrations of titanium (III) citrate (1.7mM, 2.4mM, 3.1mM) and sodium dithionite (8.6 mM, 11.5 mM) were used to achieve low redox environments. Enrichments were supplemented with filter-sterilized acetate, propionate, or butyrate at a 5mM concentration. Inoculated enrichments without volatile fatty acid supplements served controls. 500µL was collected during the enrichment series and stored at -80 C until extraction.

Transfer 2B: Marine minimal media was prepared again for inoculation using 100 µL from select Transfer 1 enrichments. Titanium (III) citrate (2.4mM, 3.1mM) was used as the primary reducing agent in this enrichment series. Organic acids (acetate, butyrate, and propionate) were added to each enrichment at 5mM concentration. Enrichments were incubated at three different temperatures 21 C, 25 C and 30 C. 500 µL was collected during the enrichment series and stored at -80 C until extraction.

Transfer 3: Marine minimal media was prepared for inoculation using 100 µL from a select Transfer 2B enrichment. Titanium (III) citrate (3.1 mM) and sodium sulfide were used as reducing agents. To test the effect of media additives on the enriched microbial consortia there was a presence absence matrix consisting of the absence or presence of antibiotics, volatile fatty acids (acetate, butyrate, and propionate), and reductant. Serum bottle headspace was filled with 80% N_2/ 20% CO_2 gas. 500µL was collected weekly during the 8-week enrichment series and stored at -80 C until extraction. 250µL of sample was collected for microscopic analysis to assess presence of cofactor 420 in culture that autofluorescence blue without the presence of a cellular stain. Liquid sample

(1 mL) was collected and 750µL of samples were fixed in 5 mL of fixative consisting of 16% paraformaldehyde (5 mL), 8% glutaraldehyde (10 mL), sterile ddH_2O (5 mL), and 3X PBS (20 mL) at room temperature for 2 hours in preparation for scanning electron microscopy. Fixed cells were then buffer rinsed, rinsed in 1% OsO_4, buffer rinsed, ddH_2O rinsed, a series of graded EtOH rinses (50%, 75%, 90%, 100%), underwent critical point drying, and sputter coated as outlined by the University of Delaware Bioimaging center protocols.

Headspace methane concentrations were measured monthly for Transfer 1, Transfer 2A and Transfer 2B and weekly for Transfer 3 by gas chromatography using a flame-ionization detector (Agilent 7890B, Wilmington, DE, USA). Methane is separated isothermally within a HP-Plot Q column (Agilent, 30 m x 0.530 µm inner diameter, 40 µm film thickness). We conducted manual injection of 100uL headspace sample using a gastight syringe. Injector temperature was 250° C with a set oven temperature of 60° C and detector temperature of 250° C. Methane peaks were integrated using Agilent ChemStation Data Analysis software version F.01.03. Methane concentrations were determined from a standard curve of equilibrated standards and the ideal gas law. Liquid samples (500µL) collected for taxonomic analysis, had DNA extracted from 250µL of sample using the Qiagen DNeasy PowerSoil Pro kit (Germantown, Maryland). Extracted DNA was sent to the UCONN MARS facility for amplicon sequencing of the 16S rRNA gene targeting the V4 region (primers 515F and 806R) using the Illumina MiSeq paired-end sequencing platform via the v2 2x250 base pair kit (Illumina) following their standard protocol (Parada et al., 2016). Raw forward and reverse sequences were paired,

and quality checked; sequences that passed QC were further processed using the 16S rRNA gene analysis pipeline implemented in MOTHUR version 1.46.1 (Schloss et al., 2009). Forward and reverse sequences were aligned and quality filtered using MOTHUR, yielding amplicons ranging in sizes of 130-200 bp in lengths, where ambiguous nucleotides and homopolymer stretches were removed. We opted against the use of amplicon sequence variants (ASV) considering the amount of available computation and created operational taxonomic units (OTU). OTUs were created with a 3% dissimilarity and were aligned and classified against the Silva SSU database, version 138 (Gurevich et al., 2013). Nontarget OTUs and taxa <1% were removed from representative sequences prior to further downstream analysis. Metagenomic sequencing was done on extracted DNA from 8 select samples from Transfer 2A. Metagenome libraries were prepared and sequenced (300 bp paired ends) on an Illumina NextSeq 2000 instrument housed at the University of Delaware's Sequencing and Genotyping.

Diversity analyses of enrichments were performed in R using the following packages: VEGAN and tidyverse (Dixon, 2003; Wickham et al., 2019). OTUs were classified to the class level and assigned a taxonomic representative for beta diversity analysis among samples. Data has been deposited in the NCBI repository under BioProject number XXXX.

Results

Transfer 1

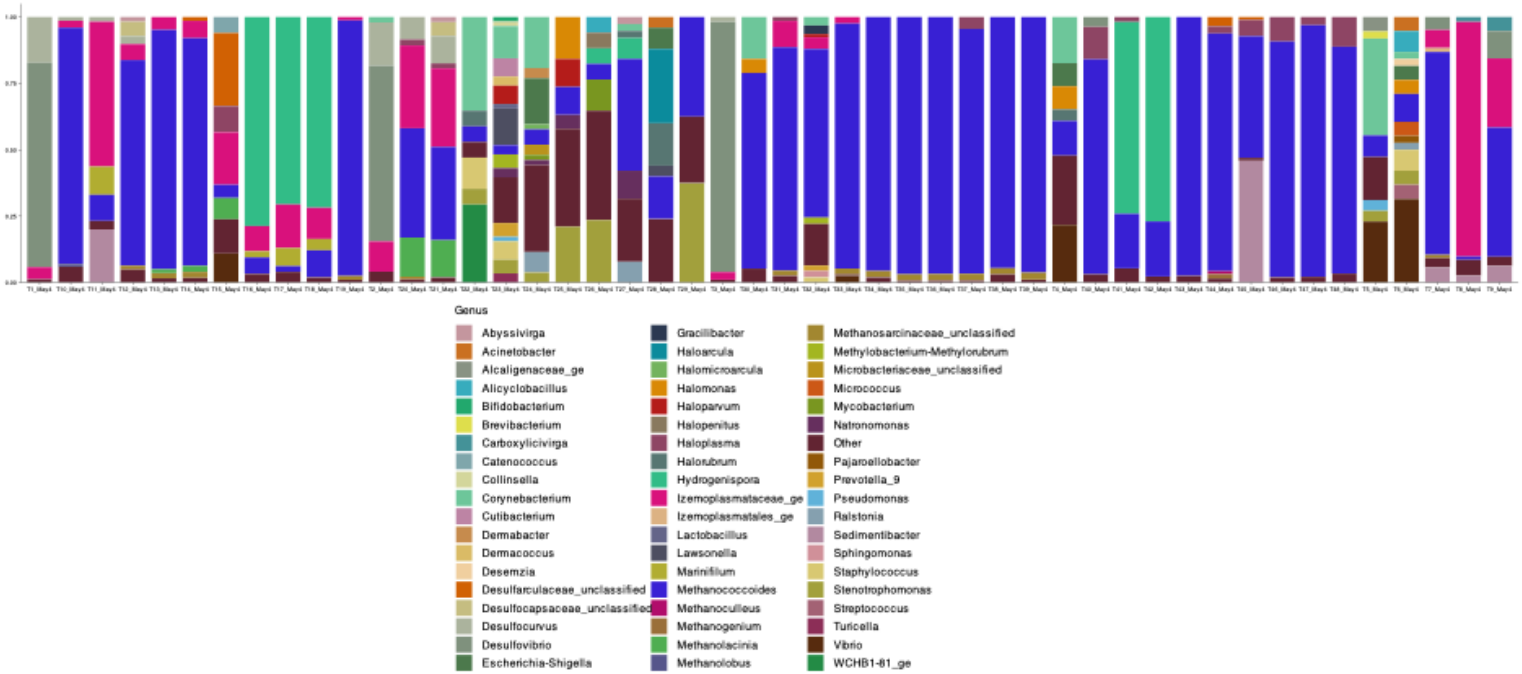

Figure E1. Abundant microbial taxa based on relative 16S rRNA gene percent abundance that have been identified to Genus level at 90-days post transfer. Data shows the dominant abundance of *Methanococcoides* across samples.

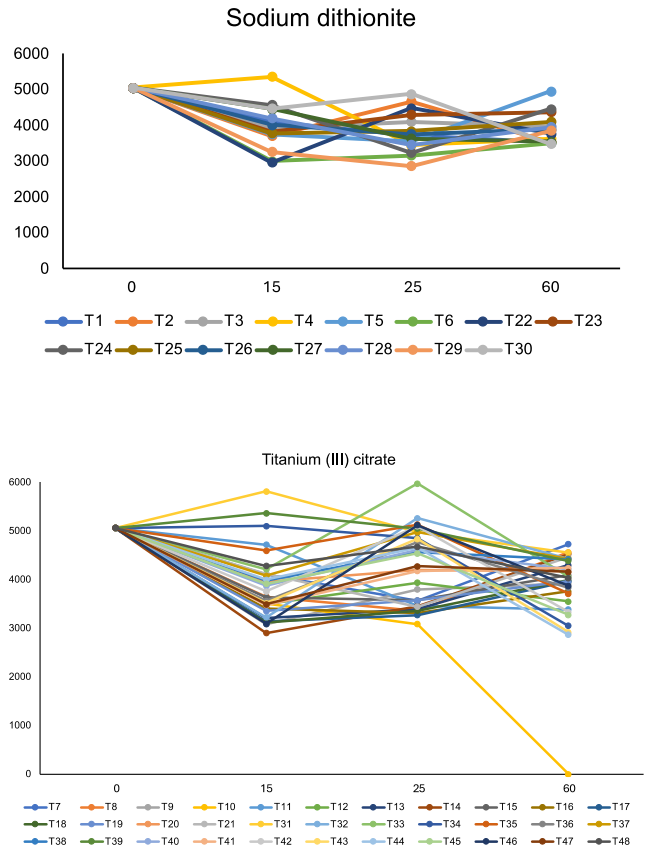

Figure E2. Headspace measurements for methane (µmol) over 60-days for enrichments from Transfer 1 using titanium (III) citrate and sodium dithionite.

Transfer 2A

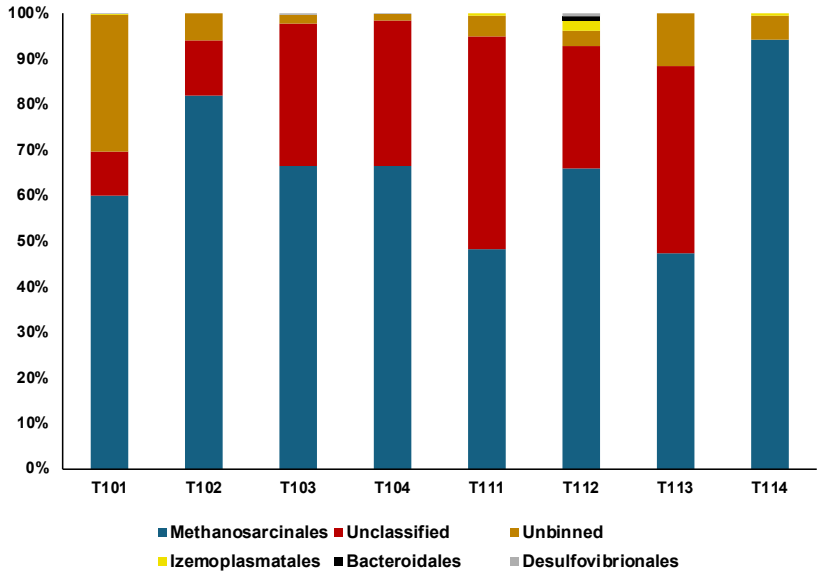

Figure E4. Metagenomes from select enrichments identified to the Order level. T101/T111 supplemented with acetate, T102/T112 supplemented with butyrate, T103/T113 supplemented with propionate, and T104/T114 have no organic acid supplement.

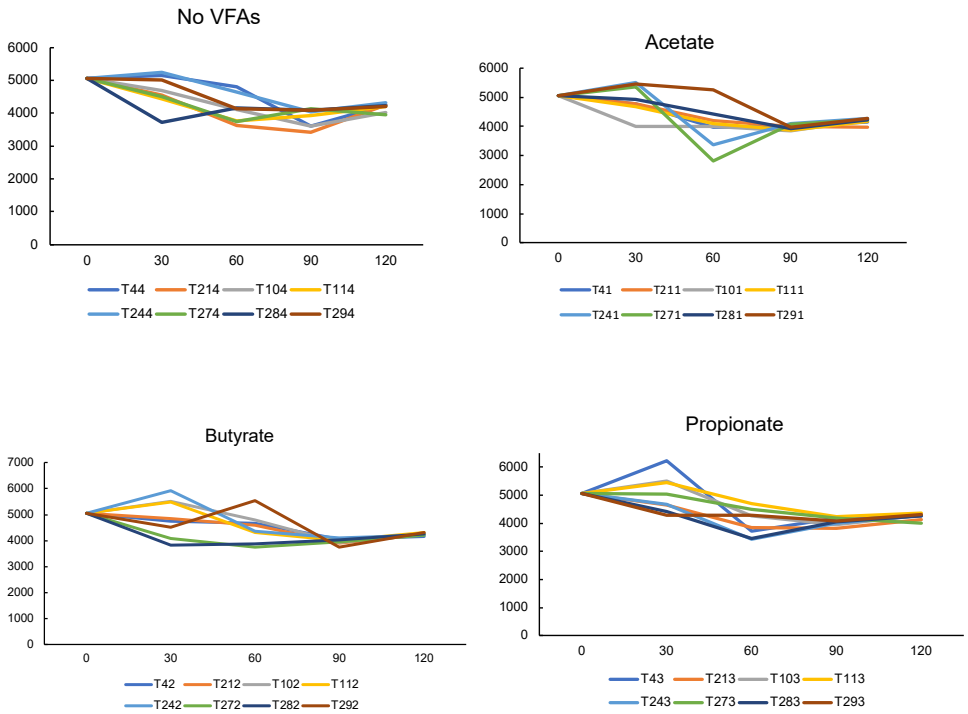

Figure E5. Headspace measurements for methane (µmol) over 120-days for enrichments from Transfer 1 using acetate, butyrate, and propionate as carbon supplements.

Transfer 2B

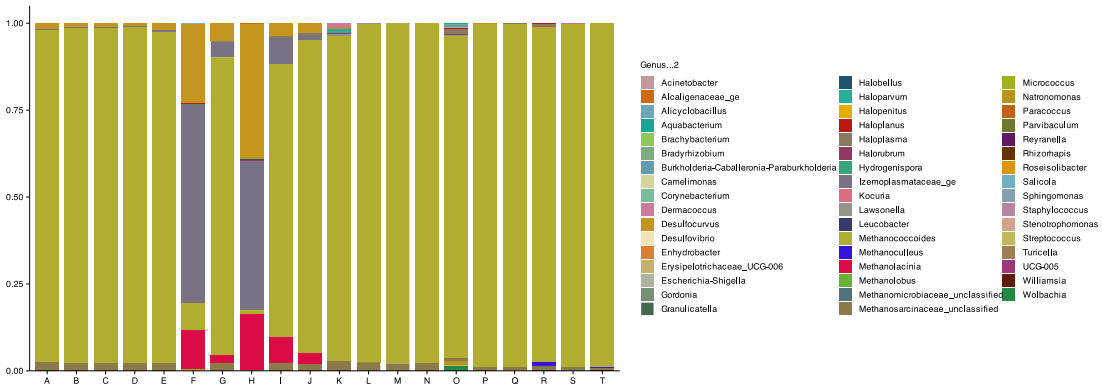

Figure E6. Abundant microbial taxa based on relative 16S rRNA gene percent abundance that have been identified to Genus level at 30-days post transfer. Data shows the dominant abundance of *Methanococcoides* across samples.

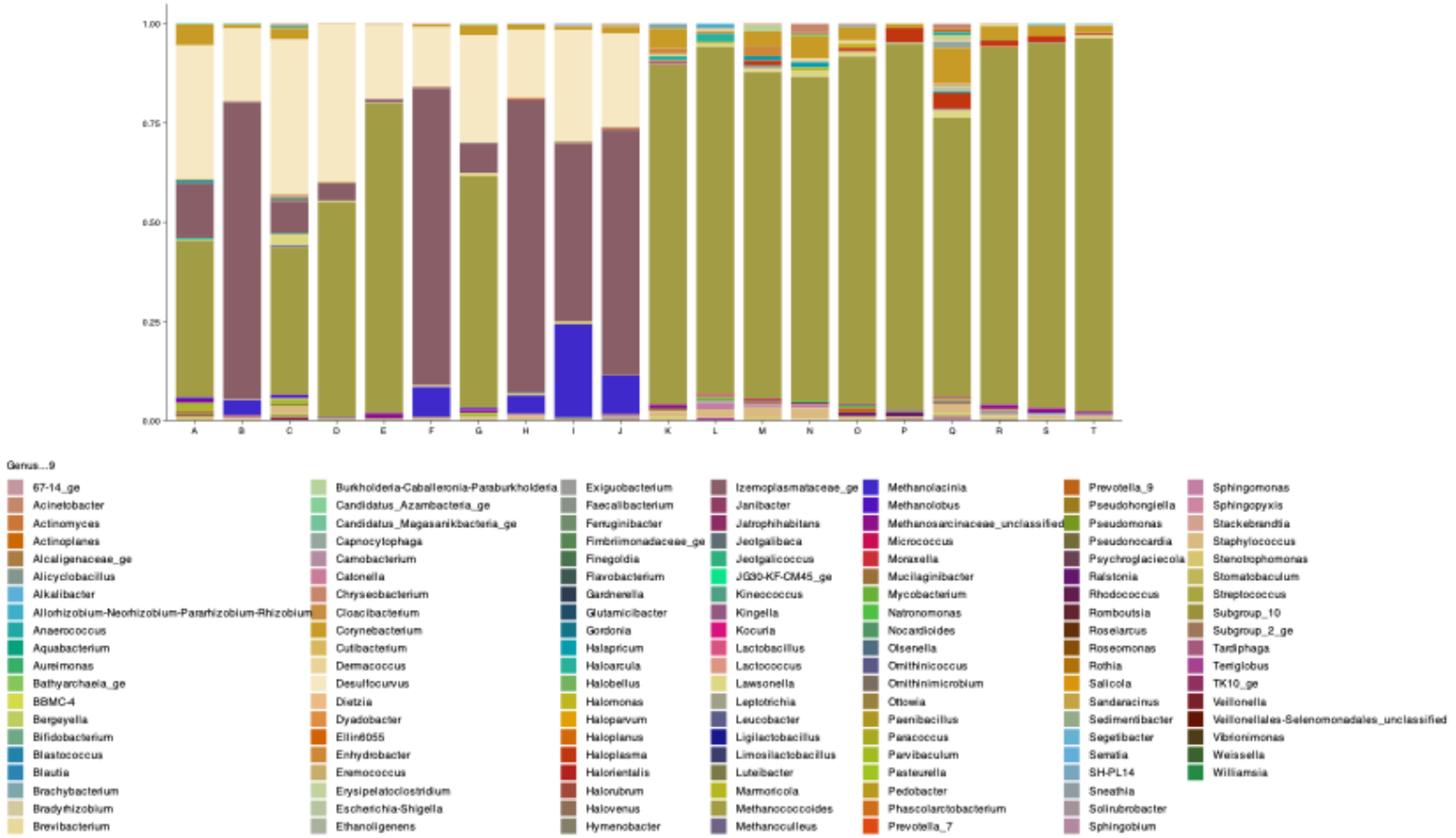

Figure E7. Abundant microbial taxa based on relative 16S rRNA gene percent abundance that have been identified to Genus level at 60-days post transfer. Data shows the dominant abundance of *Methanococcoides* across samples.

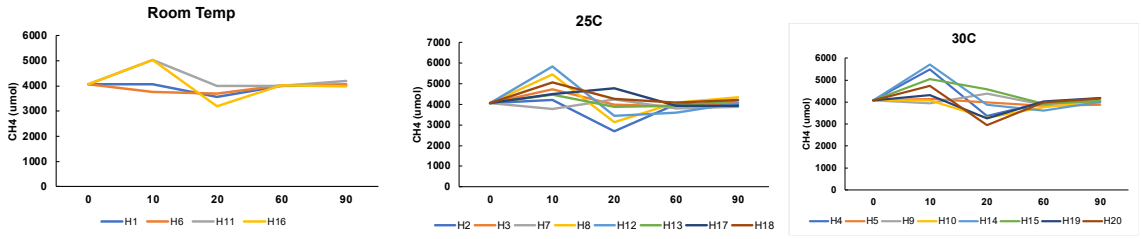

Figure E8. Headspace measurements for methane (µmol) over 90-days for enrichments from Transfer 1 at 21 C (Room Temperature), 25 C and 30 C.

Transfer 3

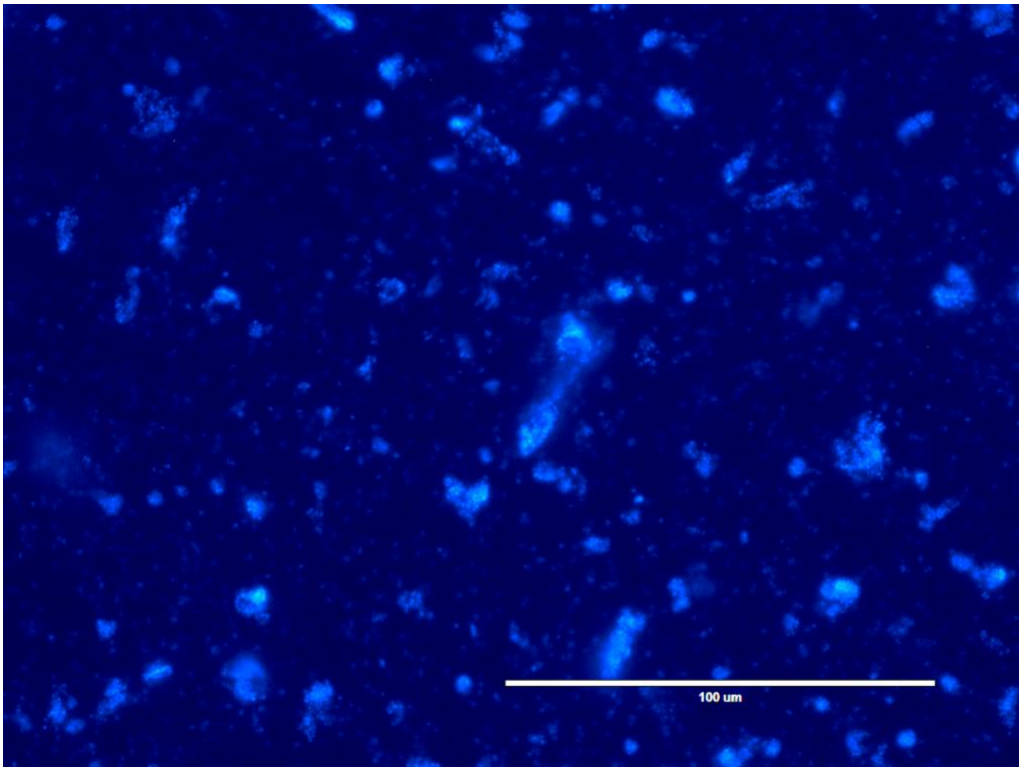

Figure E.9 Microscopy showing samples autofluorescence blue indicating active 420 cofactor production from likely methanogenic activity.

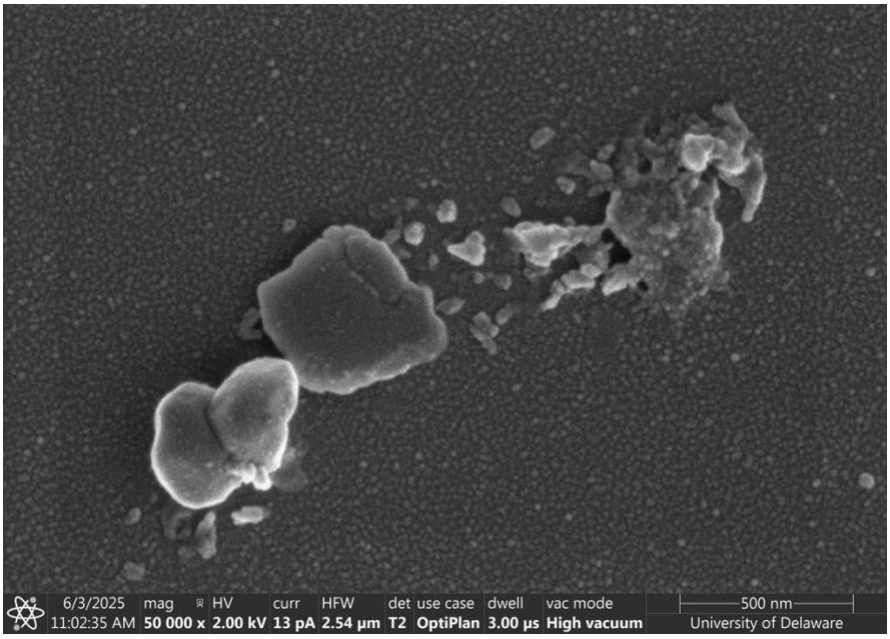

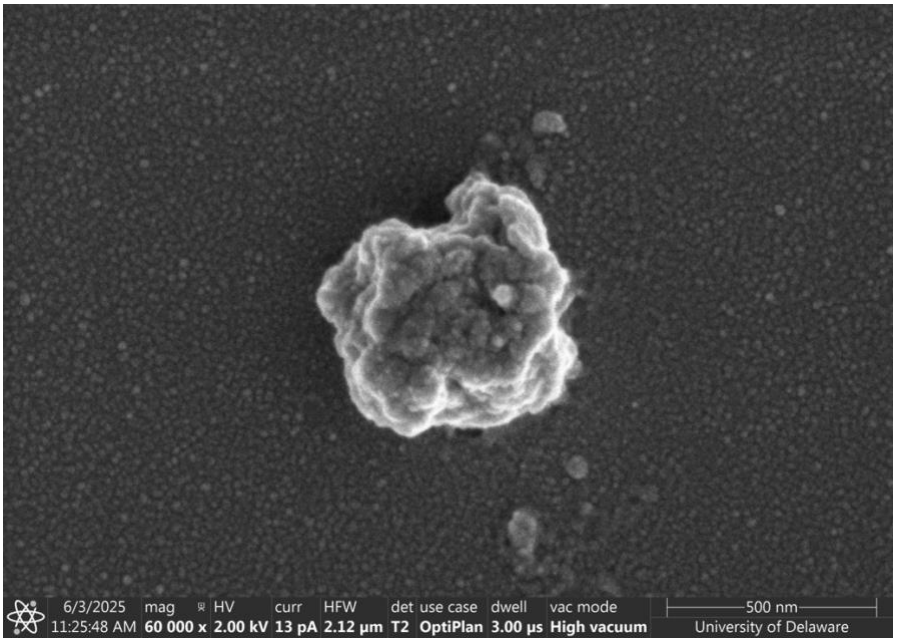

Figure E10. Scanning electron microscopy done on select enrichments from Transfer 3 with titanium (III) citrate.